VTT Technical Research Centre of Finland

Simulation of underwater sound radiation from ship structures in full frequency range

Tanttari, Jukka

Published: 25/06/2014

Document Version
Publisher's final version

[Link to publication](#)
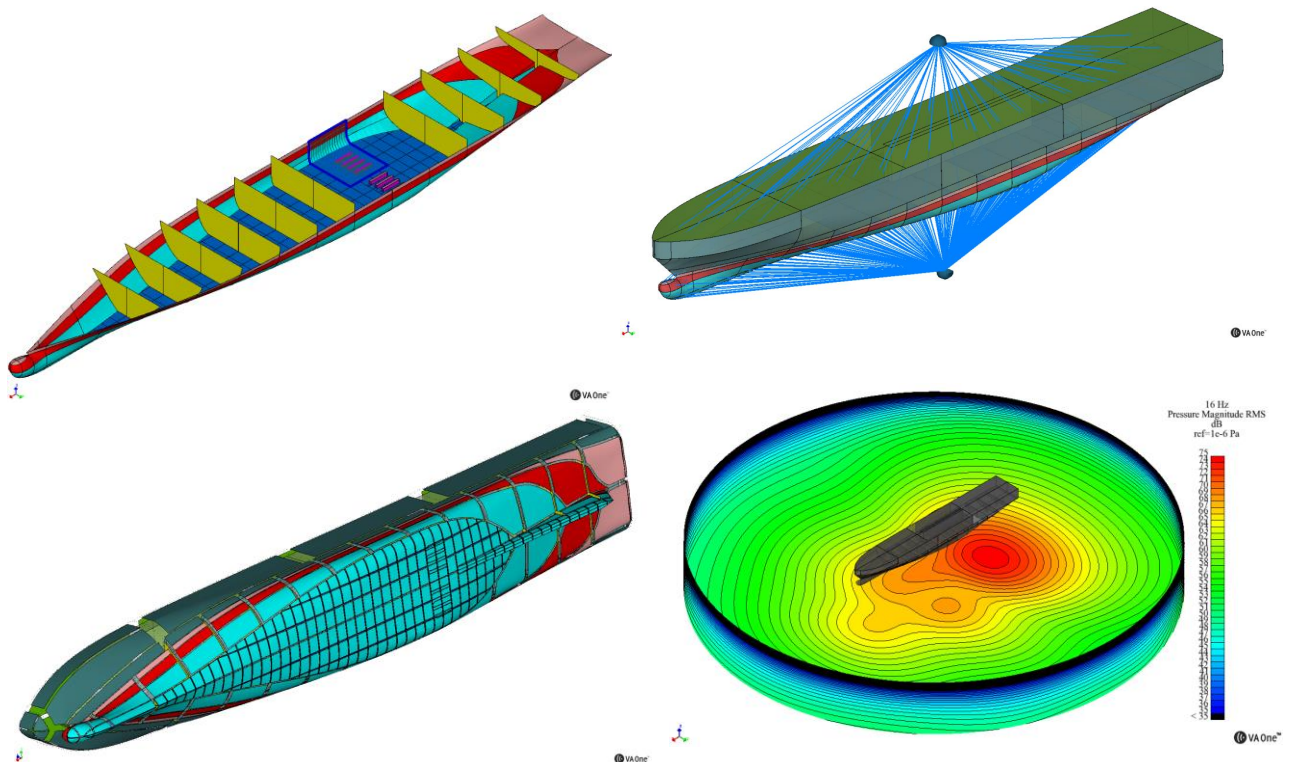
FIMECC/EFFIMA/SEEE/UNNO
Deliverable D.2.3

Simulation of underwater sound radiation from ship structures in full frequency range

Authors: Jukka Tanttari
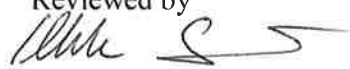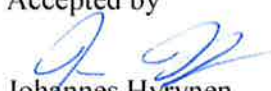
Confidentiality: Public

Report's title	
Unno - D.2.3 Simulation of underwater sound radiation from ship structures in full frequency range.	
Customer, contact person, address	**Order reference**
FIMECC Ltd / Tekes	
Project name	**Project number/Short**
Fimecc/Effima/2010/ISM – Unno	71112-1.4.2/Unno
Author(s)	**Pages**
Jukka Tanttari	76
Keywords	**Report identification code**
ship, underwater noise, SEA, FEM, BEM, modeling, prediction	VTT-R-00724-12

Summary

To goal was to review and demonstrate methods available for prediction of underwater sound radiation from large ship structures for full frequency (ca. 10...100000 Hz) range.

Background based on associated recommendations and standards was reviewed first. The frequency range dealt with is extensive, even from 1 Hz to 100 kHz.

Physical background and prediction methods available were reviewed next. Although most prediction methods are quite mature today, the sheer size of ships as well as extended frequency range makes the prediction task very demanding. There is a lack of reliable examples of prediction examples and correlation between experiments. Prediction of sound pressure in discrete points or a small area far from a ship is inherently subject to large uncertainty, even is totally isotropic unbounded conditions.

A small structure was the first example. The (ideal) low-frequency range extends up to ca 250 Hz and high-frequency range upwards from 2500 Hz. Point forces were used as excitation. The methods were used over whole possible frequency range. The most drastic finding is the remarkable effect of "Fluid Loading" option of VA One on sound radiation in SEA-models. It was concluded that SEA without "Fluid Loading" overestimates the radiation and a model with it underestimates. However, it is not wise to draw strict conclusions from a single example. This question that should be studied more.

A part of a 164 m long ship was then modelled. It was noticed that a standard "local" type FE model is not feasible to simulations at frequencies over 10 Hz. By modeling only the lower part of the ship with FE and the rest with SEA the upper frequency range could be raised up to ca. 25-30 Hz. To reach 100 Hz or more with a meaningful sized model, the FE part must be smaller. This was tried. A full SEA model was also created as well as a BEM model. The results again scatter quite much. It was also demonstrated how the SEA-prediction at low frequencies could be refined by using input power calculated using FEM.

An analyst must be aware of differences in methods. A SEA model does not account for global vibration fields, only "local" ones. HAJ formulations used between FE-structure and fluid used assume that the structure is baffled. Better approximation is obtained using BEM. SEA and FE-SEA models assume random excitations, whereas correlation effects can be taken into account in full FE. Radiation analysis using BEM is possible in both random and deterministic excitation cases.

This kind of modeling project is instructive. Much of the learned is in the form of tacit knowledge.

Confidentiality	Public

Tampere 25.6.2014

Written by	Reviewed by	Accepted by
Jukka Tanttari Principal Scientist	Ilkka Saisto Research Team Leader	Johannes Hyrynen Head of Research Area

VTT's contact address
P.O. Box 1300, FI-33101 Tampere Finland

Distribution (customer and VTT)
Customer 1 Copy   VTT 1 copy

Preface

This work was carried out between November 2012 and May 2014 under the framework of FIMECC SHOK programme EFFIMA project SEEE task UNNO (Underwater Noise).

Tampere 25.6.2014

Author

Contents

1 Introduction

The expansion of shipping and ships over the past 40 years correlates with the increase in ocean ambient noise levels. Thus ship underwater noise emission has become a crucial issue, especially in sensitive marine environments [1, 2, 3]. This has led to commendations for maximum underwater radiated noise levels produced by research vessels by the International Council for the Exploration of the Seas [4], see Figure 1 and Figure 2. The tendency is that noise emission will be more and more regulated in the future. The "source levels" (see below) are defined as 135-1.66 log(f_{Hz}) at 1...1000 Hz and as 130-22log(f_{kHz}) at 1...100 kHz. Frequency range in measurements is usually somewhat less [see 1 to 9], starting usually from 10...50 Hz partly because of limitations from background noise and partly because of procedures defined in measurement standards.
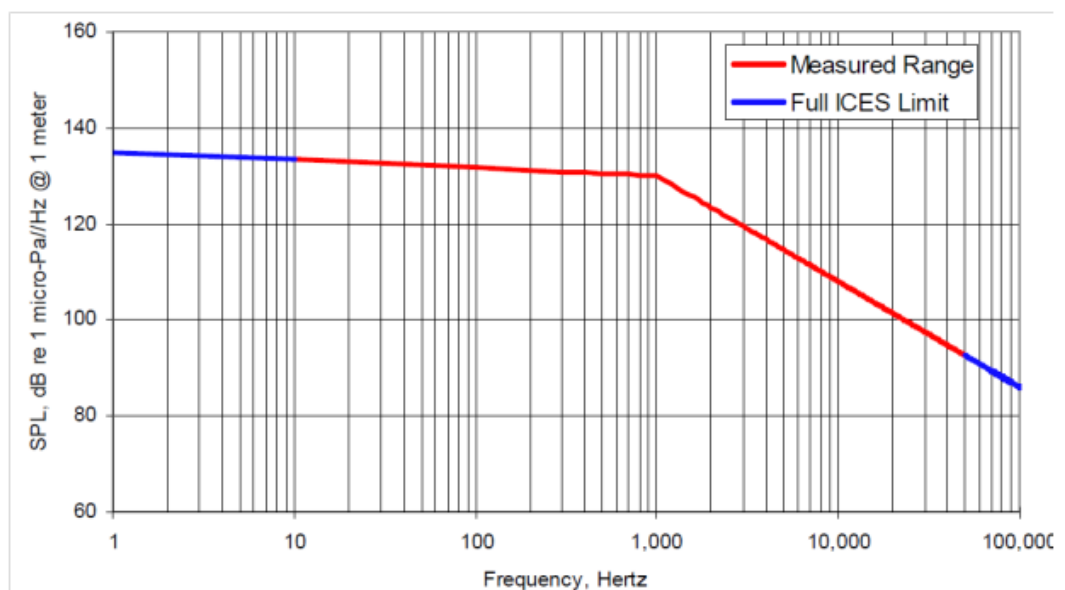
Figure 1. ICES curves defined as Power Spectral Density (PSD). Red part shows frequency range 10...50000 Hz. Taken from Bahtiarian [5].
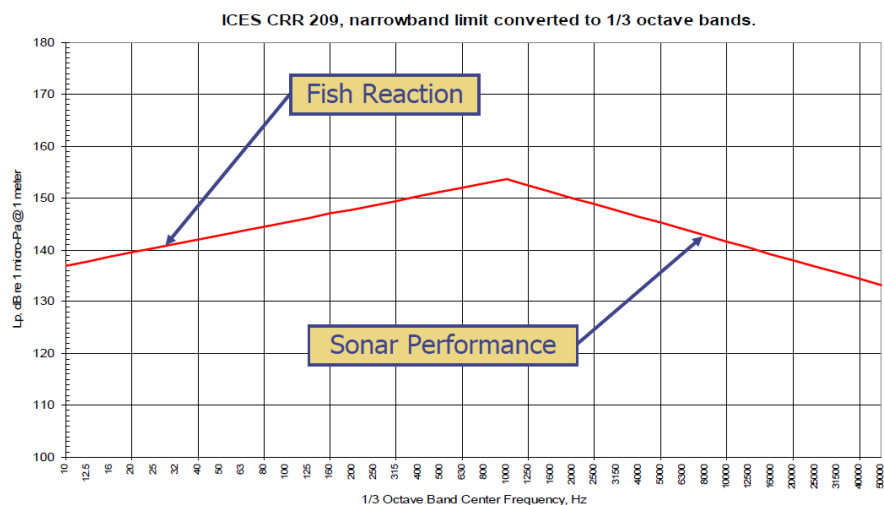
Figure 2. ICES curves defined as 1/3 octave limits. From Bahtiarian [5].

A measurement standard [7] has been published by the Acoustical Society of America (ASA). The emission called "source level" is expressed as sound pressure level normalized to 1 m distance from a fictional point source. Spherical spreading assumption -6dB per doubling of distance (1/r law for pressure, $1/r^2$ for intensity) is used in the normalization.

The measurements according to [7] are conducted during a pass-by in a period the acoustic center of the ship is between ±30° angle from horizontal line defined by Closest Point of Approach (*CPA*) and hydrophone location. Three hydrophones (for grade A or B) or a single one (for grade C) are used depending on "accuracy". Distance of the Closest Point of Approach (d_{CPA}) as well as the hydrophone positioning and water depths are tied to the ship length. If the length of a ship is 200 m, d_{CPA} = 200 m, hydrophone depths are 54, 115 and 200 m and minimum water depth is 600 m for grade A (Precision method). There is also another, somewhat different method from DNV, described in [8]. It is also based on "source level at 1m" principle. Ships speed etc. are described is the relevant documents [4, 8].
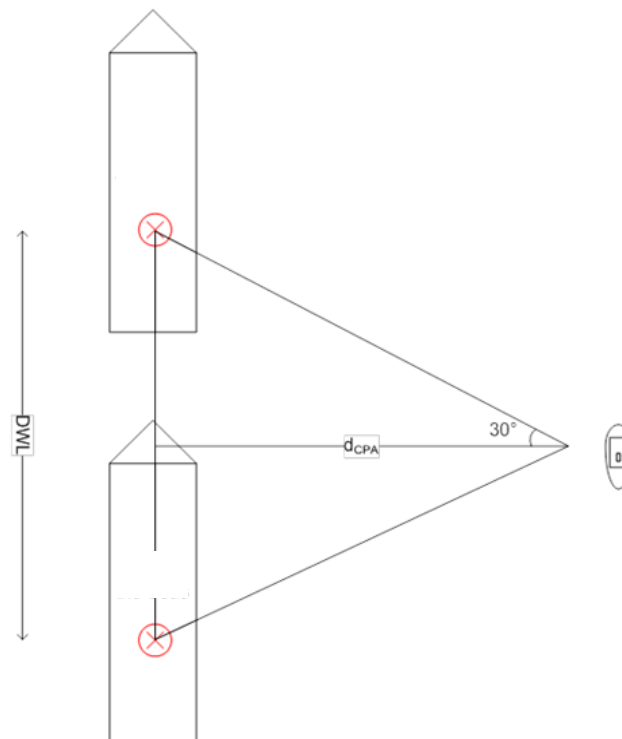
Figure 3. Measurement geometry in the ASA method. From Lankila [9].

There has been strong criticism against this kind of methods [10]:

- Attempts to characterize ship underwater noise *emission* by a single "source level" from measurements in few points in far-field is subject to large uncertainty
- Radiated noise is generally directional, due to the distribution of sources along the hull, scattering at the hull and reflections at the sea surface
- Different "source level" definitions may be required for different applications

Surface reflections easily induce up to 20 dB error between true and measured (i.e., back-calculated to the assumed source location) source levels of time-

harmonic point sources. See chapters 3.2 and 4.1. The possibilities to measure sound emission underwater are of course limited. However, in air acoustics an emission characterization like this would never be accepted.

A natural consequence of noise criteria is the question of noise prediction. Concerning civil vessels there are not many reports on calculation of emission at least throughout the frequency range using meaningful methods. (ICES recommendation is from 10 Hz to 100 kHz). All noise is treated as random and broadband, so that 1/3 octave measurements may be directly converged to Power Spectral Densities (PSD) by smearing the values over the frequency band. For periodic noise containing discrete frequencies this is not fully correct.
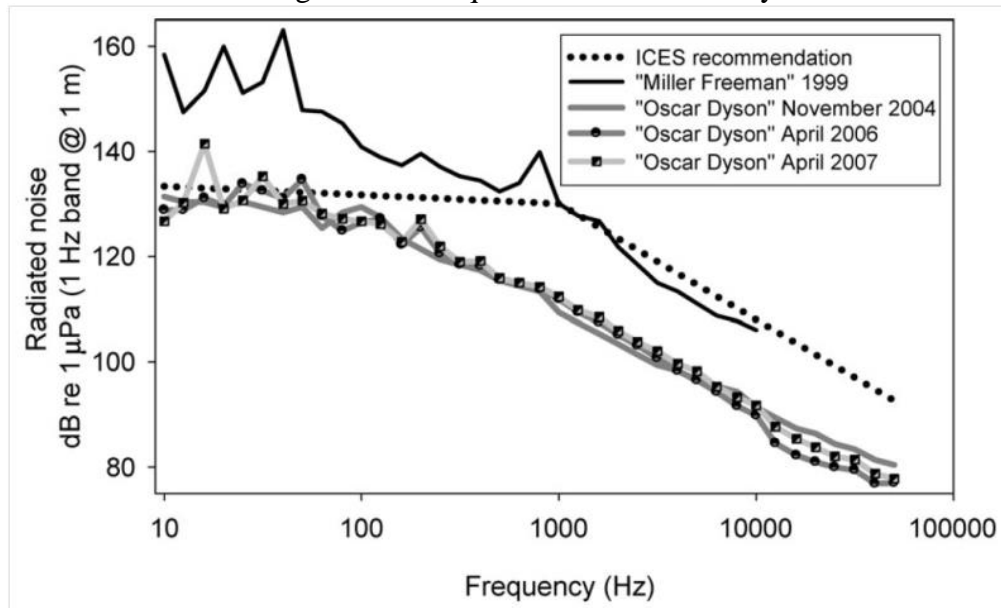
Figure 4. Some measurement results compared to ICES recommendation. From de Robertis et al [2].

Noise prediction in general, and especially in case of ships, is not easy. Ships are extensive structures. Simplifications and modeling automation are necessary. Structural details and especially source strengths may be unavailable or unknown. Different kinds of methods are needed at different frequency ranges.

Water is heavy fluid. Because of this, hydro-acoustic and structural vibration fields are strongly coupled and they must be solved simultaneously, at least at "low" frequencies. At "low" frequencies the wavelength of sound is large compared to the length scale of structural vibration patterns. This leads to highly reactive (mass type) radiation loading. Sound radiation to far field is weak but a strong reactive (non-propagating) near-field extending to tens of meters away from the ship may occur. This makes near-field measurements quite tedious and error prone.

Water surface is a pressure release boundary as "seen" from the water side. Sound pressure is very low and particle velocity high on the surface. An almost perfect reflection of sound takes place. The phase of sinusoidal sound component is reversed. All this may have a great influence on sound radiation from parts "near" the surface.

2   Goals

To goal is to review and demonstrate methods available for prediction of underwater sound radiation from large ship structures for full frequency (ca. 10...100000 Hz) range.

The main emphasis is on noise emission originating from on-board mechanical and acoustical sources. Direct hydrodynamic sound generation by propellers, wakes etc. is mostly out of the scope of this report.

3   Generation, radiation and quantification of ship underwater noise

3.1   General on noise generation and radiation

There is [11,12,13,14,15] a wealth of information about physics of underwater sound radiation, frequency ranges of different sources, as well as guidelines for vibration isolation and other elements of successful noise control. An example compendium of sources with their frequency ranges is in Figure 5.
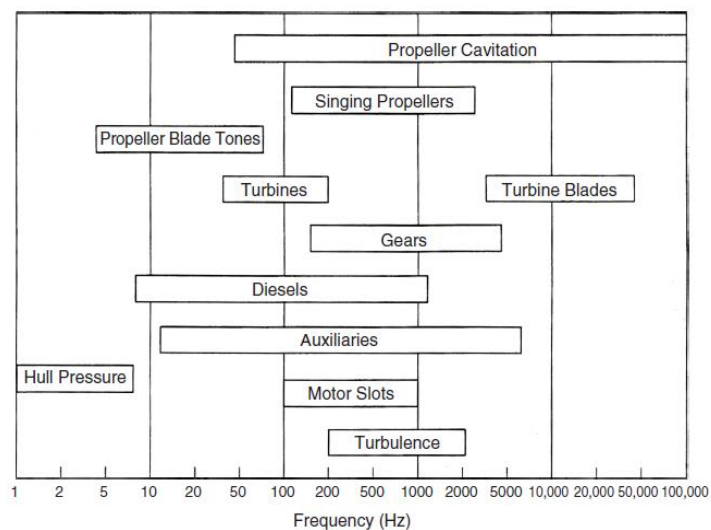
Figure 4   Frequency ranges of noise radiated by ship noise sources.[21] (From Ref. 18, Chapter 46, Fig. 3.)

Figure 5. Underwater radiation sources from Fischer&Collier [11].

An archetypal case of high-frequency underwater radiation originating from on-board mechanical source (gearbox) is shown in Figure 6.
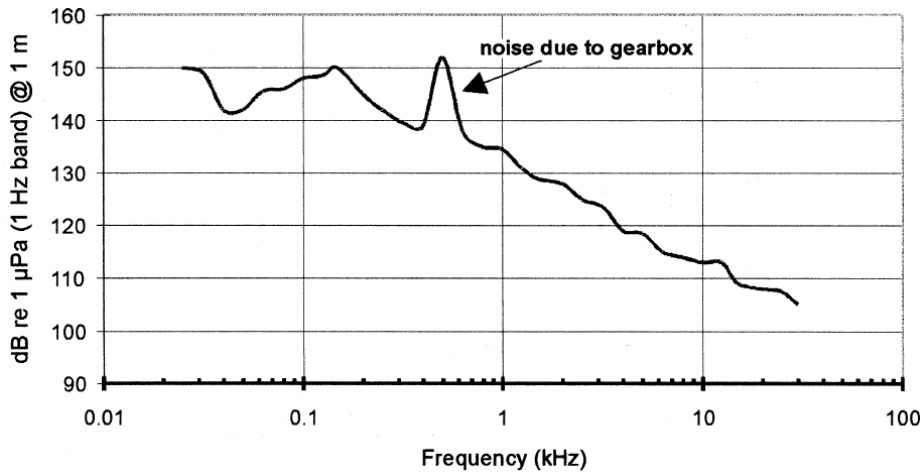
Figure 6. Gearbox whine seen in underwater noise signature. "Tridens", 11 knots. From Mitson [4].

In underwater ship acoustics, sound emission is not predicted in terms of sound power (as would be consistent to other areas of environmental noise and acoustics), but in terms of the somewhat peculiar "source level". A typical equation of traditional prediction methods is in the "first order estimation" formula below [11]:

$$L_S = L_v + 10\log\sigma_{Rad} + 10\log A_p + 10\log n + 73 \tag{1},$$

where L_S is the source level i.e., underwater sound pressure level in dB re 1μPa at 1m distance from a hypothetical point source, L_v is the space average vibration level in dB (re to reference value undocumented in [11]) at the hull plating, σ_{Rad} is radiation efficiency, A_p is the area of a single hull panel and n is the number of radiating panels. 73 dB is a constant needed to scale the equation correctly by taking into account the reference values of logarithmic terms.

In prediction purposes, there are some fundamental problems in the formula 1. It does not distinguish between hydrodynamic (reactive) or geometric near fields and geometric far field (see Figure 7). If σ_{Rad} represents the "real part" of radiation impedance, then L_S represents the geometric far-field pressure normalized to the 1 m distance. It is not the same value that is measured near the ship, where the reactive near field might dominate. Note also, that there is no guarantee that geometric far field with spherical spreading even exists in real underwater conditions.

Hydrodynamic Near Field | Geometric Near Field | Geometric Far Field

Vibrating body

$$\angle\left(\frac{\tilde{p}}{\tilde{u}}\right) \to \pi/2$$

$$\left|\frac{\tilde{p}}{\tilde{u}}\right| \ll \rho_0 c$$

$$I \neq p^2/\rho_0 c$$

I circulation

$$I \neq p^2/\rho_0 c$$

$$I \not\propto r^{-2}$$

I not radially directed

$$\angle\left(\frac{\tilde{p}}{\tilde{u}}\right) \to 0$$

$$\frac{\tilde{p}}{\tilde{u}} \to \rho_0 c$$

$$I = p^2/\rho_0 c \sim r^{-2}$$

I radially directed
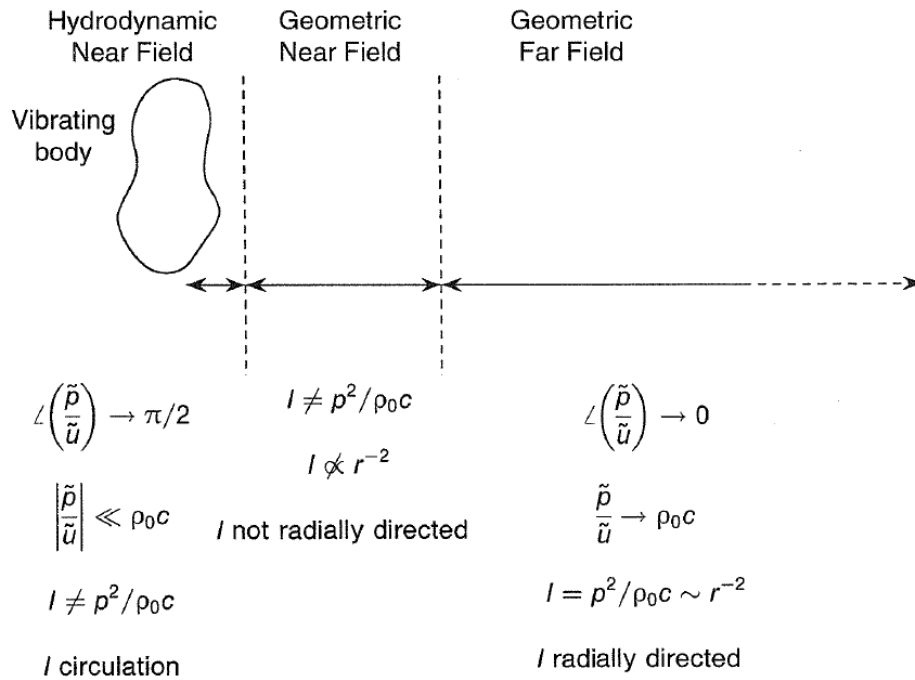
Figure 7. Acoustic near and far field of a vibrating body. From Fahy [16].

Another problem is the radiation efficiency. It is the normalized radiation resistance of a certain structure having a certain velocity distribution. It is a by-product from solve of sound radiation calculation, not a structural constant available a-priori. Of course, rough empirical values might be useful. Anyway, the equation should be seen more a scaling formula than a prediction equation.

Vibration velocity level is greatly influenced by the fluid loading. The fluid loading is often expressed in terms of added mass. The amount of added mass is a function of frequency and it can be extracted from the radiation impedance matrix governing the discretized radiation problem. The radiation impedance matrix is a product of solving the radiation problem, so L_v and σ_{Rad} are, in principle, not available without solving the radiation problem in the same time when solving the vibration problem.

The complexity of the source-transmission-radiation problem is illustrated in Figure 8. The engine emits structural energy into the foundation and acoustic energy into the machine room. The structure-borne path caused by the interior acoustic field is called here the 2nd Structure-borne Path. Noise generation is reviewed in more detail by Uosukainen [17].
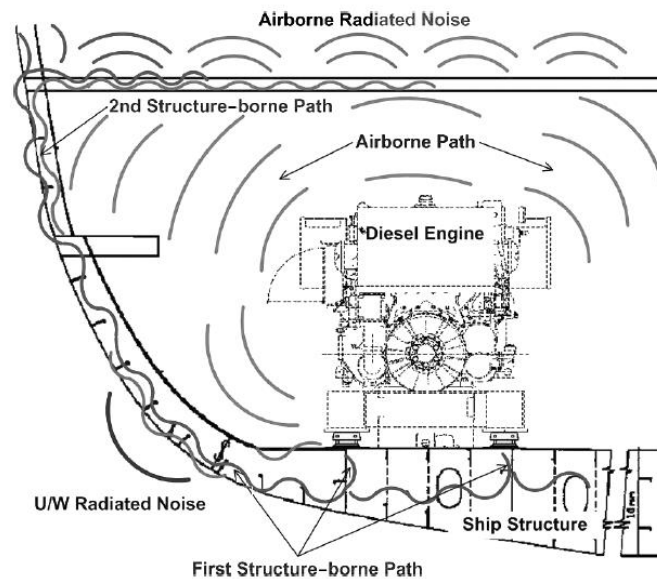
Figure 1 Source/path acoustical model.

Figure 8. Vibro-acoustic propagation paths in a ship. From Fischer&Collier [11].

3.2 Surface reflection - Lloyd's mirror effect

A nearly perfect phase-reversing reflection called the Lloyd's mirror effect takes place on a free, calm water-air surface [18,19,20]. As seen from water side, sound pressure at the surface is very low, almost zero, and particle velocity is high. An example of sound pressure as function of distance is shown in Figure 9.
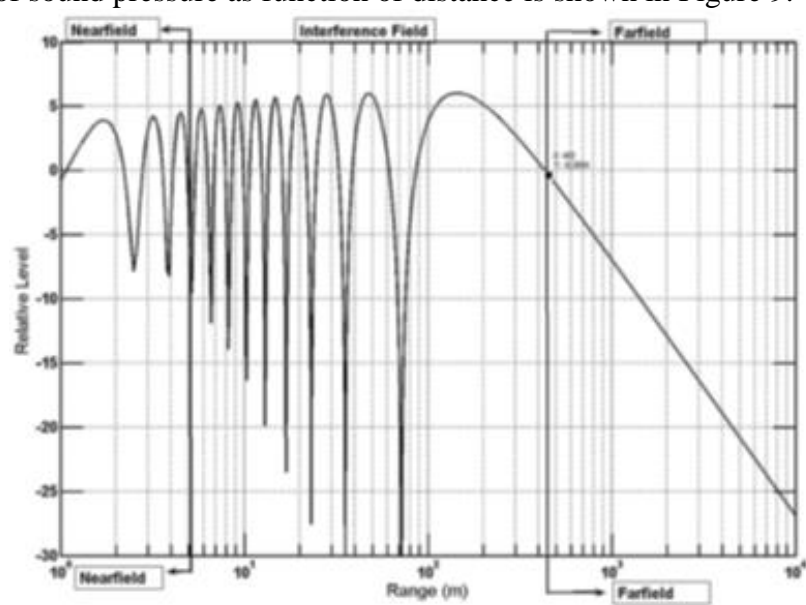
Figure 9. Interference pattern for a 5 kHz point source located 6 wavelengths (1.8 m) from water-air surface. Receiver depth is 20 wavelengths (6 m). Spherical spreading corresponds to 0 dB, so in far field the spreading loss is more than 6 dB per doubling of distance. From Carey [20].

Sound field produced by a monopole in unbounded water and 6 meters below water-air surface is shown in Figure 10. On left, the surface is not taken into account. On right, the surface is a pressure-release boundary. From the lower right plot of Figure 10 it is easy to understand, why single-point underwater

measurement results in emission characterization especially in case of narrow-band sources is problematic. Also note the pressure minimum on the surface.

Influence of bottom reflections may be almost anything, depending on bottom acoustic characteristics. In shallow waters, sound apparently propagates in a 2-dimensional channel formed by the surface and bottom. In deep waters, and large distances, the dependency of speed of sound on hydrostatic pressure and temperature has remarkable tunnelling effects on sound propagation. These effects are usually not taken into account in predictions.
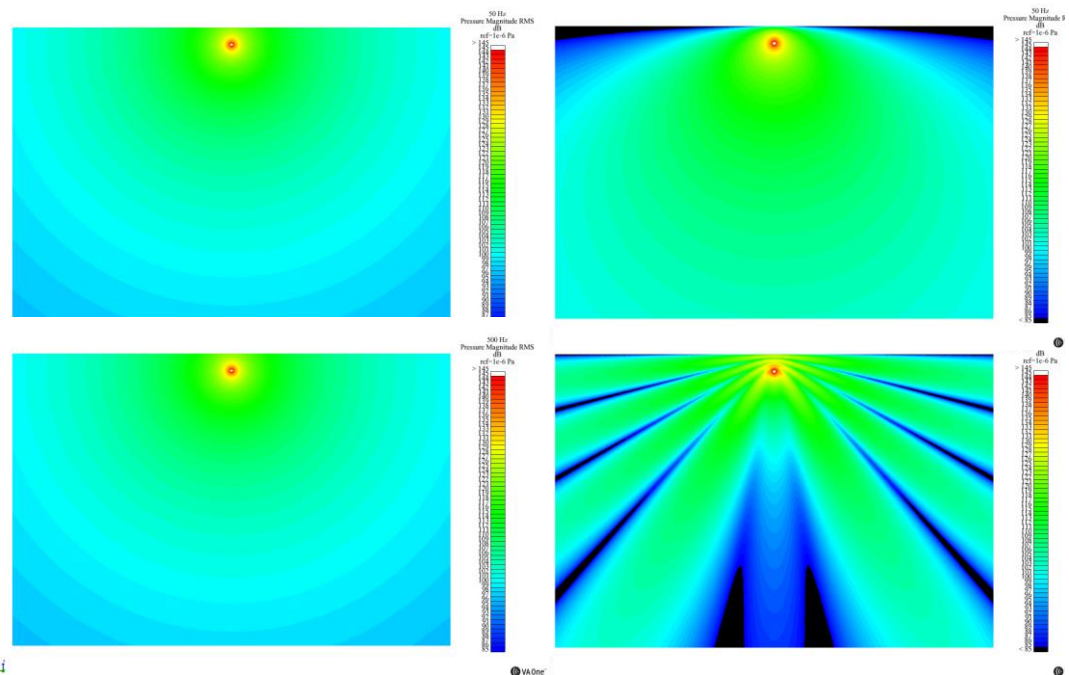
Figure 10. Calculated pressure field of a monopole source (at x=0, y=0, z= -6m) in water. Left: pressure field at xy-plane, unbounded water. Right: pressure field at xy-plane, water-air surface at z = 0 m. Frequencies are 50 Hz (upper) and 500 Hz (lower) and the scale 85…145 dB re 1µPa. The monopole strength, expressed in free field rms pressure, is 100 Pa (160 dB) at 1/4π meters. Plotted area is 75 m horizontally and 50 m vertically.

3.3   Radiation loading (fluid loading)

A vibrating structure generates forces (pressure field) to surrounding fluid at the structure-fluid contact interface. In return, fluid exerts forces on structure. These reaction forces (pressure fields) may have a significant effect on magnitudes and eigenfrequencies of structural vibration. This is indeed the case with the part of a ship hull loaded ("wetted") with water.

When fluid (water) is unbounded, the water loading is "seen" mainly as inertia (added mass, entrained mass) by the structure at low frequencies [21, 22]. When frequency is increased, the character of loading changes from inertial to resistive, indicating efficient radiation of sound power to the far field. The exact transition is largely dependent on the spatial shape of vibration and size of the structure. Low order modes with large net volume displacements have the highest added masses.

An example of added mass (inertial fluid loading) and apparent viscous damping coefficient (resistive fluid loading) of 1,1- and 1,3-modes of a vibrating, baffled 3.0 x 1.75 m panel (see Figure 11) is shown in Figure 12 and Figure 13. The added masses were calculated from the dynamic equation of the radiating plate yielding the imaginary part of radiation loading.

At low frequencies the added mass of the 1,1 –mode is equivalent to 1 meter thick layer of water on the structure. The added mass of 1,3 –mode is considerably less. There is a drastic drop in added mass as frequency is increased. The critical value corresponds to frequency at which characteristic structural wavelength is about ½ of the acoustic wavelength. These frequencies correspond to ca. 220 Hz and 750 Hz with 1,1- and 1,3- modes respectively. Transition from inefficient to efficient power radiation corresponds roughly to the same frequency range.
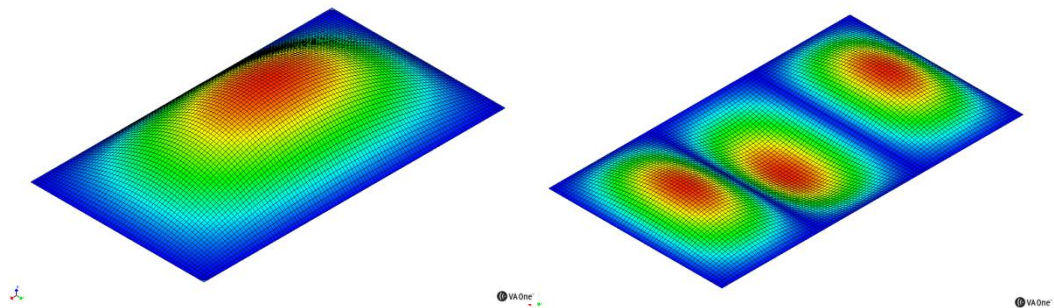
Figure 11. 1,1- and 1,3, modes of an example plate with dimensions 3.0 x 1.75 m.

It is customary to present the fluid loading as normalized radiation impedance (radiation impedance is basically effective force seen by the structure divided by average or generalized velocity of a surface), called the radiation ratio, σ_{Rad}. Radiation ratio has a real part corresponding to resistive loading and imaginary part corresponding to inertial loading. Radiation ratio is basically a radiation load ratio: load Z_{Rad} "seen" by the actual ratio divided by the real resistive "seen" by a same area S from of a hypothetical infinite planar piston radiator:

$$\sigma_{Rad} = \frac{Z_{Rad}}{\rho_0 c_0 S} \qquad (2).$$

Complex sound power W_{Rad} defined using the radiation ratio is

$$W_{Rad} = \rho_0 c_0 \sigma_{Rad} S \langle v^2 \rangle \qquad (3),$$

where $\langle v^2 \rangle$ is the spatial average of squared vibration velocity. Real and imaginary parts of the radiation ratio are shown in Figure 14. Imaginary parts (mass) dominate at low frequencies, real parts at high frequencies.

Figure 12. Added mass of 1,1- and 1,3, modes of the example plate with one side wetted with sea water.
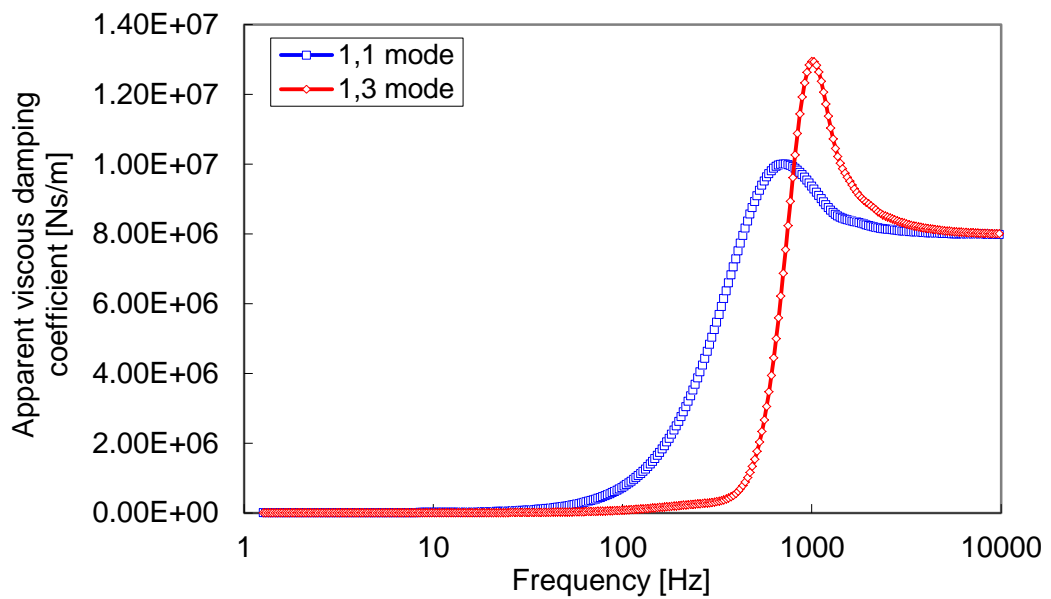
Figure 13. Apparent viscous damping coefficient of 1,1- and 1,3, modes of the example plate with one side wetted with sea water.
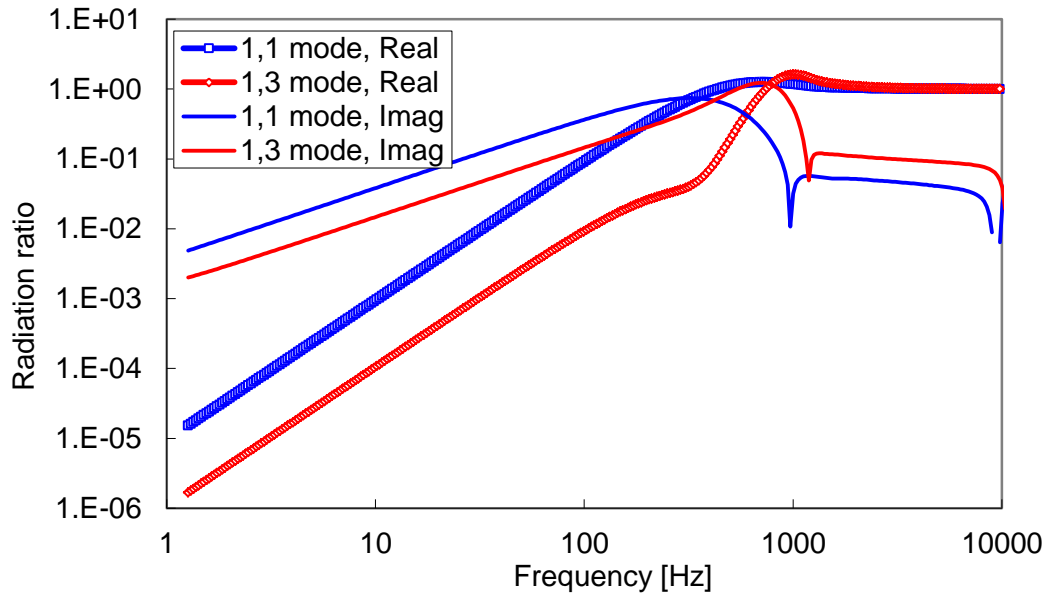
Figure 14. Real and imaginary radiation ratios of 1,1- and 1,3, modes of a plate with one side wetted with sea water.

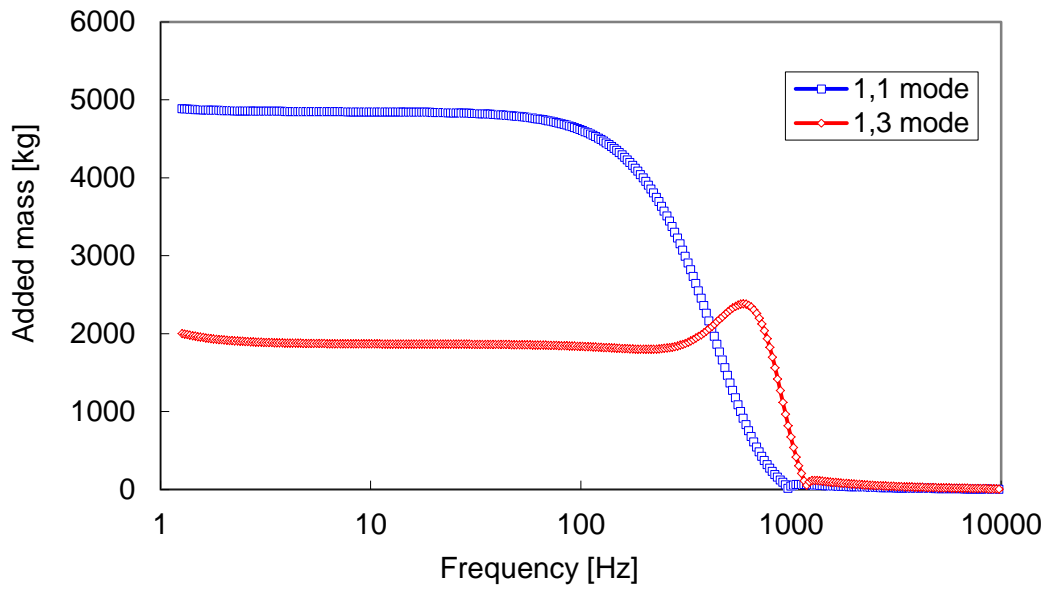Simple approximate formulas for added mass are presented in many textbooks. According to [21, 4.57], the low-frequency added mass (per unit area) of a mode may be approximated from

$$m_e \approx \frac{\rho_0}{k_m} \qquad (4),$$

where k_m is the structural wavenumber of the mode. This equation gives ca. 2600 kilograms for mode 1,1 and 1500 kg for mode 1,3, i.e., quite reasonable estimates compared to values calculated using the numerical model. The equation is known to underestimate added masses of low-order modes [21].

The most general way to get the added mass is to solve for the coupled equations for fluid-structure interaction (i.e., radiation) and analyze either the behaviour of the imaginary part of the radiation impedance matrix of the structure.

The main point here is that added masses per unit area at low frequencies may be huge compared to the area mass of structure. Consequently, sound power is dominantly imaginary, meaning the energy sloshing front and back between the structure and the fluid. The apparent damping of the structure may be smaller than that of in-vacuo structure. As frequency is increased, the onset of efficient active (real) power radiation may be quite rapid and increase of apparent damping significant.

4 Prediction methods

4.1 Prediction strategies, quantities and model validation

Emission of underwater noise might be quantified using, e.g.,

1. Sound pressure in specific point(s),
2. Average sound pressure at specific distance,
3. Sound pressure ("source level"), i.e., sound pressure measured in the geometric far field and back-propagated using some spreading assumption to a distance of 1 m from a hypothetical point source and
4. Sound power

"Sound pressure" and "sound power" usually mean absolute values or the associated levels in a proper dB-scale. In air acoustics, sound power is the principal quantity used in characterization of noise emission of machinery and equipment. It includes all acoustic energy propagating to environment through a defined *closed surface around the source*. Thus it is a very robust quantity. In underwater acoustics, it is possible to calculate sound power, but it is very tedious to measure it, because of practical limitations coming from instrumentation, acoustic environment, ship movements, etc.

As discussed above in chapter 1, the current state-of-art is to evaluate the theoretical point-source sound pressure at 1 m distance ("source level") from far field measurements carried out using 1 to 3 hydrophones in deep water or "fjord" bottom [7, 8]. It is not possible to directly validate this hypothetical source level because

1. Ship is not a point source (and if it were, the point would be inside the ship) and
2. Underwater propagation does not necessarily follow 1/r –law (i.e., 6dB per doubling of distance). Due to various effects, spreading loss might be different. When the measurement distance from the source is large, the normalization using the 1/r-law is a potential source of large errors.

The frequency range covered is one critical issue. In good conditions it is possible to measure from 10 to 50000 Hz, or even more, using hydrophones. It is also possible to cover this range with vibro-acoustic calculations using different techniques at different frequency ranges. However, it is difficult to evaluate onboard or propeller source strengths throughout this frequency range.

Another important issue is frequency resolution. Source strengths, transfer functions and thus pressures in the sound field are functions of frequency. If the resolution is not consistent for all quantities, predictions and comparisons might be difficult or even impossible. It is usually possible to change all narrow band data to 1/3 octave resolution. But, if data is only in 1/1- or 1/3-octave form, it is not possible to use it with confidence in narrow band calculations.

4.2   Information, uncertainty, complexity and frequency ranges

To better understand different modeling techniques, it is worth to think about structural and acoustic wave-fields in terms of wavelengths compared to typical dimensions.

In the range of "low frequencies", all components in a system are small compared to wavelength. In terms of modal description of wave-fields, the response of the system involves a small number of modes. At "high frequencies", all components in a system are large compared to wavelength and the response involves a large number of modes. In the "mid-frequency range" some components are small and some components are large compared with a wavelength. While the term "frequency" is usually used, the classification is more closely related to the dynamic complexity of a system [23].

The amount of information needed to predict and describe the exact system response increases rapidly with frequency. In the high-frequency range, amount of information needed to exactly describe the response is vast. Just think if the ship in chapter 6 should be modelled in every last detail. Proper prediction requires that the amount of input information is consistent with the amount of output information. One can view this as conservation of information [23].

In practice, there is limited information available. The lack may be because of the precision to which structural properties of the system are known. The system may also be still at the design stage and the details are just not ready. This may be reviewed as "uncertainty" in the properties of a system. Note that at high frequencies the wavelength scale is in the same order than uncertainties. Also note that decrease of element size or increase of element order does not provide any new input information about the system.

An example of ensemble statistics of a system is given in Figure 15. Response curves of uncertain (perturbed) individuals vary considerable, while ensemble average curve provides a meaningful estimate about the probable behaviour of the system. It is the probable behaviour the statistical calculation methods search for.
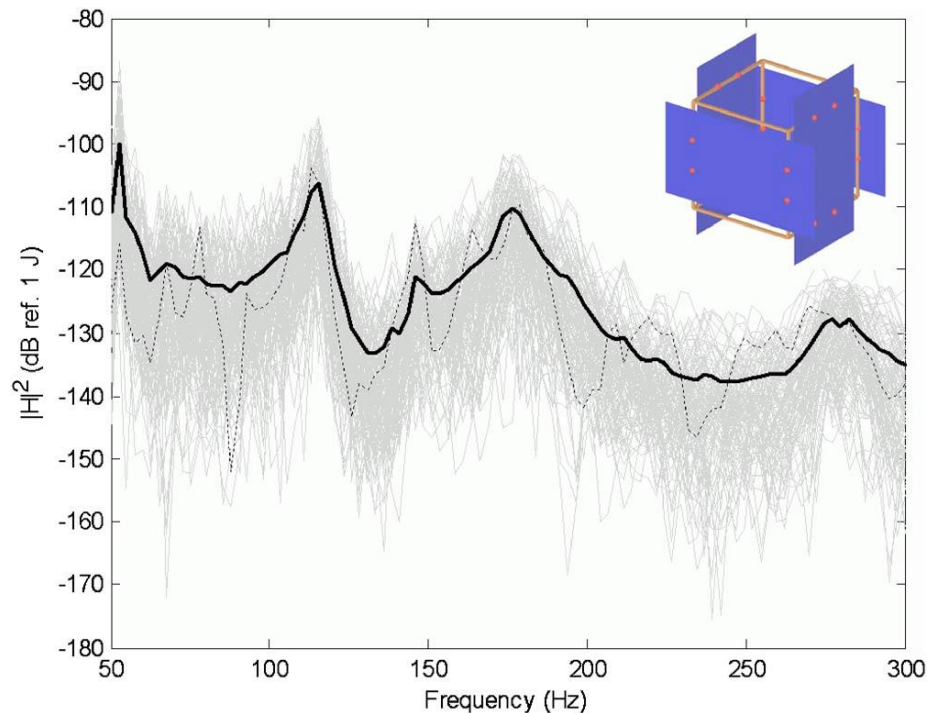
Figure 15. Response functions of a point force excited frame-plate system. Grey curves: 200 slightly perturbed systems; dotted: one particular realization of the system; thick black: ensemble average of the random population. From Cotoni et. al. [24].

Thus, methods making use of all available information of the system but *do not demand to fabricate uncertain details* are the most useful to an analyst. In the low frequency range the needed information is usually available and deterministic approach is feasible. In the high-frequency range the systems usually have significant amount of uncertainty and statistical methods are feasible. In the mid-frequency range not all components are "complex" and an assumption of significant uncertainty in the subsystem properties is not necessarily appropriate for all subsystems. A natural question is then, if these methods (deterministic and statistical) be combined in a meaningful way, so that all available information of a system may be utilized.

4.3 Low-frequency methods

Analytical solutions to vibration or acoustic problems rarely exist. Instead, Finite element (FEM) and Boundary Elements Method (BEM) are used to yield approximate solutions to the associated partial differential (FEM) or boundary integral equations (BEM) in defined spatial domains. FEM is generally used to solve both mechanical vibration and acoustic fields in closed domains, while application of BEM is relatively acoustics and sound radiation oriented. BEM is commonly used as a second step procedure using FEM-calculated vibration fields as input. Semi-infinite elements are also used to model extended fluid regions when using FEM.

Domains are discretized, matrix equations developed and then solved with appropriate boundary conditions and excitations. These methods may be described deterministic in the sense that equations are solved for solutions in discrete points. This, to be meaningful, requires precise (deterministic) description of the system

in the domain and its boundary conditions. Methods are well established [21, 25] and not repeated here.

In ship acoustics, the feasible upper limit of FEM/BEM is somewhere around 5...100 Hz depending on the size of the vessel [26, 27]. The limit is governed both by the computer capacity and knowledge or description of structural details. Examples of FE- and BEM-models of ships are in Figure 16 and Figure 17.

Node ID	Uncoupled (Hz)	Coupled (Hz)	Damping (-)
1	6.2	5.2	0.034
2	7.4	5.9	0.049
3	7.7	6.9	0.015
4	9.5	7.4	0.010
5	11.0	7.5	0.010
6	12.0	7.8	0.015
7	12.2	7.9	0.011
8	12.3	8.2	0.011
9	12.8	8.3	0.016
10	13.1	9.2	0.021
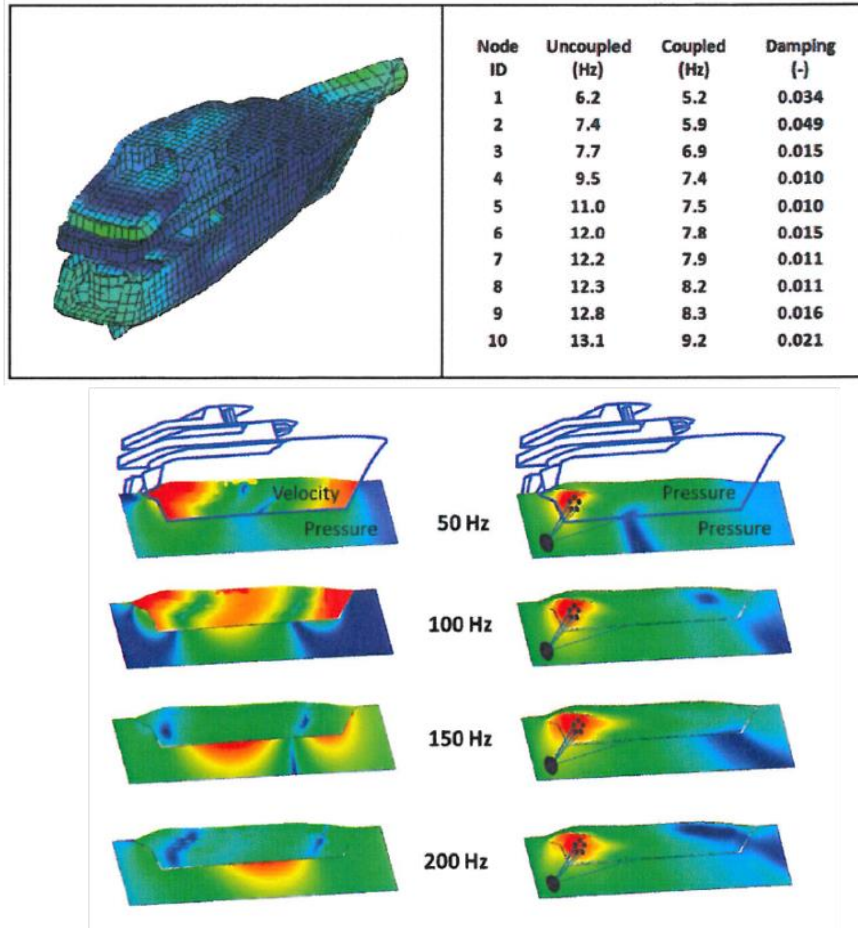
Figure 16. Structural vibration using FEM and underwater radiation from structural vibration and propeller using BEM. Length of the ship is ca. 70 m. From Blanchet & Caillet [27].
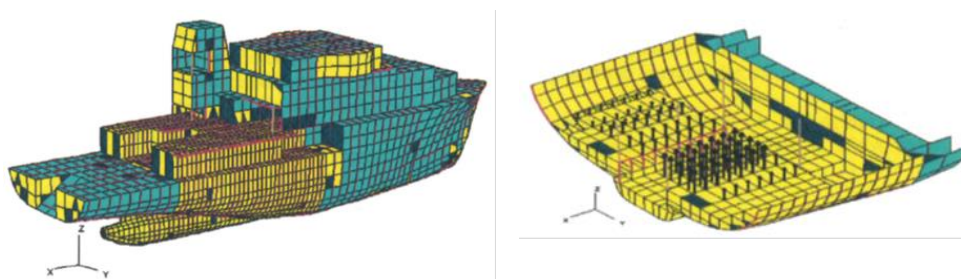

Figure 17. Ship FEM model used in BEM-prediction of underwater radiation from machinery excitation. Length of the ship is 58 m. From Gilroy [26].

Commercial software utilizing FEM/BEM include Actran, Virtual.Lab and VA One, to mention a few [45, 46, 47].

The BEM may be used in two main ways:

1) Direct use of standard BEM: The FE structural vibration and acoustic field in BEM fluid are solved in one step in coupled fashion. This is a very time and computer resource consuming operation. Practical upper limit for BEM mesh is ca. 20000 nodes unless extensive computational resources are available.

2) Two-step solution [28]:
   a. The structural vibration of the coupled system is solved using "HAJ" formulation [52], i.e., radiation loading is solved using a special Wavelet-based numerical technique based on Rayleigh integral.
   b. The structure is changed to a "forced response" type and acoustic field is solved, as a second step, using FMM BEM. The advantage of this procedure is that up to one or two million nodes in BEM mesh is still feasible. Large area of the bottom for example may be described. The assumption is that the bottom etc. has no effect on structural vibration, i.e., HAJ-formulation yields correct structural responses.
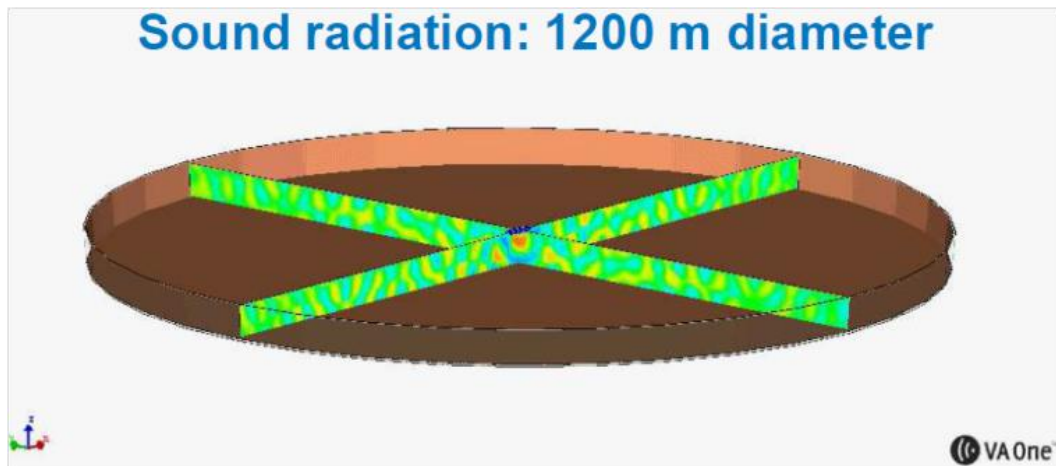

Figure 18. Sound radiation in domain of 1200 meters diameter at 40 Hz in shallow water using FMM BEM. From Blanchet [28].

4.4　Statistical energy analysis

Statistical Energy Analysis (SEA) is a method working best at high frequencies and with random, distributed excitations. In SEA, statistical descriptions of system components are employed in order to simplify the analysis of complicated vibro-acoustic problems [23, 29]. SEA is often viewed as being a method for describing the storage and transfer of vibrational and acoustic energy between subsystems of "weakly" coupled modes. The energy storage capacity of a given subsystem is described by a parameter termed the modal density; the coupling between subsystems is described by parameters termed coupling loss factors (CLFs). Mean (expected) values of responses are solved for. Responses are averaged over subsystem domains, frequencies and, to be strict, population of systems with uncertainties.

Conservation of energy (Power-energy balance of "reverberant" vibrational energy) is applied to each subsystem (equation 5). This results in a set of simple linear simultaneous equations (equation 6) for the expected (mean) values of subsystem energies. For subsystem j the power balance equation is

$$\omega \eta_j E_j + \sum_k \omega \eta_{jk}\, n_j \left[\frac{E_j}{n_j} - \frac{E_k}{n_k} \right] = P_j \tag{5},$$

where ω is mean radian frequency, η_j is total loss factor of subsystem j, E_j is energy in subsystem j, η_{jk} is coupling loss factor from subsystem j to subsystem k, n_j is modal density in subsystem j and P_j is external input power to subsystem j. For a system of n subsystems the set of equations is usually written

$$\omega [C]\{E\} = \{P\} \tag{6},$$

where $[C]$ is the system matrix containing loss- and coupling loss factors. The matrix formulation may be either symmetric (solved for energy per modal density E_i/n_i) or non-symmetric (solved for total energy E_i).

From the wave point of view, a subsystem is represented as a collection of propagating waves. The energy storage capacity of a given subsystem is related to the expected group velocity and dimension of the subsystem. The coupling loss factors at a given junction are found by calculating the local transmission of energy into the 'direct fields' of a number of receiving subsystems, due to the presence of a 'diffuse reverberant field' in an excited subsystem.

Note that a SEA model represents a random system, i.e. population of nominally similar systems having uncertain (not exactly known) properties. The justification for this is that vibro-acoustic responses of any group if "identical" structures or products show large scatter at high frequencies. This is due to small, unpredictable differences in geometry, material properties, boundary conditions etc. uncertainties which have the same length scale as wavelength and thus have a great influence on the details of response.

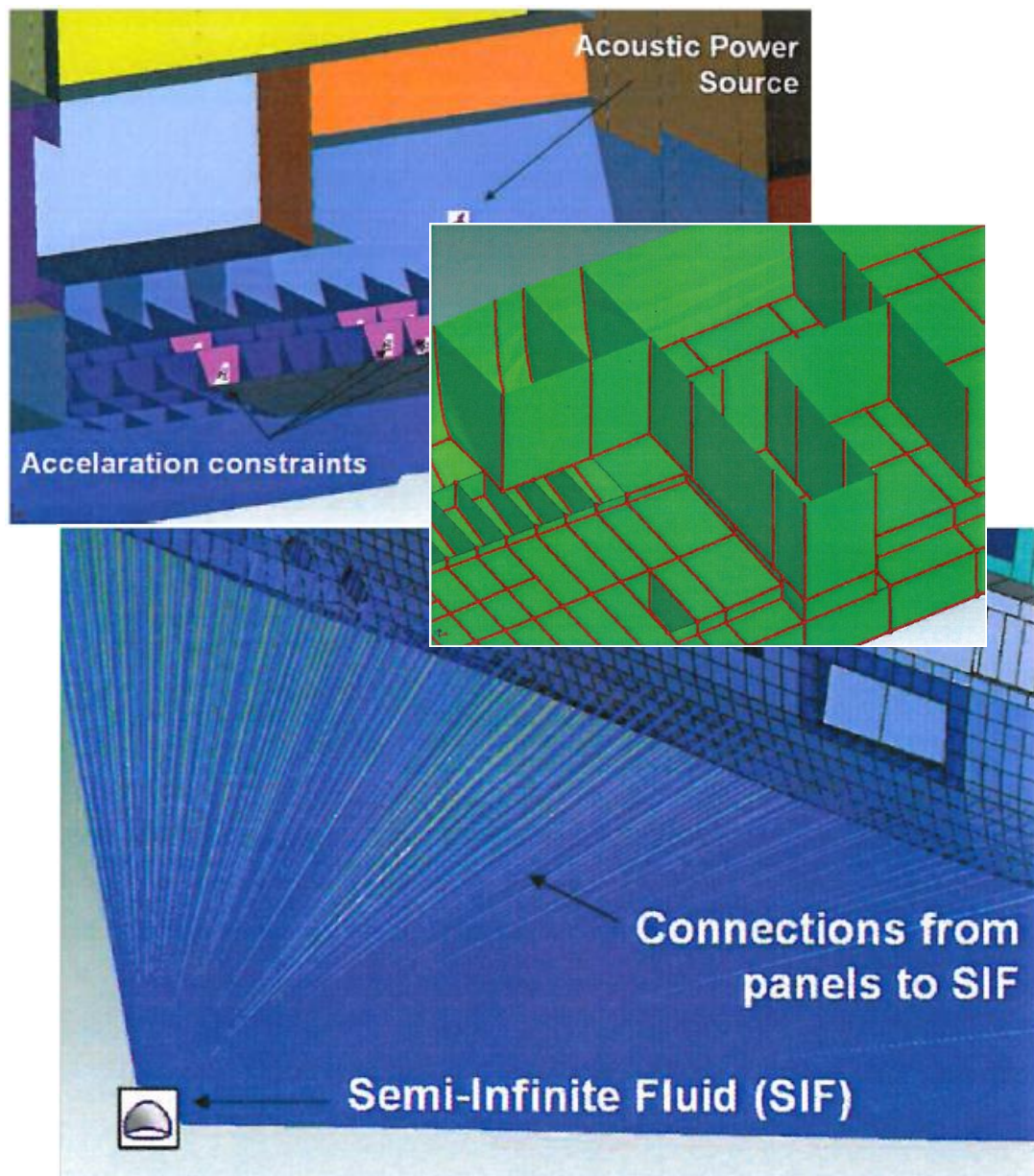Some examples of a ship SEA model building is shown in Figure 19.

Figure 19. Details of a ship SEA model. From Blanchet & Matla [30].

Commercial SEA-programs include VA One by ESI Group, SEAM by Cambridge Collaborative and SEA+ (Virtual.Lab) by LMS (Originally by InterAC) and Designer-Noise by Noise Control Engineering, Inc. [47, 48, 49, 50]. Numerous in-house codes exist as well.

4.5 The hybrid FE-SEA method

In most practical situations the analyst is interested to simulate acoustics on a wide frequency range (compare to full ICES recommendation limits 1…100000 Hz). In the lower end of this range, a deterministic model might be feasible and in the higher end a purely statistical model might work quite well. However, there is an inevitable frequency range in which some parts of the system are complex and thus good candidates for SEA subsystems while some other parts show long wavelength "deterministic" behavior.

Main equations and procedures of the hybrid FE-SEA method are presented below. This is because the method is still rather new and still unknown. Complete description may be found from references [32, 33]. Analysis consists of the following phases:

1) FE models of the deterministic subsystems ("master system") are created. Models of the SEA subsystems are created as well. Degrees of freedom q of the FE-part may belong to a larger structure (q_1) or just to a local junction (q_2) between two SEA-subsystems see Figure 20.
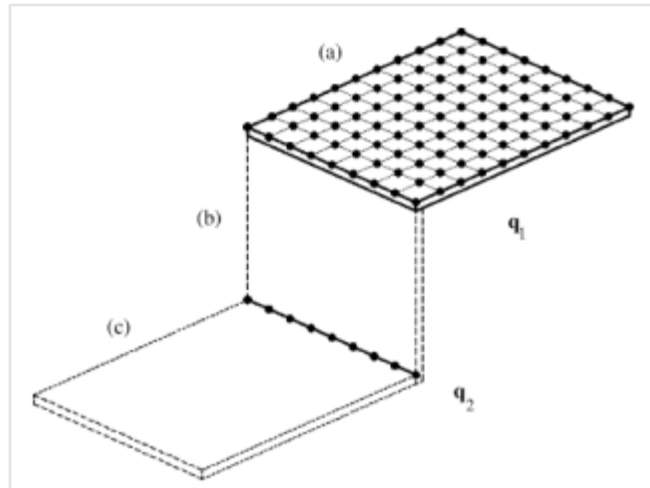

Figure 20. FE-SEA -model. (a) is a FE-subsystem, (b) and (c) are SEA-subsystems. From Shorter and Langley [32].

2) FE- and SEA-subsystems are coupled together. The assembled dynamic matrix equation of the FE-subsystem is

$$D_{tot}q = f_{ext} + \sum f_{rev} \tag{7},$$

where f_{ext} is external load (force) vector and f_{rev} is the reverberant random load vector arising from the SEA subsystem response. Dynamic stiffness matrix D_{tot} is composed of the part associated with the FE-subsystem, D_d, and the part associated with the dynamic stiffness of the direct field of the k SEA subsystems "seen" by the FE subsystem, D_{dir}:

$$D_{tot} = D_d + \sum_k D_{dir}^{(k)} \tag{8}.$$

The dynamic stiffness matrix of the direct field is utilized in calculation of power transfer from FE subsystem coupled to the SEA subsystems.

3) The power balance equation for the SEA subsystem j is

$$\omega\left(\eta_j + \eta_{d,j}\right)E_j + \sum_k \omega\eta_{jk}n_j\left[\frac{E_j}{n_j} - \frac{E_k}{n_k}\right] = P_{in,j} + P_{in,j,ext} \tag{9},$$

where ω is angular frequency, E is vibration energy, η_j and $\eta_{d,j}$ are loss factors for dissipation respectively in the SEA and FE subsystems, η_{jk} is coupling loss factor, n_j is modal density and $P_{in,j,ext}$ is power injected from the FE-subsystem. $\eta_{d,j}$ is a

new term compared the classical SEA formulation. SEA parameters $\eta_{d,j}$ (damping loss factor of FE-subsystems "seen" from SEA-subsystem) and $\eta_{jk}\,n_j$ (coupling loss factors between SEA subsystems) are calculated using the FE model. For details see [32].

Input power from FE subsystem to SEA-subsystem j is calculated from

$$P_{in,j,ext} = \left(\tfrac{\omega}{2}\right) \sum_{rs} Im\left\{D_{dir,rs}^{(j)}\right\}\left(D_{tot}^{-1}\, S_{ff}\, D_{tot}^{-1*T}\right)_{rs} \qquad (10),$$

where S_{ff} is the autospectrum of FE subsystem external excitation and rs is the row-column -index of the dynamic stiffness matrix.

4) Responses of SEA-subsystems are calculated using equation (9). Power inputs from other sources other than FE-subsystem added to the right-hand side. Response of the FE-subsystem is then calculated using

$$S_{qq} = D_{tot}^{-1}\left[S_{ff} + \sum_k \left(\frac{4E_k}{\omega \pi n_k}\right) Im\left\{D_{dir}^{(k)}\right\}\right] D_{tot}^{-1*T} \qquad (11),$$

where S_{qq} is the autospectrum of the displacement of degree of freedom q. The second term inside parentheses includes reverberant excitation forces from SEA-subsystems, described using the diffuse field reciprocity relation between the resistive part of the direct field dynamic stiffness and reverberant random loading. The reciprocity relation is the key in coupling SEA to deterministic analysis methods like the finite element method.

The main equations 9 and 11 are coupled: SEA input power depends on response of FE-part and Response of FE-part depends on energy in SEA part. Direct field dynamic stiffness of SEA subsystems is seen in the dynamic stiffness matrix of the FE subsystem, equation 8. The load term including reverberant response E_k expresses the vital reciprocal relation between reverberant random loading f_{rev} and direct field stiffness D_{dir}.

A chart of power flow in a SEA subsystem is depicted in Figure 21. A deterministic boundary separates the SEA and FE subsystems. The somewhat abstract random boundary is the formal cause of uncertainty.
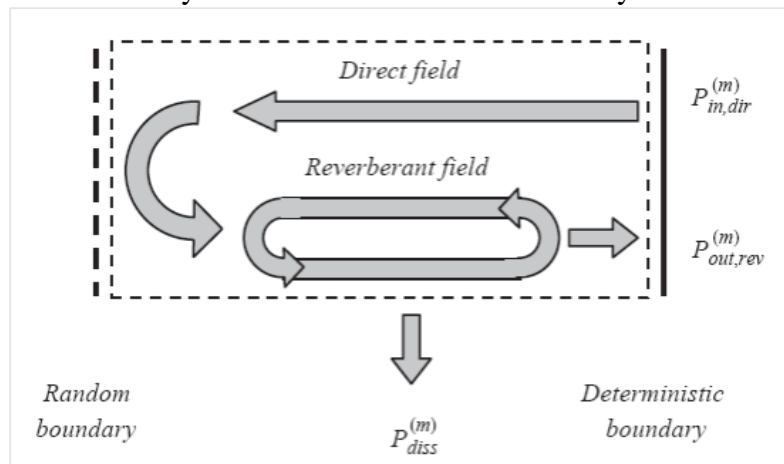

Figure 21. Power flow in a SEA-subsystem. From Shorter and Langley [32].

If there are no SEA subsystems, the method is purely FE. If there are only local small FE subsystems, the method is in principle the classical SEA enhanced with FE junction models. The coupling powers are then calculated using FEM and therefore the classical SEA relation between modal energy and power flow is not needed.

Example of assumed feasible frequency ranges of FE, FE-SEA and SEA in ship vibro-acoustics is shown in Figure 22. The important frequency range from 20 to 200 Hz is covered using FE-SEA. In the FE-SEA model the stiffest low part of the ship is modeled using FEM and the other parts using SEA. It is worth to note that in case of much larger ships the division is not so easy, because the underwater part is still an extensive structure. The meaningful range of full FEM (+BEM) might be well below 10 Hz.
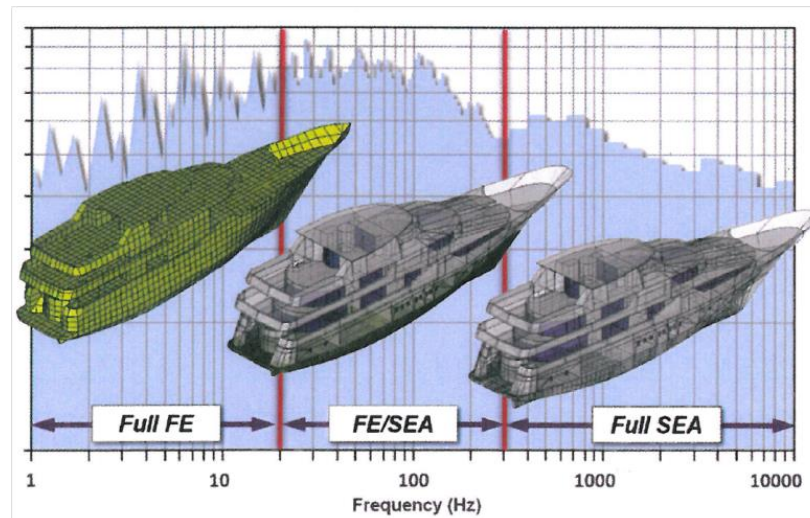

Figure 22. Frequency ranges of FE, FE-SEA and SEA in case of a luxury yacht, length 70 m. From Blanchet and Caillet [27].

VA One is presently the only commercial software applying the above described hybrid FE-SEA method.

4.6 Power injection methods

Power injection methods (see [36]) are available in, e.g., VA One software [34]. In the power injection methods the response of a complex system is viewed in terms of a simplified Energy Flow Model. An Energy Flow Model gives a relationship between the energy in various regions or subsystems of a system when uncorrelated excitations are applied to the subsystems. For a linear system it is always possible to write this relationship in the form of a matrix equation so that

$$E(f) = [EIC(f)] P_{in}(f) \qquad (12),$$

where E is the vector of subsystem energies, P_{in} is the input power to each subsystem due to the applied excitations, ω is the radian frequency of interest and [EIC] is a matrix of coefficients. EIC's are typically referred to as Energy Influence Coefficients. The mn'th EIC gives the energy in subsystem m per unit input power applied to subsystem n.

The *EIC*'s depend on specific type of excitation. Often an energy flow model is averaged over a large ensemble of different types of excitations that can be applied to a system. This kind of excitation averaged energy flow model is equivalent to an energy flow model where the subsystems are excited by spatially incoherent or delta correlated rain-on-the-roof excitations. The *EIC*s for such a model describe the energy flow properties of a system (rather than those associated with a specific excitation).

The *EIC*s are useful for diagnosis purposes, but another reason for creating an energy flow model is to view a deterministic system in terms of SEA-like parameters. The matrix equation in equation 12 can be inverted to give

$$\left[EIC\left(f\right)\right]^{-1} E\left(f\right) = P_{in}\left(f\right) \tag{13}.$$

This equation has the same form than standard classical SEA-equations. When scaled by frequency *f*, the off-diagonal entries of the inverse of the *EIC* matrix can be viewed as effective coupling loss factors (*CLF*s) that describe the transmission of energy between a set of subsystems. An effective coupling loss factor obtained from a single system need not obey the SEA reciprocity relationship (which only holds for the SEA ensemble). Similarly, the effective CLFs may be negative or infinite. If the subsystems in a system are complex, then the effective CLFs for a single system are usually similar to those obtained after ensemble averaging, strictly positive and obey the SEA reciprocity relationship.

4.6.1   Virtual Experimental SEA

In the "Virtual Experimental SEA" experiments used to obtain SEA system matrix from a physical structure are carried out virtually in a FE model. The basic processes is to "measure" power input and energy outputs in all subsystems and then construct the frequency-averaged SEA system matrix based on that information. The subsystem power inputs and energies are solved using FE-computed receptance matrices and subsystem effective masses. Then the EIC-matrix is composed. The rain-on-the roof excitation is approximated using typically 5 to 10 uncorrelated point forces. Five to 20 frequency points are used inside a frequency band.

Example of a warship (partial) FE model for VSEA is in Figure 23. Reported number of modes up to 500 Hz is 50000, reported modal density is up to 1000 modes/Hz (author: this might be incorrect; 100 sounds more realistic) and the practical upper limit of the model 400 Hz. 1360 observation nodes were used. The structure was decomposed into 20 subsystems.
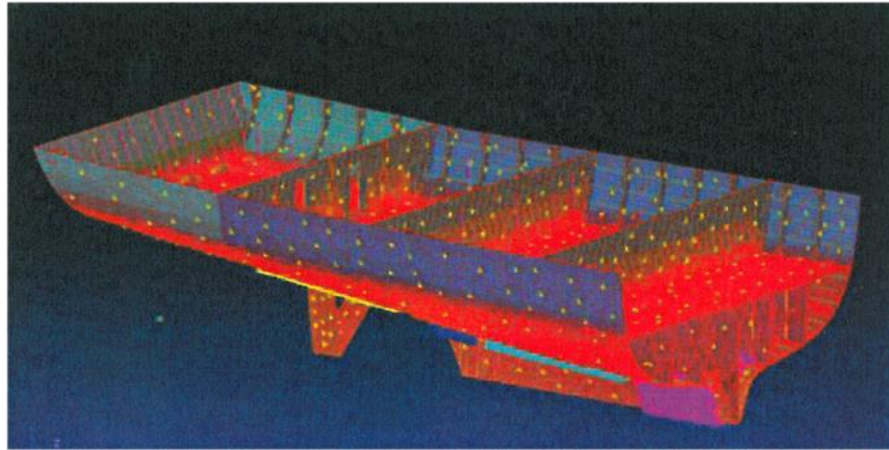
Figure 23. A warship VSEA FE model and grid of observation points. From Borello [35].

4.6.2 EFM

The EFM is an exact implementation of the power injection method when applied to numerical FE models [36]. Excitation forces are applied to all degrees of freedom and energies are computed according to response in all degrees of freedom of a FE model. The method makes use of the local mass and stiffness matrices of an FE model to provide exact calculations of the energies in various subsystems per unit rain-on-the-roof excitation applied to a given excited subsystem. This removes the need to define an equivalent mass for the subsystems in a system. It also removes the bias errors associated with the use of a limited number of sample points in the VSEA method. Computational burden is of course considerably higher than in VSEA.

4.6.3 Wavequide methods

Waveguide methods, e.g., [43, 44], were used extensively in the past to predict vertical propagation of structure-borne sound and interior noise levels. They are, more or less, a class of semi-empirical power injection or transfer matrix methods. Numerical methods might be useful to enhance these old methods.

4.7 Power flow and energy flow finite element methods (PFFEM, EFFEM)

The techniques described in chapter 4.6.1 and 4.6.2 relies on extracting power-energy information from FE-models using post-processing techniques. FE models are formulated as dynamic matrix equations and lead to SEA-type "lumped" subsystem energy description.

There are also attempts to formulate the structural energy flow more directly using energy (or energy density) or power as a continuous field variable. In these methods right-hand side (known) quantity is input power and unknown quantity is the energy density subject to suitable differential operators. The difficult thing has been that different structural components lead to different type of differential equations (compare to equations of 3D elasticity) [37].

An energy finite element method based code NoiseFEM [38], was developed in late 1990's at Germanischer Lloyd. One aim was to facilitate the use of an energy based prediction method for and, in particular, efficient reuse of geometrical and structural data from already existing finite element models. Input powers are predicted using experiments, semi-empirical formulae and refined local FE models.

It is mentioned in passing that earlier the task of generation of a SEA model was seen as a major obstacle. Today, this limitation is somewhat relaxed since automatic algorithms to create SEA models or subsystems directly from suitable FE or CAD geometries exist.
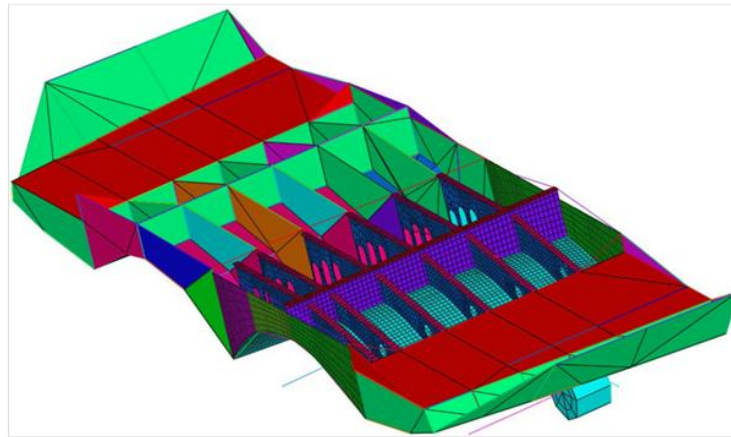

Figure 24. Part of global and local FE model used to predict power inputs from machinery. From Cabos [38].
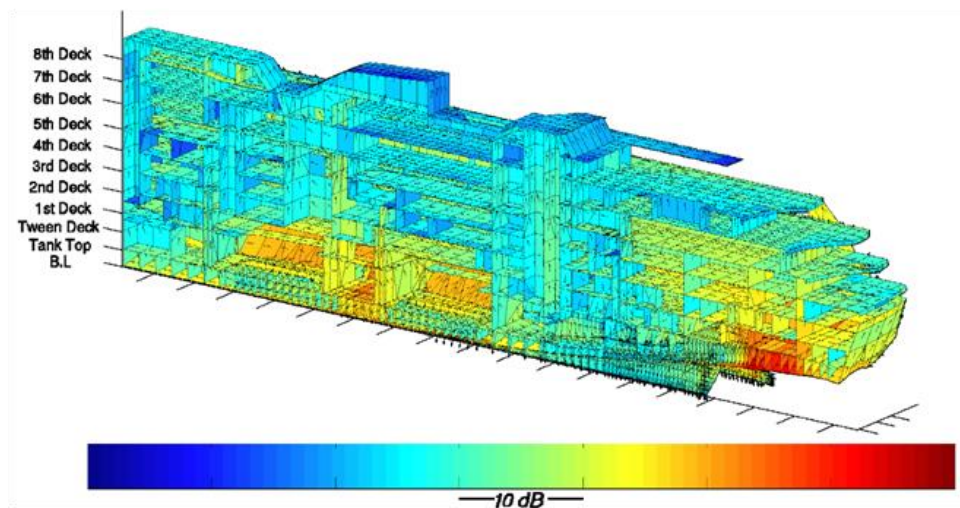

Figure 25. Energy FEM predicted structural intensity (magnitude using colors and direction using vectors) in a passenger ship. From Cabos [38].

EFEM code development has also been carried out by the Noise Control Engineering, Inc., Martec, Inc. and Defence Research and Development Canada (DRDC) from the request of Office of Naval Research (US Navy) [39]. They conclude that "the ideal implementation would be a hybrid system of EFEA and SEA for the analysis and understanding of ship noise and vibration. The EFEA approach would be appropriate for structure-borne energy flow in and around the source, where the vibration gradient is high, and the SEA approach would be

appropriate for modeling the transport of energy away from the machinery space."
The author is not aware of possible continuation of this work.

Kim et al [40] and Han et al [42] from Korea have reported about on-board and underwater noise predictions using EFEM at 31.5, 500 and 8000 Hz. Some results at are presented below. The sound field results at 8000 Hz clearly suffer from spatial aliasing or numerical noise. Measurements were also carried out, but they are not clearly reported in the reference. The software is probably in-house. The study of Kim et al was supported by the Marine Research Institute of Samsung Heavy Industries Co., Ltd. The study of Han et al was supported by the Agency for Defence Development Naval System R&D Institute (RDD). The authors are partially the same in both Korean studies.
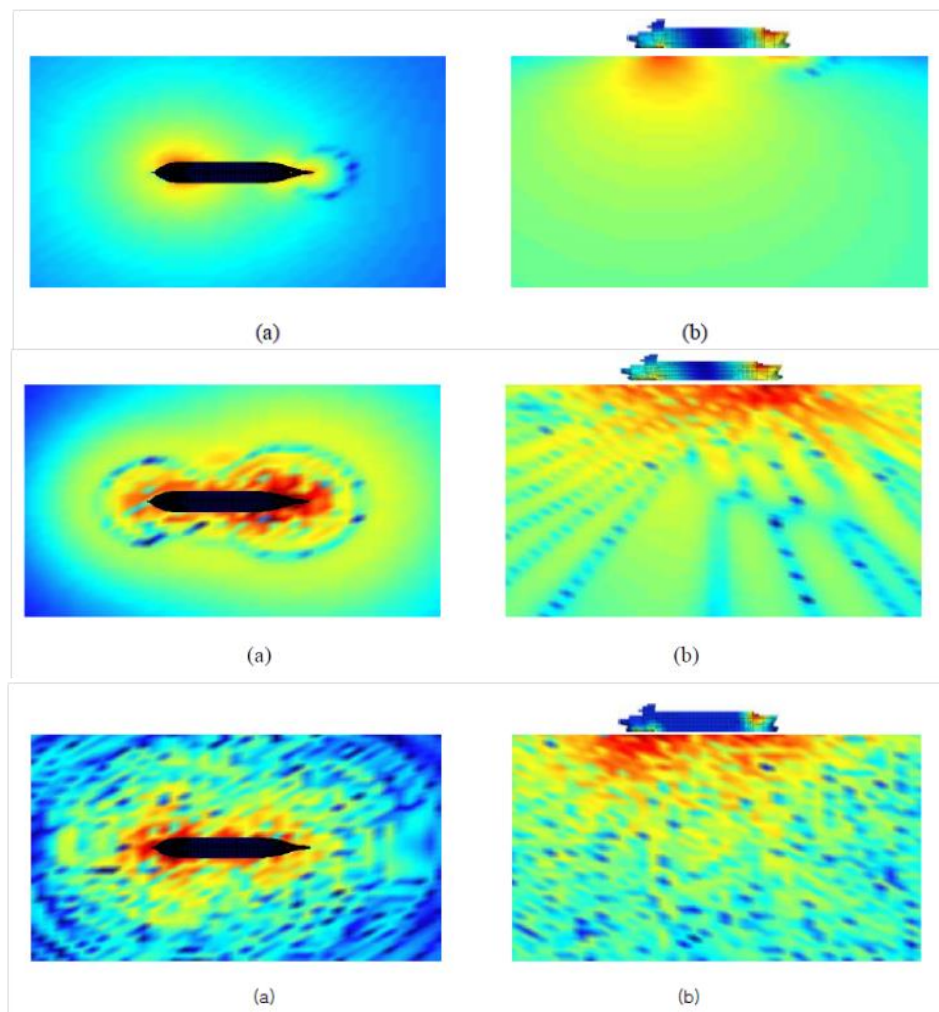

Figure 26. Predicted underwater sound pressure levels at 31.5, 500 and 8000 Hz. Horizontal plane on the left is 20 m underwater. Vertical plane on the right is on the plane if the centre line of the ship. From Kim et al [40].

A recent review of methods for structure-borne noise prediction on ships is in [41]. The authors conclude that EFEM is a very potential tool for ship noise analysis overcoming some limitations of the classical SEA. As a drawback of the EFEM they see that it represents a relatively new method with not so much feedback from experience with application to the ship structures. The authors are evidently not aware of hybrid FE-SEA. The EFEM is capable to predict energy

distributions inside subsystems (i.e., predict in discrete points) using relatively coarse FE meshes.

It is worth noting, that the PFFEM/EFFEM method does not generate any new refined input data on structural and material details. These quantities a subject to uncertainty and thus details of local energy density fields are uncertain just like dynamic variables in a FE analysis.

A commercial software package named EnFlow, based on EFEM, may be found from Comet Technology [51]. ESI Group acquired Comet Technology Corporation's IP in 2011. The present status of the EnFlow is unknown.

It must be emphasized that validation data concerning the capabilities to predict underwater noise radiation of ships correctly using any method is lacking.

5 Calculation method assessment case: a small floating structure

5.1 General

Model of a small "generic" floating structure radiating into water was created. The structure is not intended to simulate a part of a ship. To make things still simpler, no stiffeners in form of beams are used, there are only plates and cavities. From point of view acoustics, this is maybe not a fundamental issue. From point of view structural stiffness and vibration and model building time it certainly has an effect. The purpose in this point was rather to study the rationale of creating models for different frequency ranges and the associated problems, like possible inconsistencies between the results at overlapping frequency ranges.

5.2 The structure and models

The structure (Figure 27) is made of steel. It contains a relative small and stiff part with 16 (red in the figure) and 12 mm (yellow in the figure) plate thicknesses. This part serves as a "machine foundation". The rest of the structure is more flexible, 8 and 4 mm steel plates. The structure is symmetric in one plane. Structural damping was assumed to be "Welded Flexure". The length of the structure is 4.75m, width 4.15 m, height 0.89 m and mass 3211 kg.

Point forces (Figure 28) in three perpendicular directions are used as excitations. The forces are directed on foundation simultaneously. The model is solved as random, i.e. the forces have no phase reference to each other. The location of excitation makes the problem asymmetric.

Internal acoustics may be modelled using interior FE-cavity or SEA-cavity. In all cases, a SEA cavity (volume ca. 13.5 m^3) was used in all models.

Exterior underwater radiation connections are realised using Semi-Infinite Fluid (SIF) objects (Figure 29). This means that sound radiation calculation from FE structures is based on Rayleigh integral, which is accurate for planar structures and approximate for curved structures. In VA One, advanced method based on vibration field de-composition into wavelet shape functions may be used. Compared to standard procedure using "piston" shape functions, this theory [52] is more accurate for imaginary part of radiation impedance (i.e., mass loading), which is vital in case of heavy fluid loading. For SEA subsystems, radiation efficiency formulation, based on the wavenumber domain theory of Leppington et.al. [53], is used. Air around the structure has negligible effect on underwater results and is not taken into account.
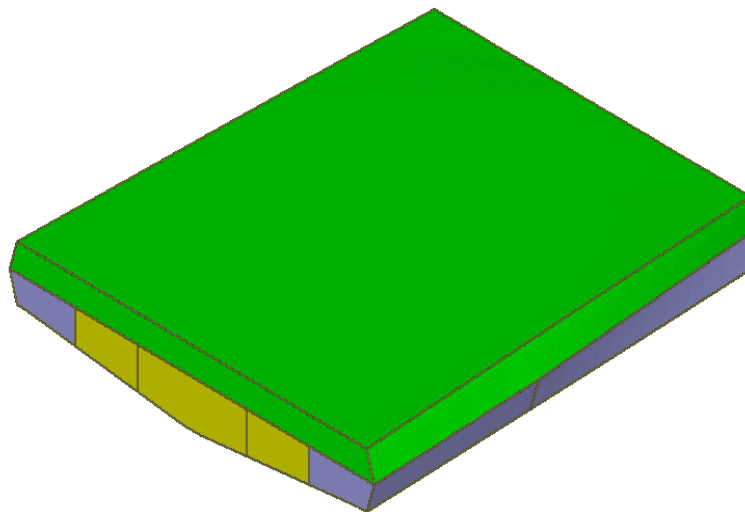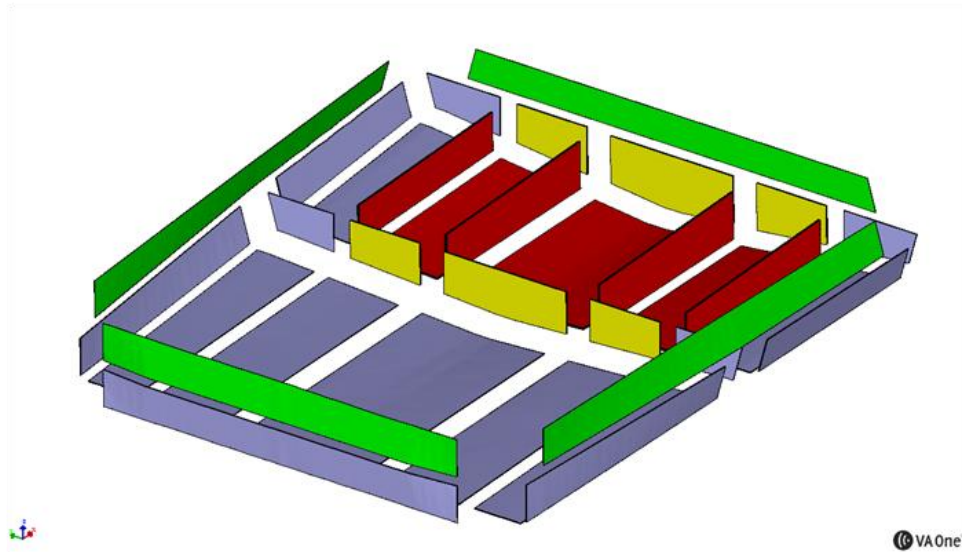
Figure 27. A Small floating structure. Upper: SEA-subsystem division, seen from "back", without "deck"; Lower: seen from "front" with "deck", Color codes for thicknesses are red: 16 mm, yellow 12 mm, violet: 8 mm, green 4 mm.
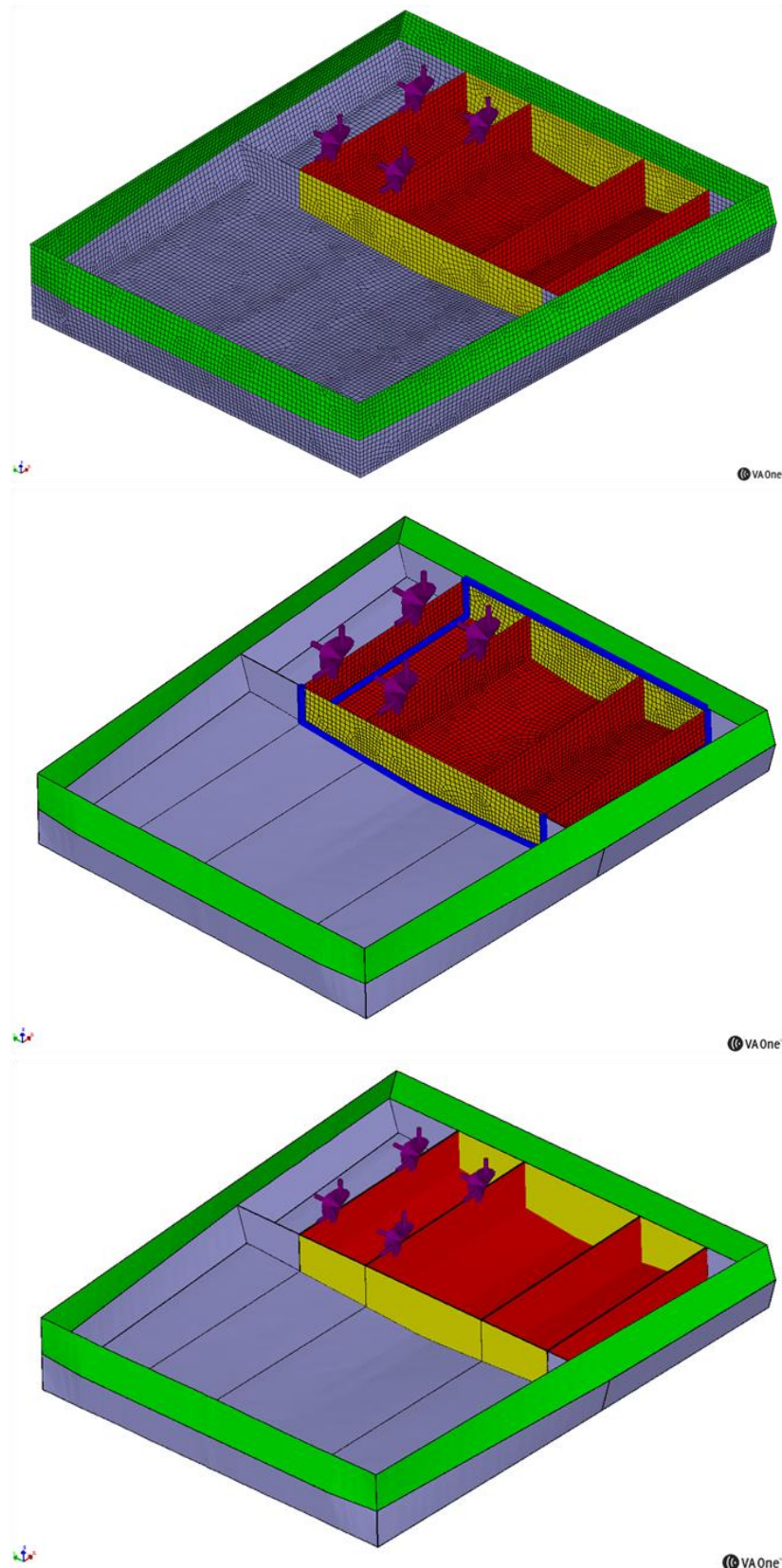
Figure 28. FE-, FE-SEA and SEA models of the small floating structure with point force excitations. Blue lines depict hybrid line junctions between the FE- and SEA-subsystems. Mesh density of the FE subsystems is ca. 40 mm. Elements are of type Quad4 (Mindlin plate). Number of structural modes is 972 up to 400 Hz in the FE –model and 1117 up to 4000 Hz in the FE part of the FE-SEA model.
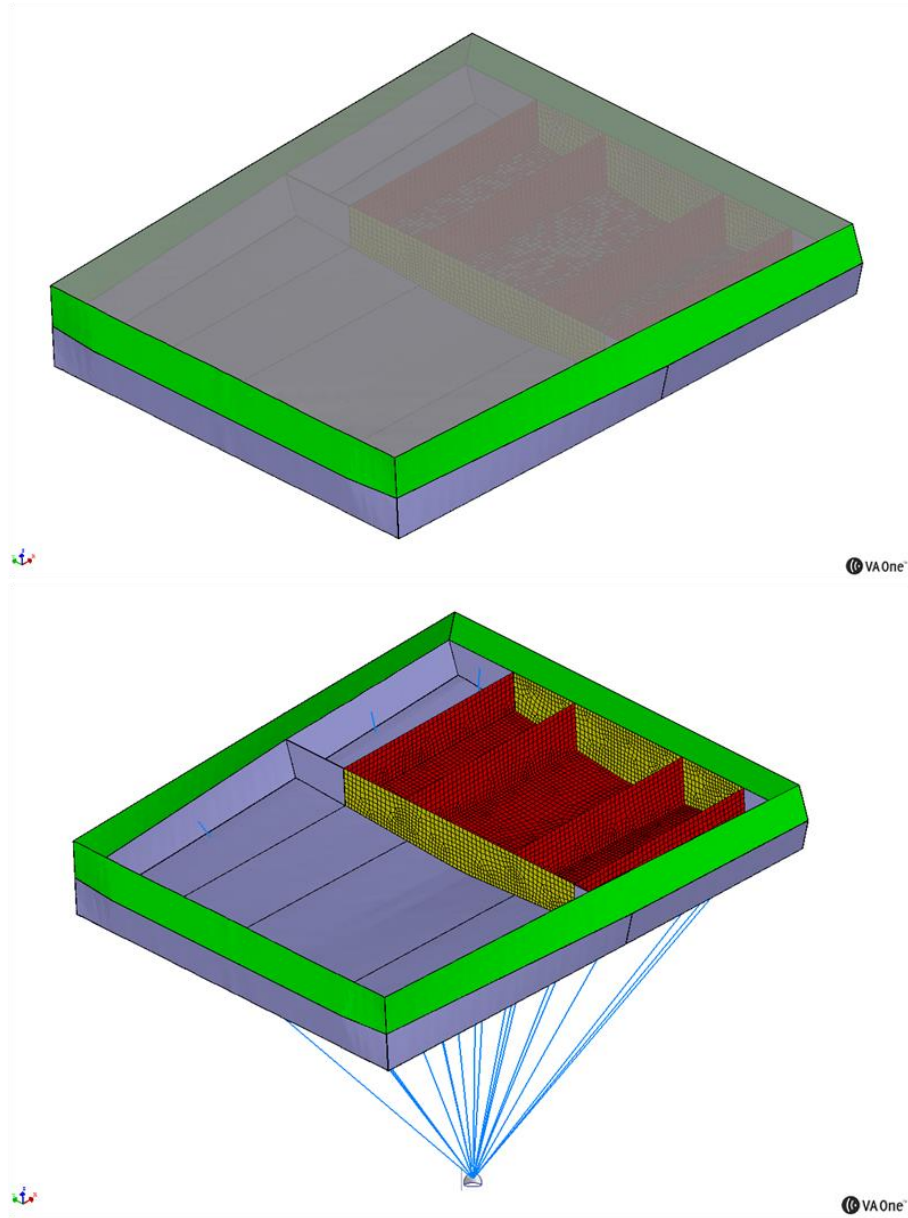
Figure 29. Top: Interior SEA cavity, Below: exterior radiation connection of the wetted subsystems to the water.

5.3 Low, mid and high frequency ranges

When partitioning the system into FE and SEA subsystems, the number of modes was used as a rough rule. At 1000 Hz 1/3 octave all subsystems have more than one flexural mode and at 2000 Hz more than three. As a conservative rule of thumb, over 2000 Hz should be adequate for a full SEA model. However, SEA-models usually work quite well from considerable lower frequencies provided input powers are correct. One explanation to this is that strongly coupled subsystems tend to function as a one larger one, thus releasing a little bit. What may be more problematic is the power input from localized sources not taking into account rigid body movement of a floating structure, a phenomenon not described by the SEA "local mode" model.

At 250 Hz most of the 8 and 4 mm subsystems have more than one mode. This may be seen as starting of the "mid-frequency" range where short-wavelength "local mode" part of the structure may be well modelled using SEA. The ideal division of the methods is roughly:

- Low frequency range   0…250 Hz   FE
- Mid-frequency range   200…2500 Hz   FE-SEA
- High-frequency range   over 2500 Hz   SEA

In Figure 30, there are some simulated vibration fields of the structure. At highest frequencies the vibration field of the FE part of the FE-SEA model is not very well described using the chose element size. However, it was decided to keep the element size at 40 mm.
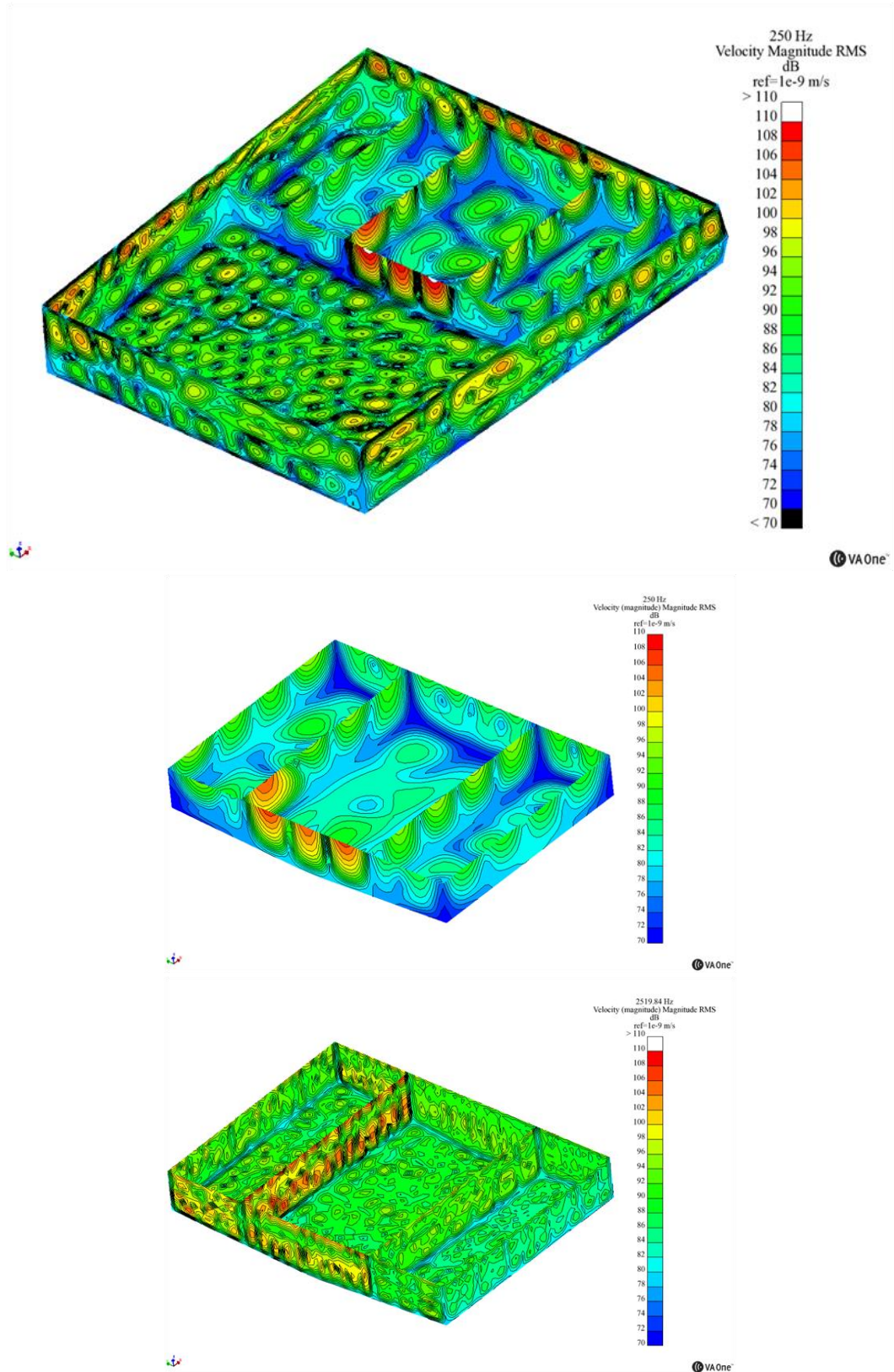
Figure 30. Simulated vibration fields of the structure. Top: FE-model at 250 Hz, Middle: FE-part of the FE-SEA mode at 250 Hz, Bottom: FE-part of the FE-SEA model at 2519 Hz.

5.4 Underwater radiation simulations and results

5.4.1 Model configurations

The FE-, FE-SEA and SEA models of the small structure and its radiation were solved in configurations described in Table 1. Both point force excitations and acoustic excitations were used. Only the models with mechanical excitations are presented below. Because of high scatter of radiation results noted, also BEM models were created and solved for the same point force loading.

All simulations were done at 1/24 octaves. The lower frequency limit of all models is 8.76 Hz in order to see results at overlapping frequencies. The upper limit of FE- and BEM- models is 250 Hz and that of FE-SEA model is 2500 Hz. The SEA model was solved up to 55400 Hz. Note that there is no exact "theoretical" lower limit for SEA model. However, the mean values predicted using SEA are expected to be useful (comparison to FE and FE-SEA is meaningful) above ca. 300-500 Hz.

12 random point forces in 4 locations were used to excite the structure. In each spatial location there are 3 forces of 1N in orthogonal directions (see Figure 28)

Table 1.Model configurations.

Method/Model	*Excitation on foundation [N]*	*SEA Plates "Fluid loading" used*	*Frequency range of 1/24 octaves in solve [Hz]*
FE	12 x 1N	-	8.76 – 250
FE-SEA	12 x 1N	No	8.76 – 2828
SEA	12 x 1N	Yes/No	8.76 – 55394
BEM	12 x 1N	-	8.76 – 250

In the models following (Table 2) methodology were used to solve for the structural response and underwater radiation:

Table 2. Methods used in radiation simulation.

Method/Model	*Structure*	*Underwater radiation*	*Radiation condition*
FE	FEM	Hybrid Area Junction ("HAJ")[1]	Baffled: rigid plane
FE-SEA	FEM/SEA	HAJ/Leppington et al theory[2]	Baffled: rigid plane
SEA	SEA	Leppington et al theory	Baffled: rigid plane
SEA Fluid loading	SEA	Leppington et al + Fluid Loading Corrections[3]	Baffled: rigid plane
BEM	FEM	Kirchhoff-Helmholtz integral equation	Baffled: rigid plane or pressure release plane

1) Rayleigh integral based theory using Wavelet base functions, see [52]
2) Analytic method radiation efficiency calculation, see [53]
3) Radiation efficiency and mass loading correction on SEA panels for heavy fluid loading, see [54, 55, 56] and chapter 5.6.

In FE- and BEM-models the structural and underwater acoustic fields are fully coupled, so that exterior radiation impedance matrices calculated using HAJ or BEM are projected onto structural modes before the full solve. In FE-SEA model only the FE part and underwater acoustics is fully coupled. In FE-SEA model SEA-part and "pure" SEA, structural and underwater acoustic fields are energetically coupled, so that underwater radiation is seen as an energy sink in SEA structures. In SEA, the "Fluid Loading" option seems to yield very low values for sound radiation. Hence comparisons were run with no fluid loading option.

When using HAJ for radiation, the structure is effectively unwrapped to a planar radiator. In BEM, the irregularity of the body is rigorously taken into account. The advantage of the HAJ-formulation for an FE subsystem is that the computation of the radiation impedance (and diffuse field excitation) is quite fast, often several orders of magnitude faster than using the BEM approach. However, differences are expected to occur.

5.4.2 SEA Fluid Loading

The purpose of the "Fluid Loading" option in SEA models is to modify radiation efficiency and add a frequency-dependent "fluid mass loading" on wetted SEA plates. This option has a particularly drastic effect on underwater sound power. This issue is discussed in more detail in chapter 5.6.

5.4.3 Underwater sound power with unit force excitation on foundation

Results as sound power levels at 1/24 and 1/3 octaves are shown below in Figure 31 and Figure 32. There is a huge difference between the SEA curves with and without the "Fluid Loading". The SEA without Fluid Loading, FE and FE-SEA models give quite comparable results above 50...100 Hz, SEA predicting ca. 5 dB lower values. The BEM-curves are considerably below the FE- and "normal" SEA-curves but above "Fluid Loading" SEA-curves. The differences are more clearly visible in 1/3-octaves, Figure 32.
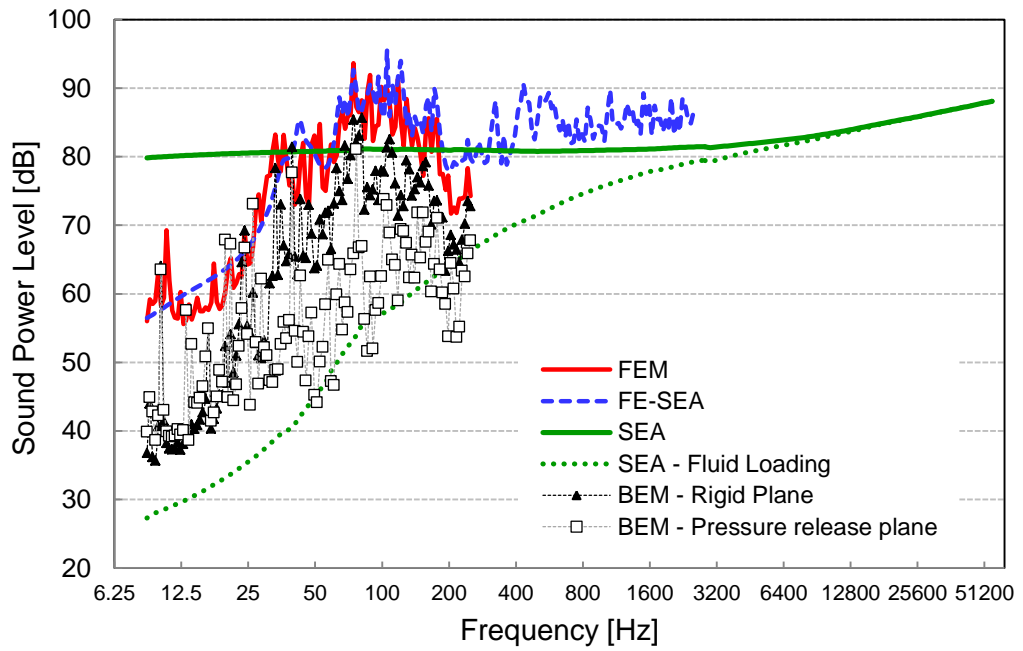
Figure 31.Underwater sound power levels at 1/24-octaves. Mechanical excitation.
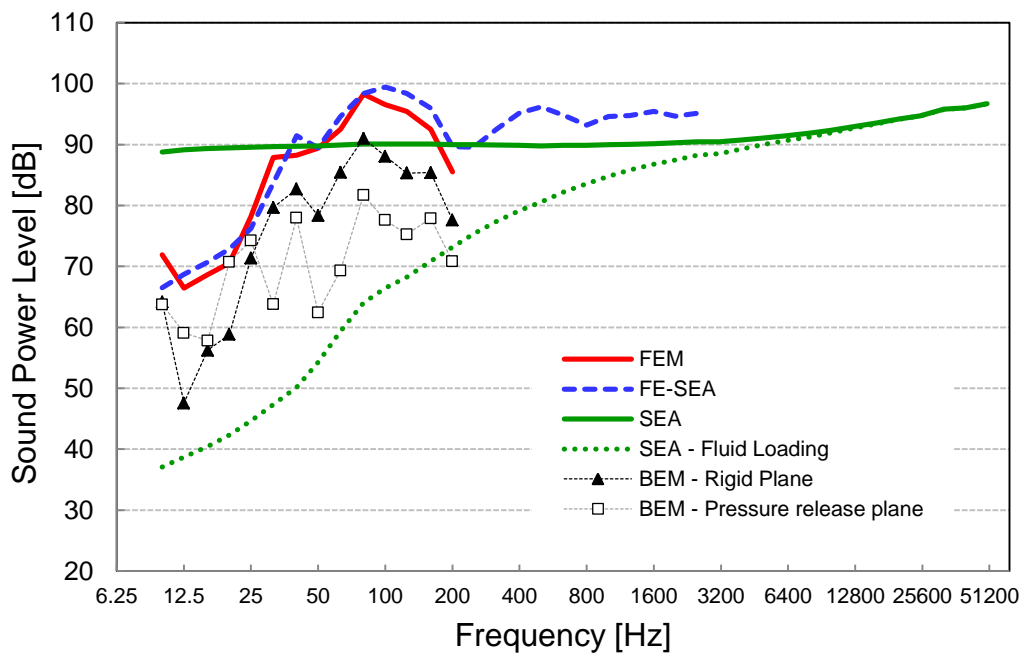

Figure 32. Underwater sound power levels at 1/3-octaves. Mechanical excitation.

Vibration velocity of a wetted bottom plate with unit force excitation on foundation is shown in Figure 33 and Figure 34. Above 100 Hz the methods, except SEA without Fluid Loading, give quite consistent results. Below 50 Hz SEA overestimates quite much.
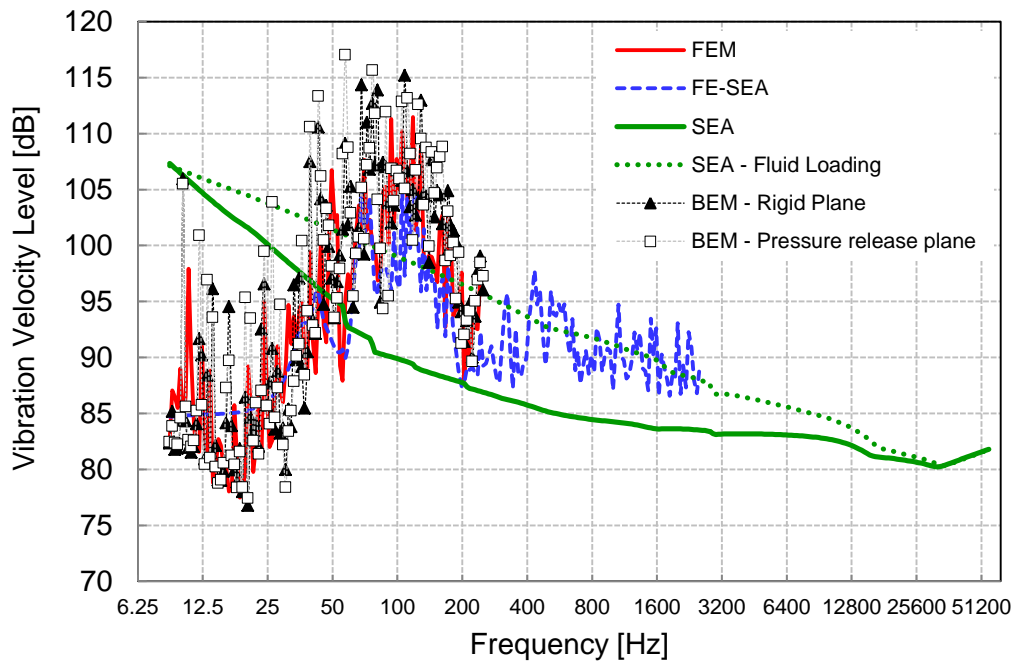
Figure 33.Vibration velocity level of a large bottom SEA plate at 1/24-octaves. Mechanical excitation.
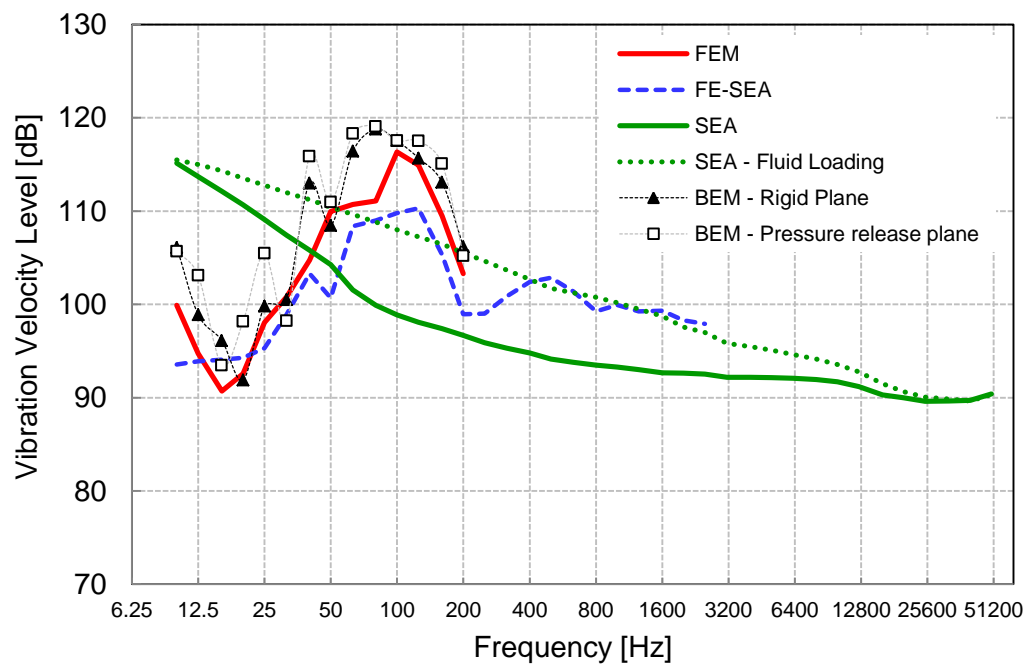
Figure 34. Vibration velocity level of a large bottom SEA plate at 1/3-octaves. Mechanical excitation.

One problem in comparison of methods is the consistency of the excitations. This is addressed in the next chapter.

5.5 SEA model refinement using corrected input power

5.5.1 Unit force excitation on foundation – structural input power

In SEA models input powers are approximated from SEA default impedances. This means that impedances of infinite plates are used to estimate the input powers. It is well known that due to that the input powers at low frequencies in SEA models differ from those calculated using FEM.

In a SEA model, point force excitation means that the power input is an expected value taken an average over ensemble of structures and excitation locations. This ensures an even power distribution over all "local" modes. In FE models the excitations are in a certain location and some modes are excited more than others. Also, in FE-model, both "global" and "local" modes are excited, but in SEA model only "local" modes are excited. The same applies on radiation; the structure radiates also via rigid body modes and global elastic modes whereas in SEA model only local modes are assumed. Number of excited modes is a statistical estimate in SEA model and result of explicit calculation in FE-models.

Power inputs from applied forces to the structures at 1/24 octaves are shown in Figure 35. There is a big difference below 50 Hz. The difference between SEA and FE/FE-SEA is almost identical to the difference in plate vibration levels (Figure 33). This is a typical difference between FE and SEA: difference in power input, which returns to the differences in structural impedances. The point force excited plates are stiff and have no many modes. In this case frequency average or infinite plate impedances give a relatively poor estimate of the structural power input.
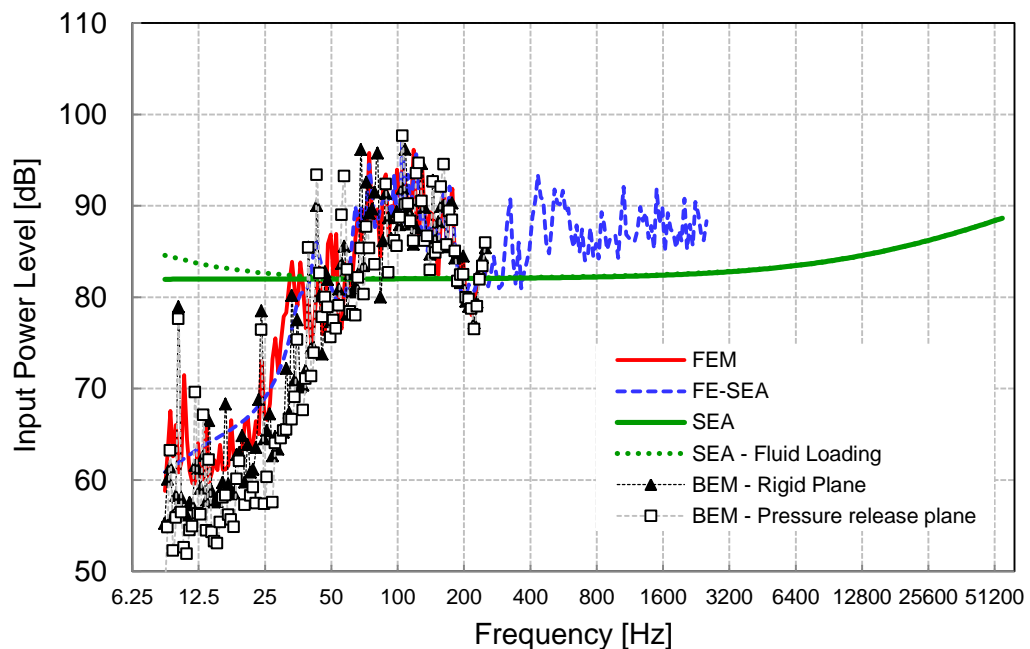

Figure 35. Total input power to the foundation in different models, 1/24 octaves.

If a more accurate estimate of input power is available, this can, in principle, be used in SEA models to make the model more accurate at low frequencies. Better low- and mid-frequency estimation of sound power is obtained when input powers from FE-SEA model are used in the SEA model, Figure 36.

Note that this is tricky! The input power used here is <u>not</u> independent from sound radiation. The net power is always consumed by losses and <u>in this case,</u> most of the input power into SEA system (when no Fluid Loading used in model) is consumed by radiation to exterior as other losses are small. Thus the correlation of the "SEA Refined Input Power" and FEM is unrealistic good in sound radiation – same input, same answer. The radiation area is large compared to the structure size. This emphasizes the problem.
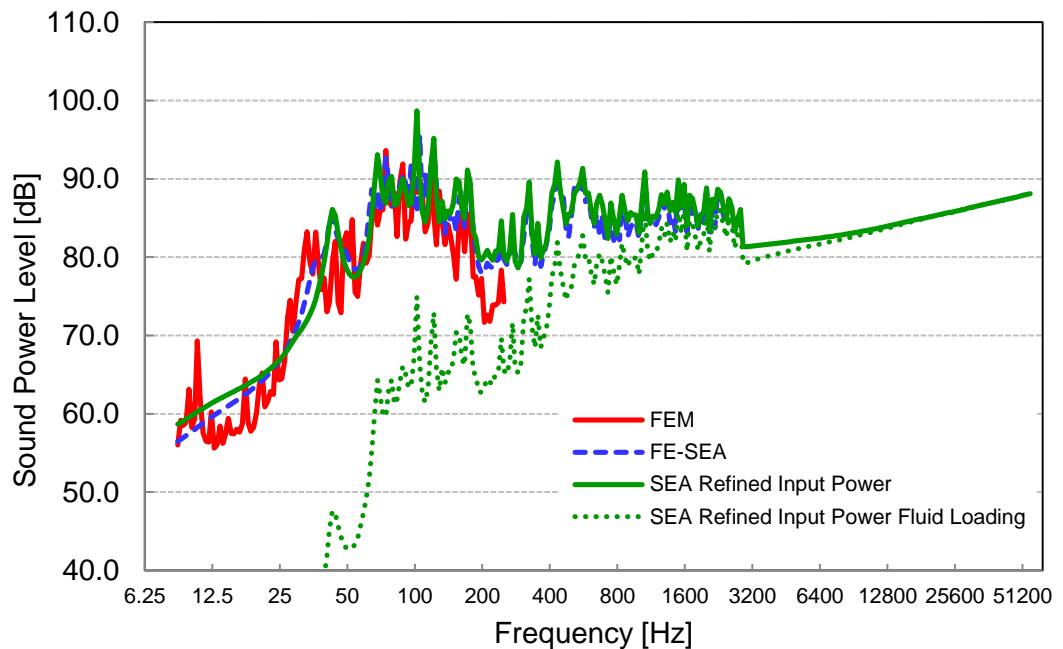
Figure 36. Predicted underwater sound powers at 1/24 octaves, foundation input power from FE-SEA used in SEA model.
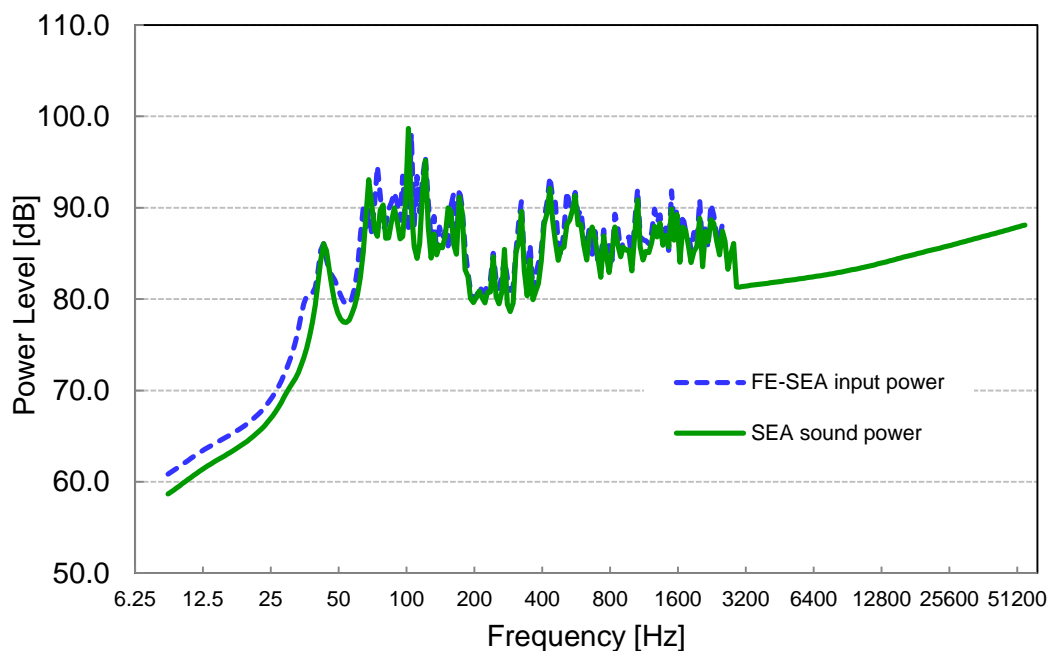

Figure 37. Comparison of refined input power from FE-SEA and SEA radiated sound power.

5.6 Fluid Loading and low-frequency radiation of SEA subsystems

Critical frequencies of the plates in water are in the range of 20 kHz to 50 kHz and thus the radiation conditions are "subcritical" throughout the most of the frequency range. There is much acoustic "short-circuiting" in the vibration field and plate edges, excitation points and other discontinuities have an important role on sound radiation. Theoretically, free flexural waves of an infinite plate do not radiate at all below the critical frequency.

Some articles argue how the existence of heavy fluid loading fundamentally changes radiation characteristics of point and line excited structures, see [21, 54, 55 and 56]. Monopole type radiation from an excitation area of a point force should change to dipole type due to special effects the fluid have on structural vibration. Physical background is that fluid loading adds so much mass that the excitation "sees" the fluid only and thus the excitation is of type fluctuating fluid force (i.e., dipole).

There seems not to be solid experimental material of the effect of fluid loading to radiation. Thus both options (with and without Fluid Loading effects on SEA panels) were used in this report. In VA One, the "Fluid Loading" option of SEA plates reduces radiation efficiencies of SEA panels hugely at low frequencies (see Figure 38). However, the formulation takes into account the radiation from ribs etc. which is apparently not included in calculated radiation efficiency of flexural waves. The Fluid Loading option modifies flexural wave-numbers slightly, which seems rational. As a result, the curves of FEM and SEA radiation efficiency may become quite different at low frequencies. It seems that FEM (or BEM) results for sound power are somewhere between the two SEA results. It should be repeated that no rigid body modes or other global movements capable of radiating sound are accounted for in SEA.

The net effect of lower radiation efficiency with the SEA Fluid Loading option is lower apparent damping and higher vibration response. The author sees that this option should be used with caution and possibly studied a bit more with different sizes of plates. Blanchet & Matla [30] discuss underwater noise prediction and use the "Fluid Loading" option, but they do not show any underwater results. Note that vibration of the wetted shells is less sensitive to the underwater radiation efficiency than the sound power, so structural vibration velocity is not the reliable criteria the correctness of the model in radiation prediction.

VA One has options for "Radiation from Ribs" and "Radiation from Ribs scattering". They are used in case the plates are ribbed. VA One calculates additional damping and coupling loss factors among the shell's in-plane and flexural wavefields, accounting for the coupled dynamics of the ribs. This feature not only creates a new radiation path from the resonant rib modes, but also the new coupling loss factors among the shell's wavefields affected by the dynamics of the shell whether a SIF or acoustic cavity or diffuse acoustic field is connected to the ribbed shell.
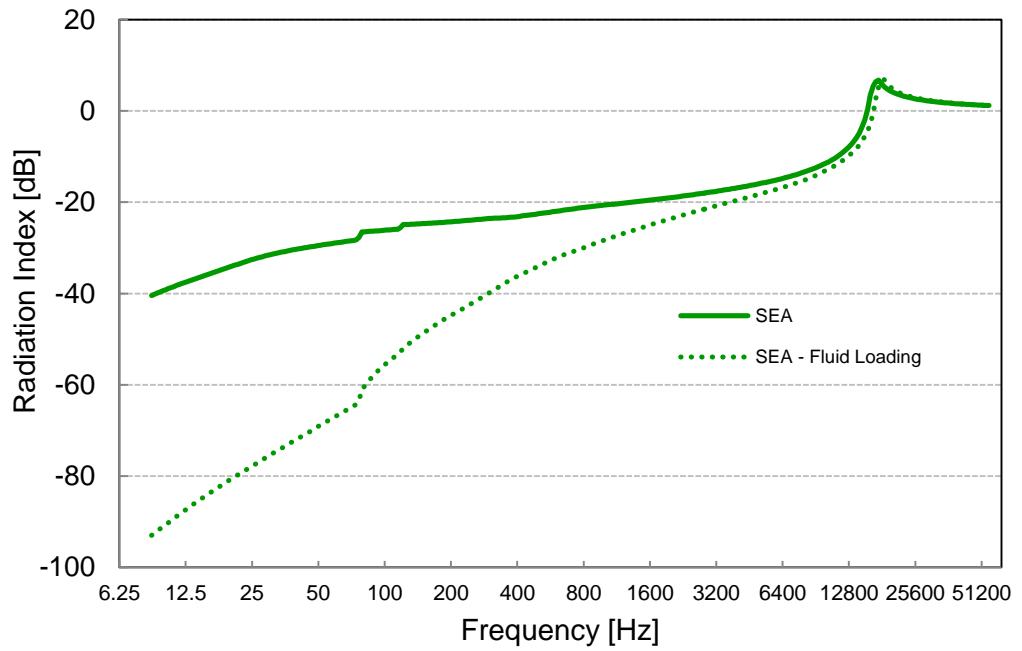
Figure 38. Typical radiation efficiency (usually termed "Radiation Index" in dB scale) curves of a SEA steel plate (3.44 m^2, 8 mm thick) wetted with water with and without the "Fluid Loading" option.
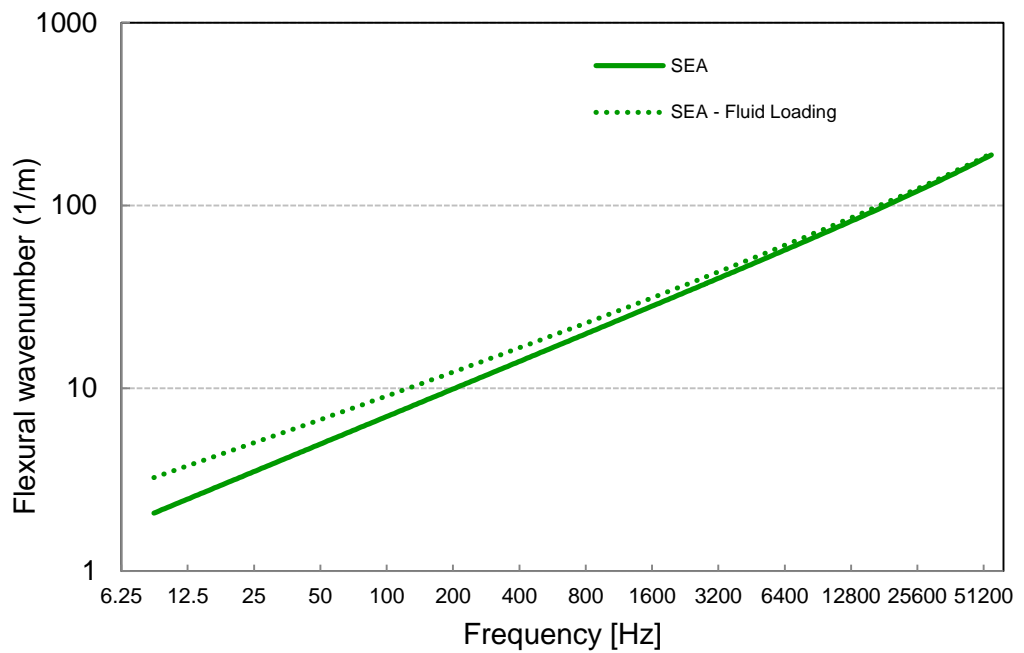

Figure 39. Flexural wavenumbers for a SEA steel plate (3.44 m^2, 8 mm thick), wetted with water, with and without the "Fluid Loading" switch.

6 A ship in full scale

6.1 General

NAPA steel model of a typical ROPAX/RO-RO vessel was created by Elomatic Oy on VTT's request [57]. The hull shape of the ship originated from a VTT's past project. In the model, there is a double bottom and three decks (tanktop, car deck, main deck). Superstructure on the main deck was not included. Ice class was chosen to be 1A Super.

The waterline length (Lwl) of the ship is 164.05 m, waterline beam (Bwl) 25.0 m and draught 6.1 m. The light weight is 9700 tons, total displacement 14156.7 tons and dead weight (DW) 4456.7 tons. The DW consists of last (65 trucks) of 2600 tons, heavy fuel oil 1226.2 tons, fresh water 352.6 tons and water ballast 277.9 tons. An overview is in figures Figure 40 and Figure 41. Frame/beam network is shown Figure 42.
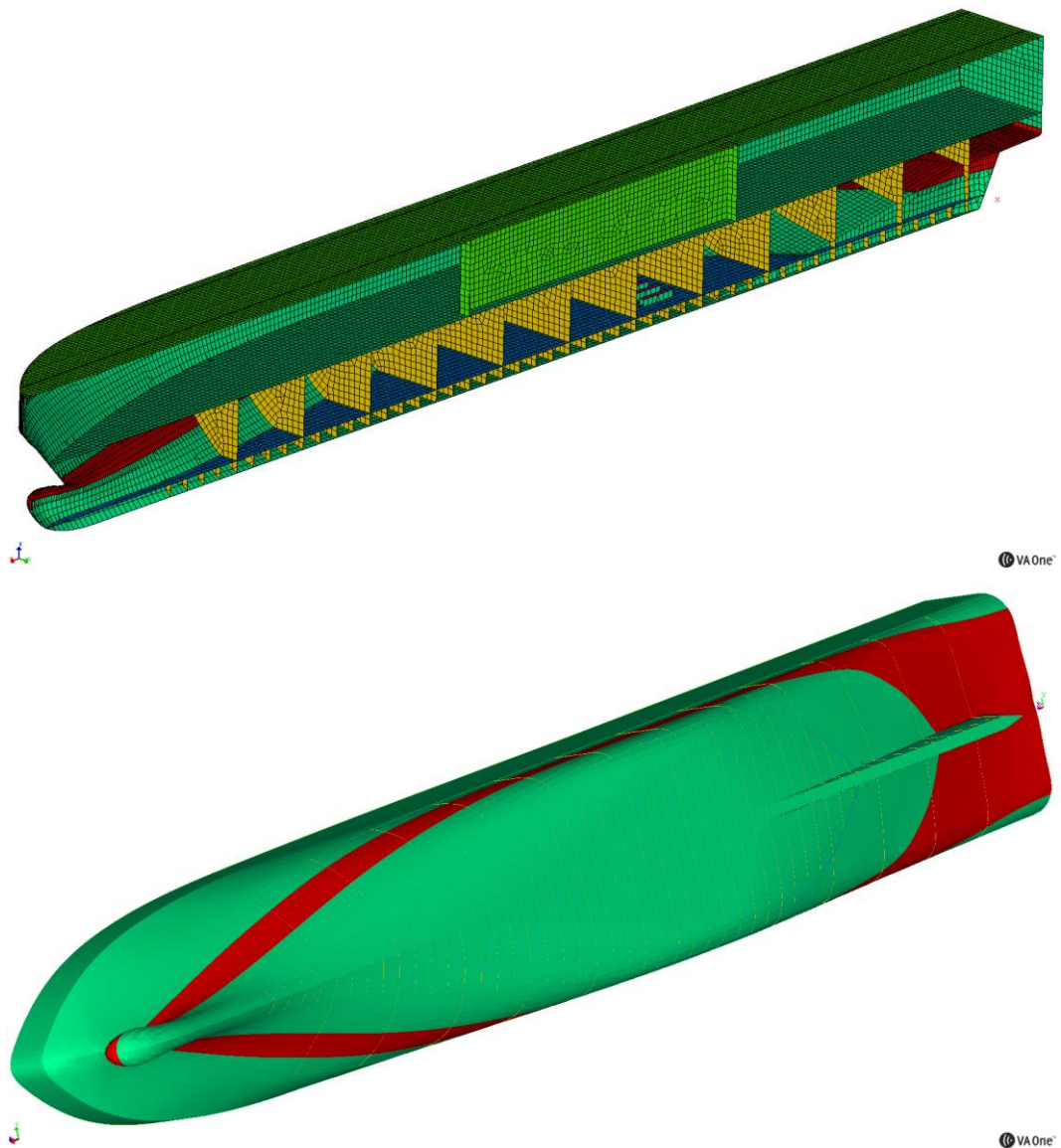

Figure 40. Overview of VTT ROPAX/RORO. Cut of the local FE model and ovewview of the bottom.
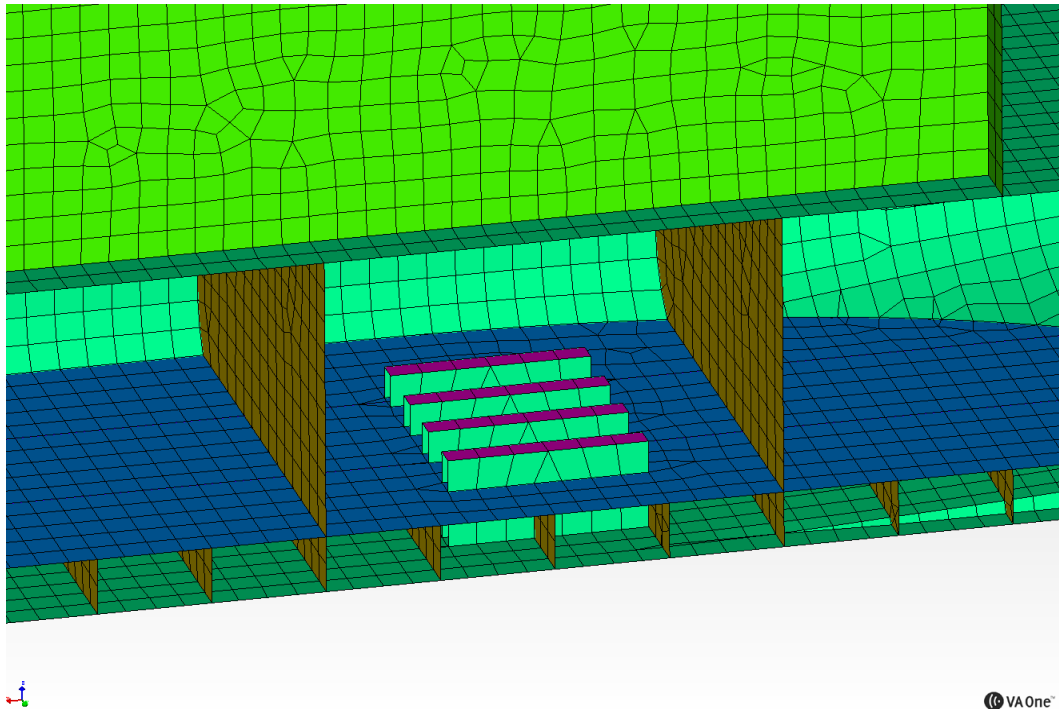
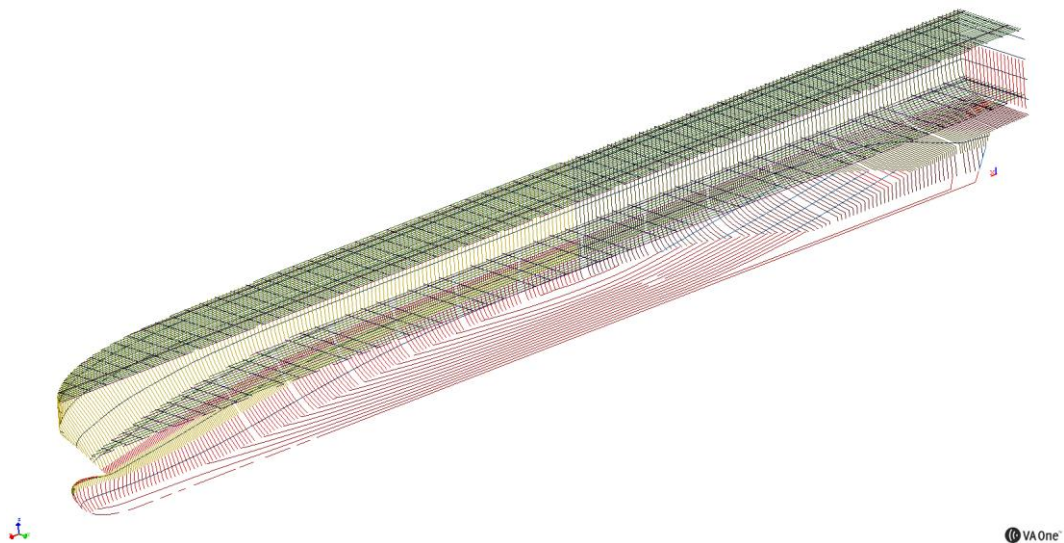*Figure 41. Overview of VTT ROPAX/RORO. Engine foundation.*

Figure 42. VTT ROPAX/RORO. FEM-model frame/beam network.

Machine foundations were designed according to specifications of an engine manufacturer [58] on basis of four W12V32 engines. The overall design was simplified to be follow symmetry.

The mesh is divided at the waterline in the middle of the strengthened 23 mm thick part. This enables the connection of wetted part of the ship to water to be realized more simply.

Two structural FEM models were created by Elomatic within NAPA software and exported as NASTRAN block data files. One is a "local" and the other is a "fine" FE-model. They have typical element sizes of 0.8 and 0.3 m, respectively. The

"local" model has ca. 105000 elements and 51000 nodes and the "fine" model 253000 elements and 165000 nodes. The elements are mainly 4-node shells type QUAD4 with PSHELL property cards. There are 8 different plate properties; thicknesses between 7 and 50 mm. The beam elements are of 2-node beam elements type CBEAM with PBEAML property cards. The original NAPA beam properties were mapped to 6 different NASTRAN properties for L- and T-beams. Beam network is shown in Figure 42. In this report, the coarser "local" model is used as basis for other models. All materials are steel.

6.2   Modeling process

Modeling process is described in Figure 43. A full FE-model was created first. The received FE-geometry was not partitioned to structural elements. Thus 14 FE-subsystems were created directly following the PSHELL (8) and PBEAM (6) properties. A full SEA model was created independently of the full FE-model. Creation of FE-SEA models were more laborious, since several trial model versions had to be created.

There are various ways to create SEA and FE-SEA models. It was seen easiest to proceed as follows. First, a full SEA model was created based on "Temporary FE Geometry)". Then it is analyzed, how large (and what) part of the full FE model is feasible as the FE subsystem (master system) of the FE-SEA hybrid model. A BEM model is basically a radiation model and it may be composed in many ways depending on solve type (deterministic/random). Anyway, the structure coupled to a BEM fluid must be a modal or forced response FE-subsystem.
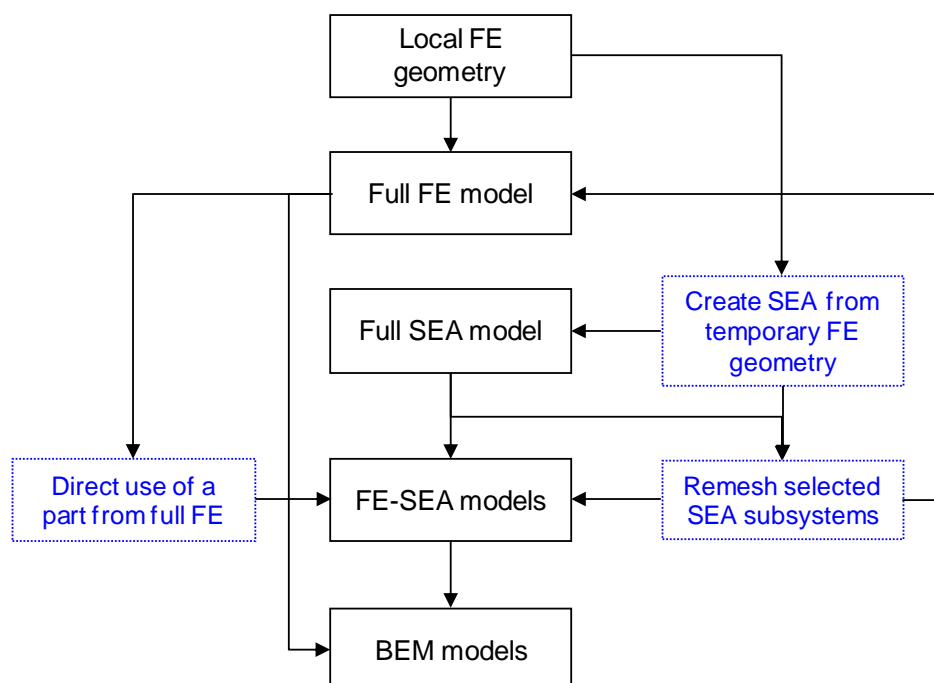

Figure 43. VTT ROPAX/RORO. Main parts of the model creation process. Mirroring, meshing etc details are not included here. Some re-creation of SEA subsystems was also needed to enable seamless coupling between SEA and FE subsystems.

One of the key issues is how to create models fluently from the original FE mesh. It is relatively easy to create FE- and SEA subsystems from temporary FE mesh. It is also possible to remesh FE model directly to smaller or larger element size. However, the re-meshing within VA One did not produce very good results, probably because the basis is the old, not very high quality mesh. Instead, when FE subsystems with smaller elements are needed, it is better to create first a detailed SEA model with plates and beams and then mesh it with the wanted mesh size. The result is much better, probably because the SEA model now serves as geometry. About this, see Figure 44 and Figure 45. *For future reference*; much work could be saved if the original FE mesh (or CAD geometry) is already partitioned to simple parts (into so-called manifolds) so that that *every part is directly usable as a SEA plate*.
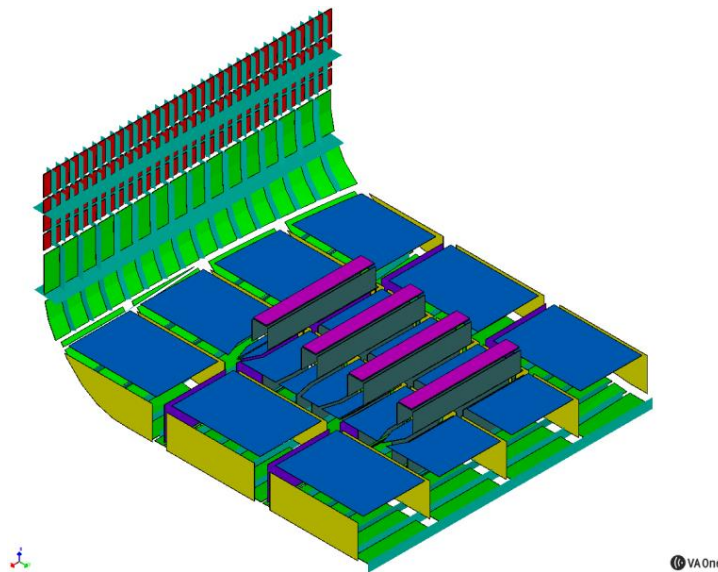

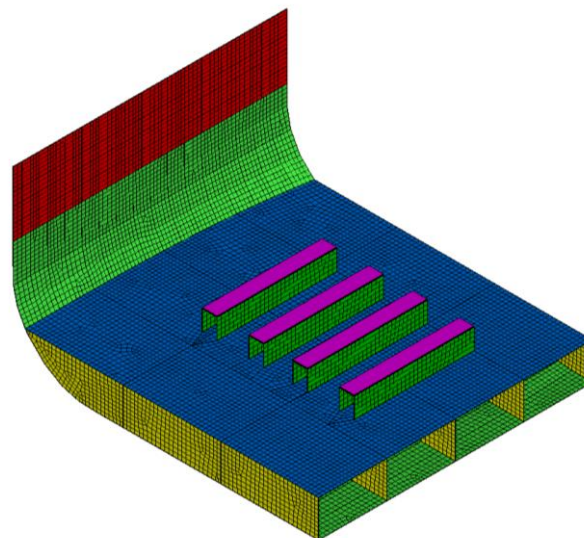*Figure 44. VTT ROPAX/RORO. Detailed SEA-model of a part.*

Figure 45. VTT ROPAX/RORO. Detailed SEA-model of a part meshed to FE.

6.3 Full FE vibroacoustic model

Modal properties of the local structural FE model were analyzed using NX NASTRAN. Mode counts and modal densities were analyzed at 3 Hz intervals up to 30 Hz. There are 3800 modes up to 30 Hz. Modal density varies from 60 modes per 1 Hz at low frequencies up to 150 modes per 1 Hz at the 22...25 Hz range, Figure 46. There are about 2000 modes below 18 Hz, so according to one rule of thumb, some 9...10 Hz is the meaningful upper limit for a full FE model of the ship.
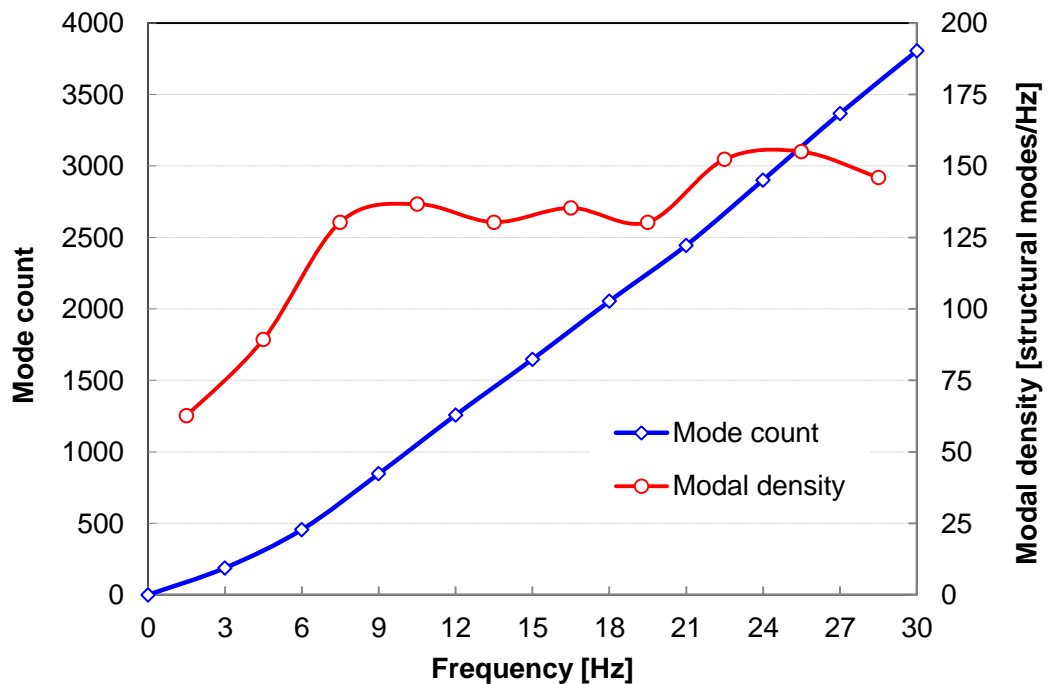

Figure 46. Mode count and modal density of the full local structural model.

A few mode shapes are plotted in Figure 47. Very many modes are associated with local responses of the "wall" structure, connecting the decks, and with the bulkheads. This is natural, since these the wall and bulkheads are relatively thin and not beam-stiffened ("wall" is 7 mm, bulkheads 9 mm). The hull and decks are very large. Also the upper double bottom has considerable response participation in very many modes. The mode shapes at the thinnest parts are somewhat distorted after 10 Hz, so the element size should be smaller in these parts when calculations are to be done up to 10 Hz. It is likely that the full local model is not very good to rigorous analysis. On the other hand, it is the stiffer lower part of the ship that is important to radiation analysis. Of course, it is possible to calculate higher frequencies using selected low order modes, like the rigid body modes.
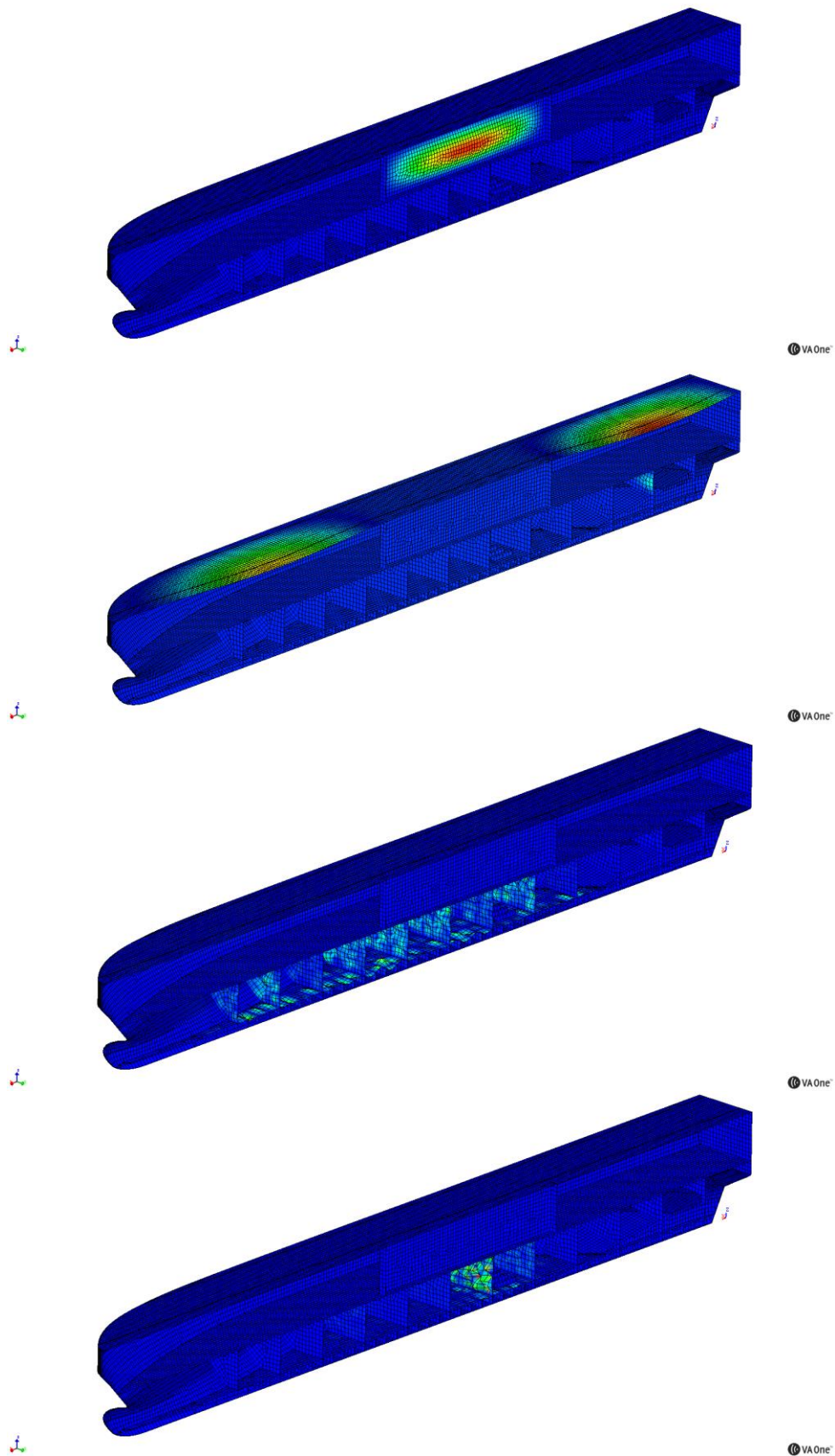
Figure 47. Global mode shapes at selected frequencies. From top to bottom:
First elastic mode (mode #7) at 0.46 Hz, a global mode at 2.01 Hz (mode #98),
a typical tanktop-bulkhead mode at 9.0 Hz (mode # 3075) and a "local"
bulkhead mode at 15.0 Hz (mode # 1651).

Note that the VA One software uses global structural modes and substructuring/component mode synthesis/superelement type strategy using series of component modes is not feasible. Instead, SEA-subsystems are used like sort of superelements connected to the FE-subsystem used as a master system.

The Face consisting of wetted element faces is in Figure 48. The face has 12085 nodes and average element size of 0.61 m. According to 6 elements/wavelength rule-of-thumb, the face is valid in acoustic radiation calculations up to 400 Hz. As low-frequency calculations will be limited to much lower frequencies, the FE Face can be significantly coarsened. At 10 Hz and 100 Hz the wavelength of sound in water is 150 and 15 m so, in principle, element size in the FE Face could be in the range 2.5 … 25 m. Of course the shape of the hull is not precisely followed if elements are very large.
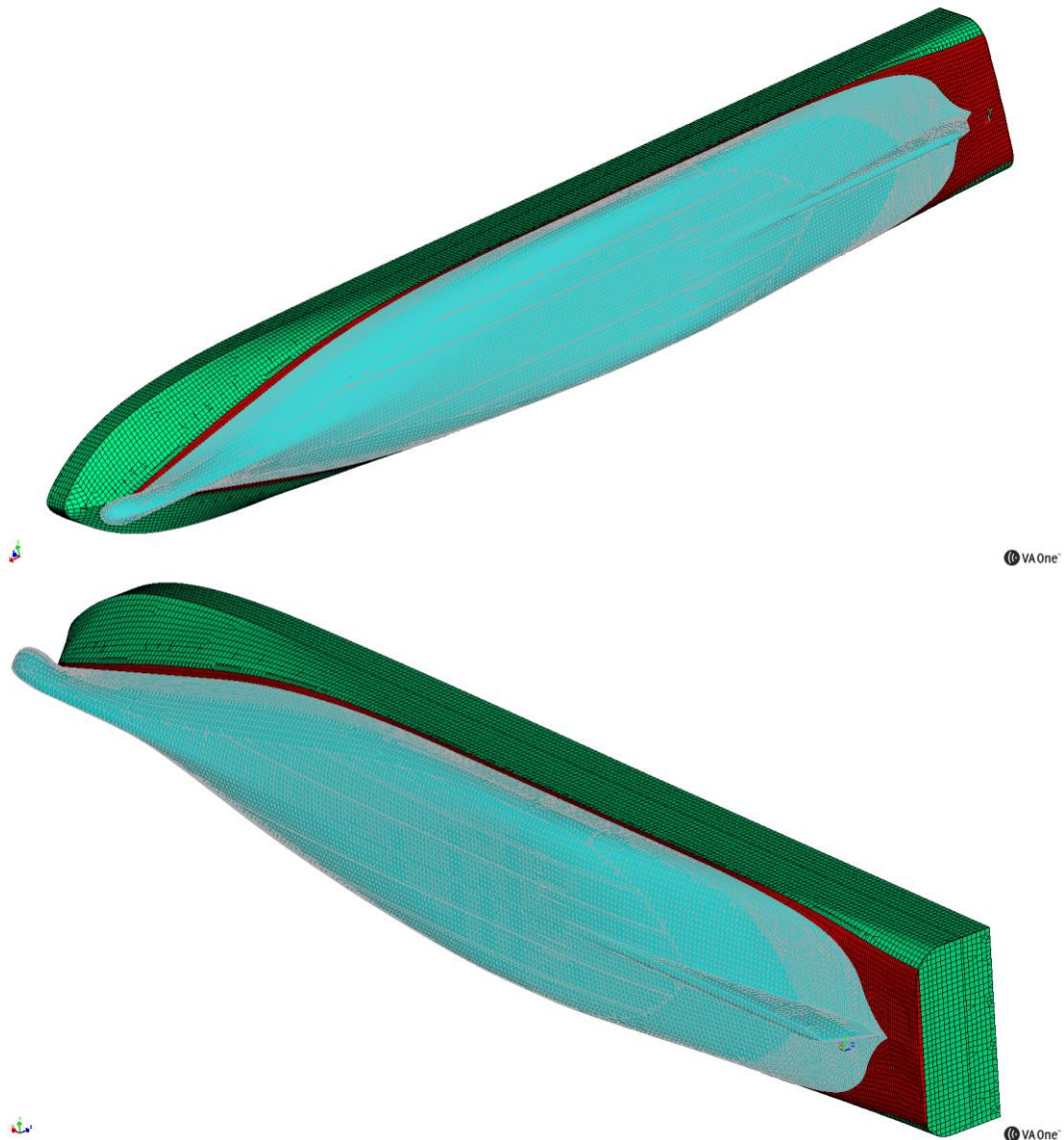

Figure 48. The FE face consisting of wetted hull elements. It consists of TRIA3 elements and it has 12085 nodes. A face is a means to connect structure to exterior fluid.

6.4 Full SEA model

Beams were modelled implicitly in the SEA model. This means that where beams and plates form a stiffened structure, ribbed panel physical properties were used. In this property a modal formulation is used to compute the vibro-acoustic properties of a plate or shell. A rectangle is fitted to the subsystem geometry by preserving area and perimeter. The natural frequencies of the simply-supported modes of the rectangular ribbed panel are found by solving an equation that includes the effects of the ribs (together with additional complicated effects such as curvature, pressurization, etc). When the bending wavelength in the base plate or shell is larger than the ribs spacing, the rib dynamics are included by smearing the rib's mass and stiffness into the base panel properties, which results in an equivalent orthotropic panel [34]. "Uniform" plate (i.e., thin plate) physical property was used for non-ribbed panels.

SEA plate and shell subsystems were first created to the S-side of the ship. The subsystems were then mirrored with respect to y=0. When a watertight system was ready, interior acoustic cavities were created using an autocreate script. Finally, underwater panels were connected to "Water SIF" with Sea Water fluid properties. Other outer panels were connected to "Air SIF".

The model consists of ca. 1350 subsystems (-structures) of which ca. 190 are acoustic cavities. There are ca 3660 junctions. As a curiosity, weight of the air in acoustic cavities (Figure 50) is 73 tons.
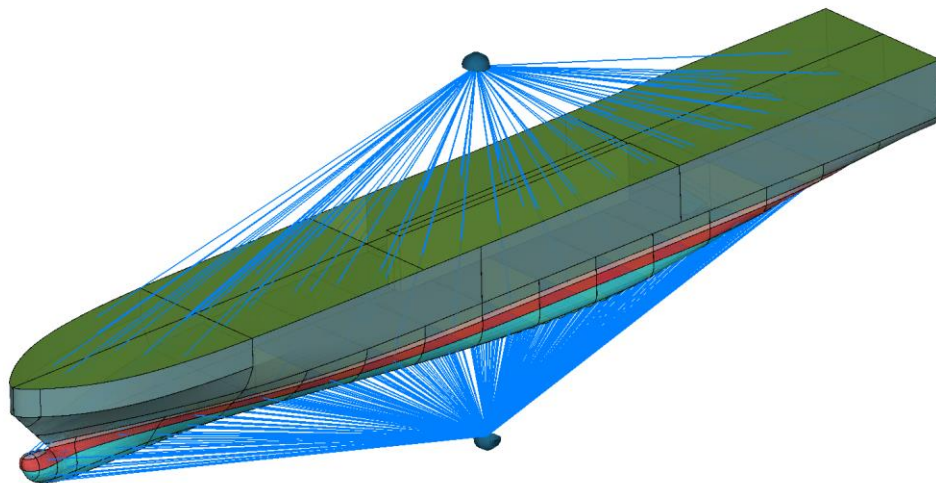

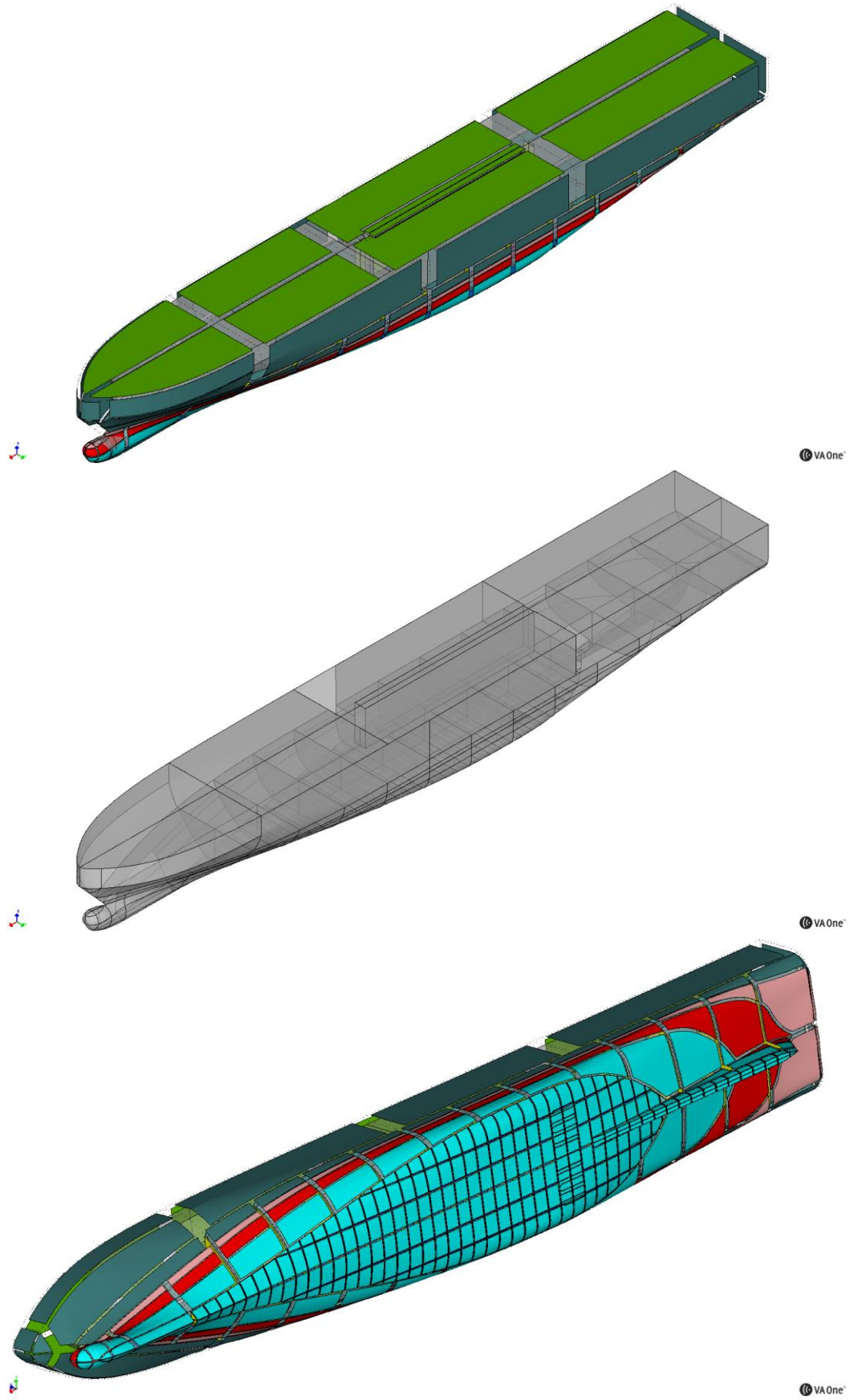*Figure 49. VTT ROPAX/RORO. SEA model overview with Water- and air SIFs.*

Figure 50. VTT ROPAX/RORO. SEA model. SEA Cavities shown in the middle figure

6.5 FE-SEA participation

To reach "low" frequencies up to, say, 100 Hz instead of 10 Hz possible with the full "local" FE-model, a hybrid FE-SEA model is an option. Another option is to create a FE-model with 100 times more elements. The candidate 1 for the FE-subsystem in a FE-SEA model is in Figure 51. Here, the structure is truncated at the waterline with exception that the red, strengthened part is included in its entirety. This FE-model includes ca. 34000 elements and 18300 nodes, so the size is roughly 30% of the full local FE model. Results of mode count / modal density analysis are shown in Figure 53. There are typically 45...60 modes per 1 Hz. Mode count of 2000 modes is reached at ca. 45 Hz and 3000 modes at 60 Hz. This suggests the model might be useful up to (max) 25...30 Hz, i.e., to the typical frequencies of 1st and 2nd harmonic of engine typical rotational speeds of 500 to 750 rpm. However, a better quality FE mesh with smaller elements would probably be needed.
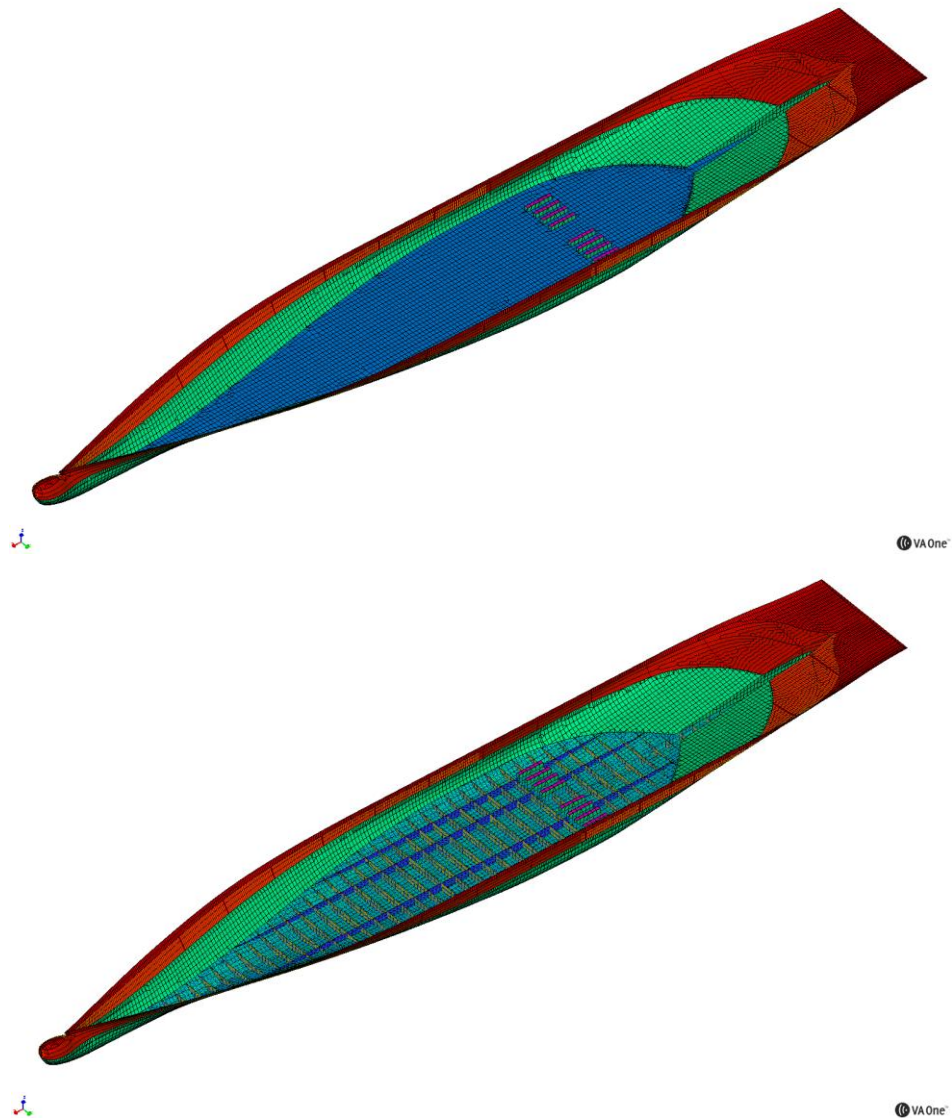

Figure 51. The candidate 1 for the FE-subsystem.

The hybrid line junctions between FE and SEA are visible in Figure 52. There are also over 1000 hybrid point junctions not shown. The calculation time of hybrid coupling loss factors may be *very* long (longer than full FE) for this kind of model.
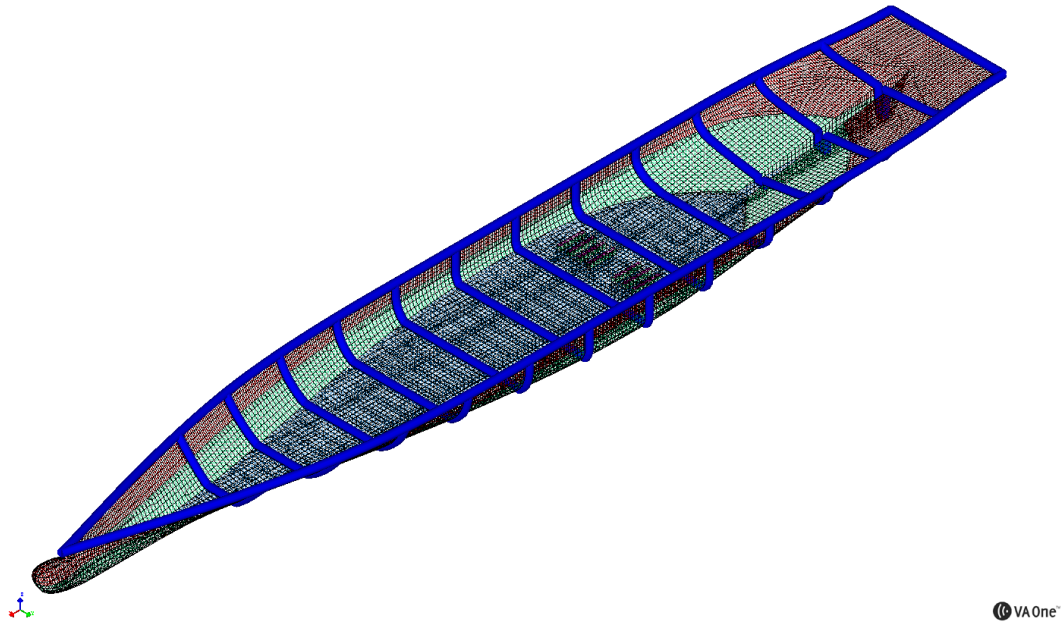

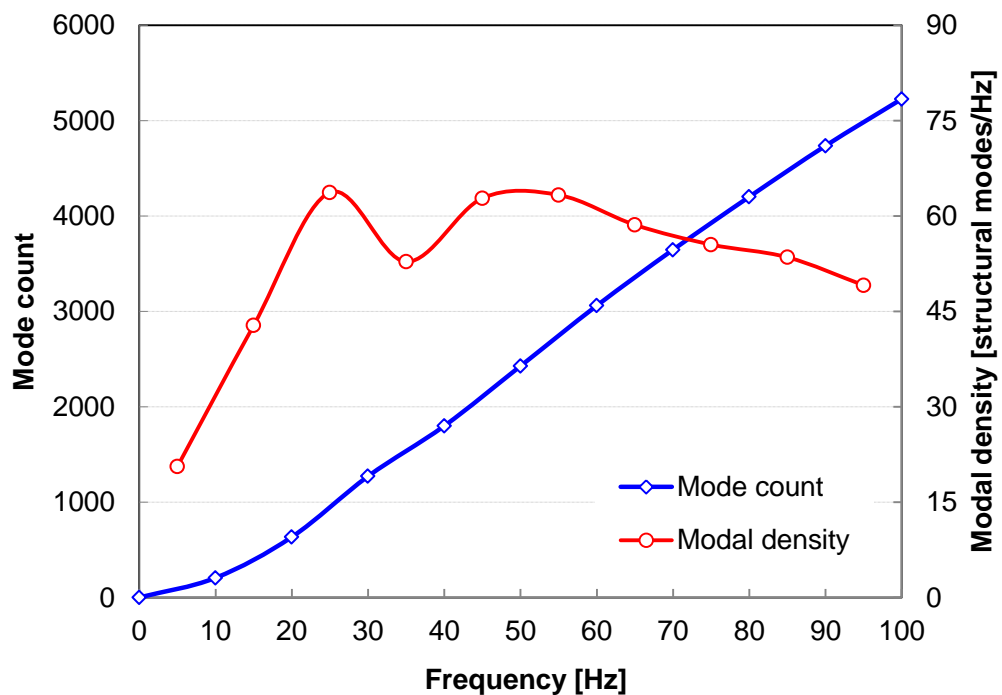*Figure 52. The hybrid line junctions (blue lines) between FE- and SEA subsystems of candidate 1.*

Figure 53. Mode count and modal density of the FE sybsystem candidate 1.

A quite radical reduction of the model size is still needed in order to reach, say, 100 Hz using a FE-SEA hybrid model. Next candidates were generated around the

machine foundations, first creating a detailed partial SEA model with explicit beams (since the full SEA model uses ribbed plates with implicit beams), then meshing it to element size of ca. 15 cm and mirroring the result at y=0. Detailed SEA model and candidate structures named 2A and 2B are shown in Figure 55. Model data is shown in Table 3. Note that candidate 2A is still an extensive structure, covering an area of roughly 11 x 22 m. Anyway, the far greater part of the wetted structure will be modelled using SEA subsystems when using either 2A or 2B.

Table 3.Model data of FE subsystem candidates 2A and 2B.

Candidate	Nodes	Elements	Modes below 100 Hz	Modes below 200 Hz
2A	55784	62480	1193	3308
2B	27998	31280	613	1682

A good modeling strategy would also to avoid of placing place hybrid junctions to very stiff places with small displacements (like corners created by junction between structures), but to extend the FE part a bit to less stiff structure (i.e., SEA plate subsystem), see Figure 54. This makes the operation more tedious since many subsystems have to be re-created. Candidates in Figure 55 are not ideal, because partition is based on natural divisions, which take place at stiff locations. However, it was decided to try the alternative 2B to prevent extra model handling work needed in solution like in Figure 54.
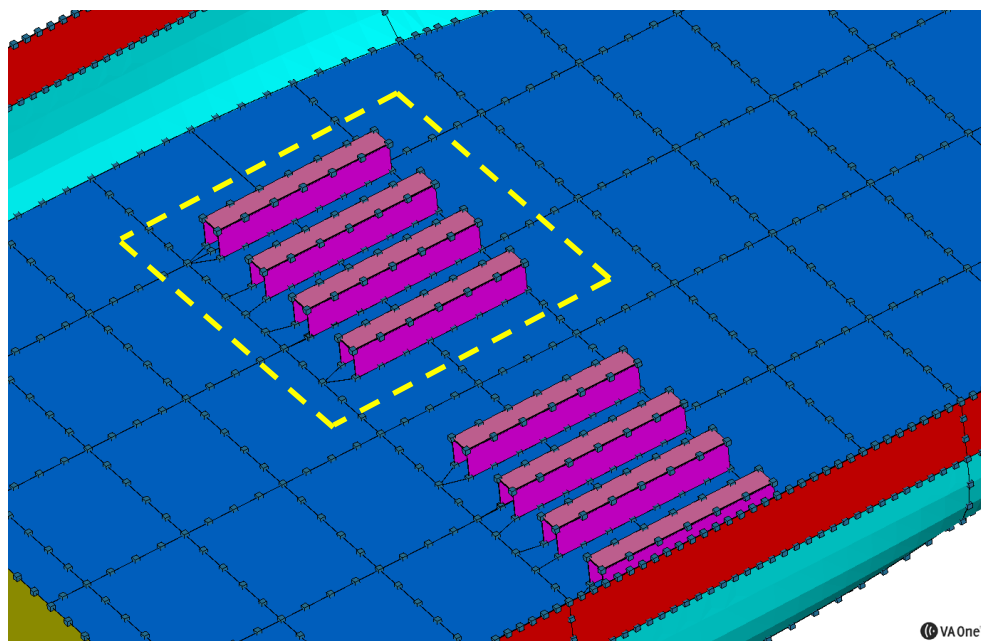

Figure 54. Example of recommended (ideal) principle for FE-SEA partition placement (dashed yellow line). Place of partition is in "loose" area, away from the stiffest parts (junctions of vertical and lateral plates) of structure.
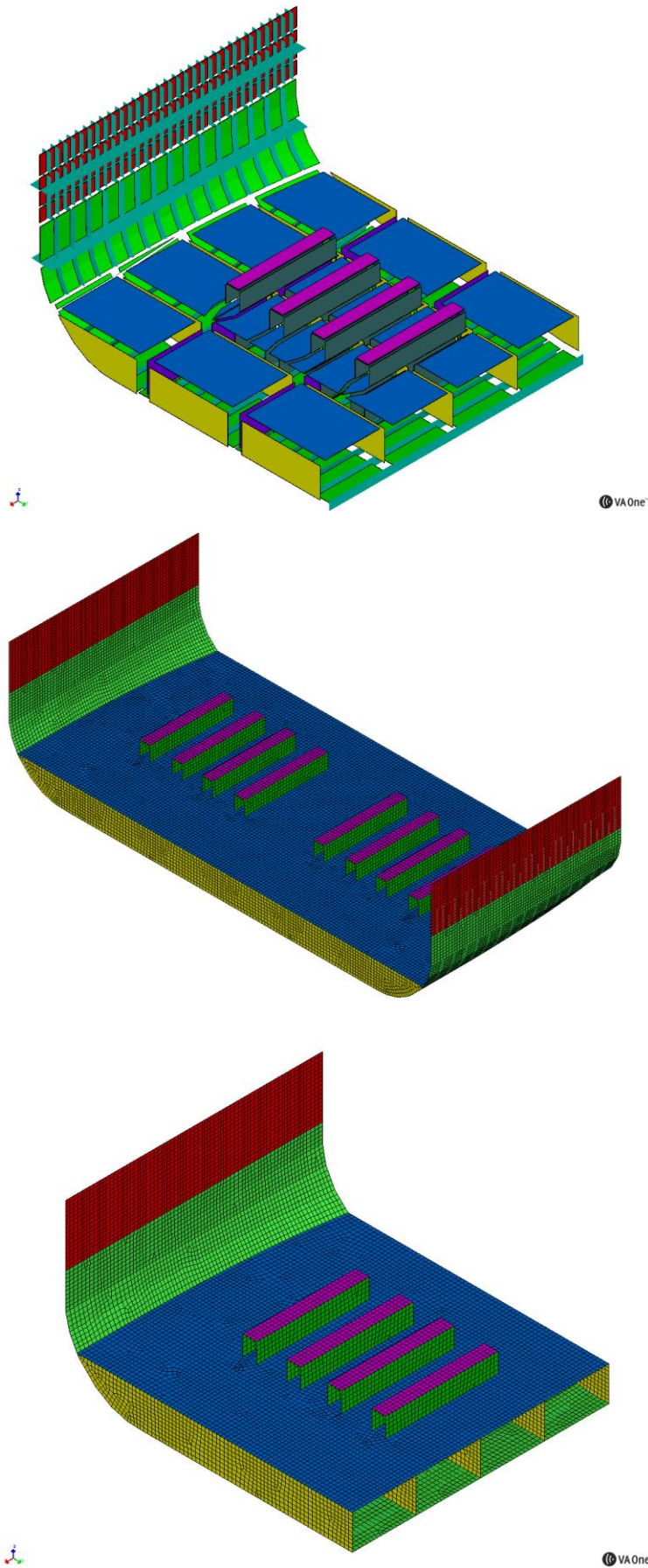
Figure 55. Detailed SEA model with explicit beams (top). Candidates 2A and 2B for the FE-subsystem (middle and bottom).

Modal behavior of 2B is depicted in Figure 56 and Figure 57. Details of model creation are depicted in Figure 58 to Figure 62.
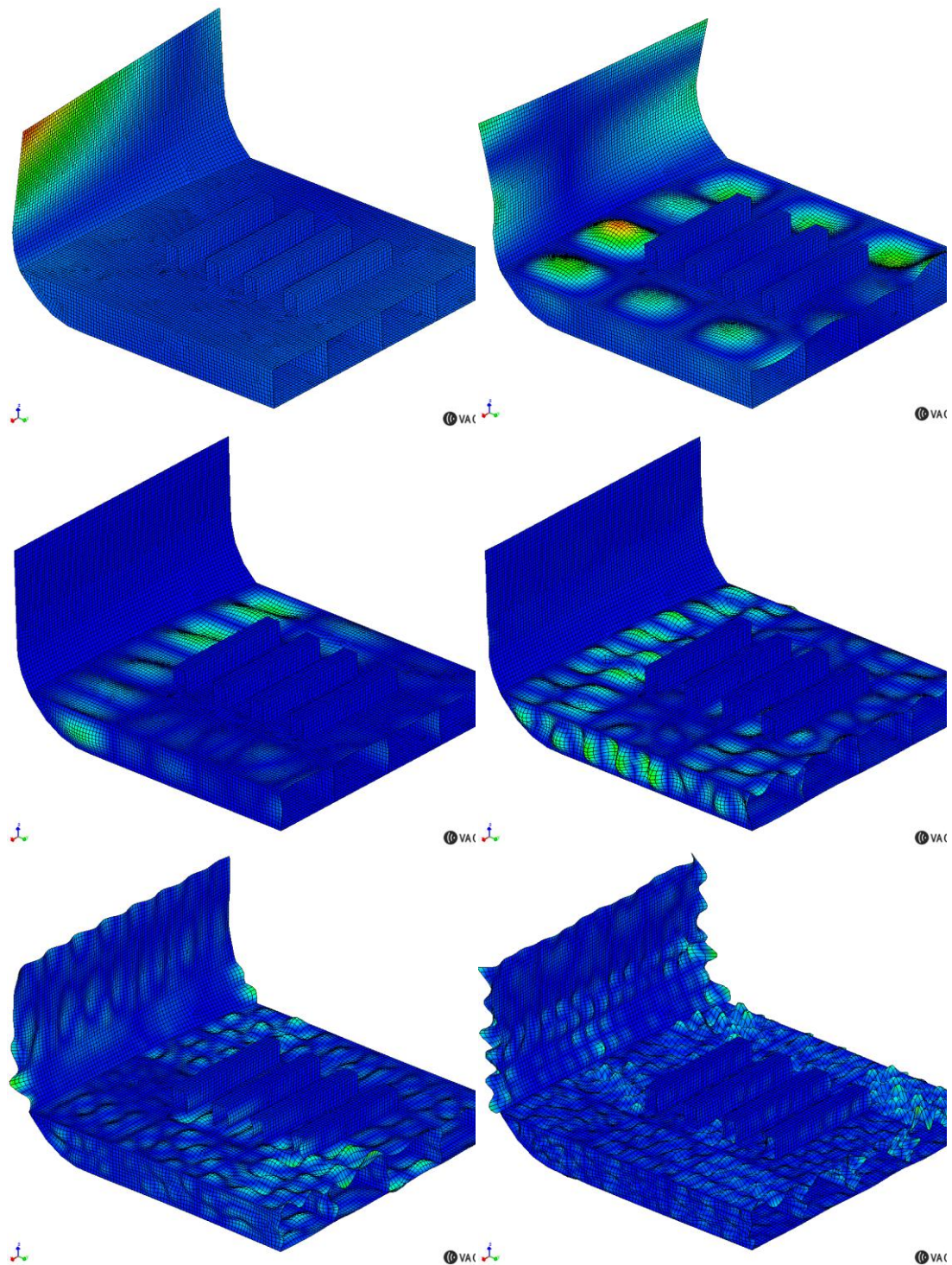

Figure 56. Modes of the candidate 2B.Top row: modes #7 (0.99 Hz) and #21 (10.4 Hz); second row: modes #46 (20.7 Hz) and #225 (50.2 Hz); bottom row: modes #617 (100.5 Hz) and #1674 (199.3 Hz).
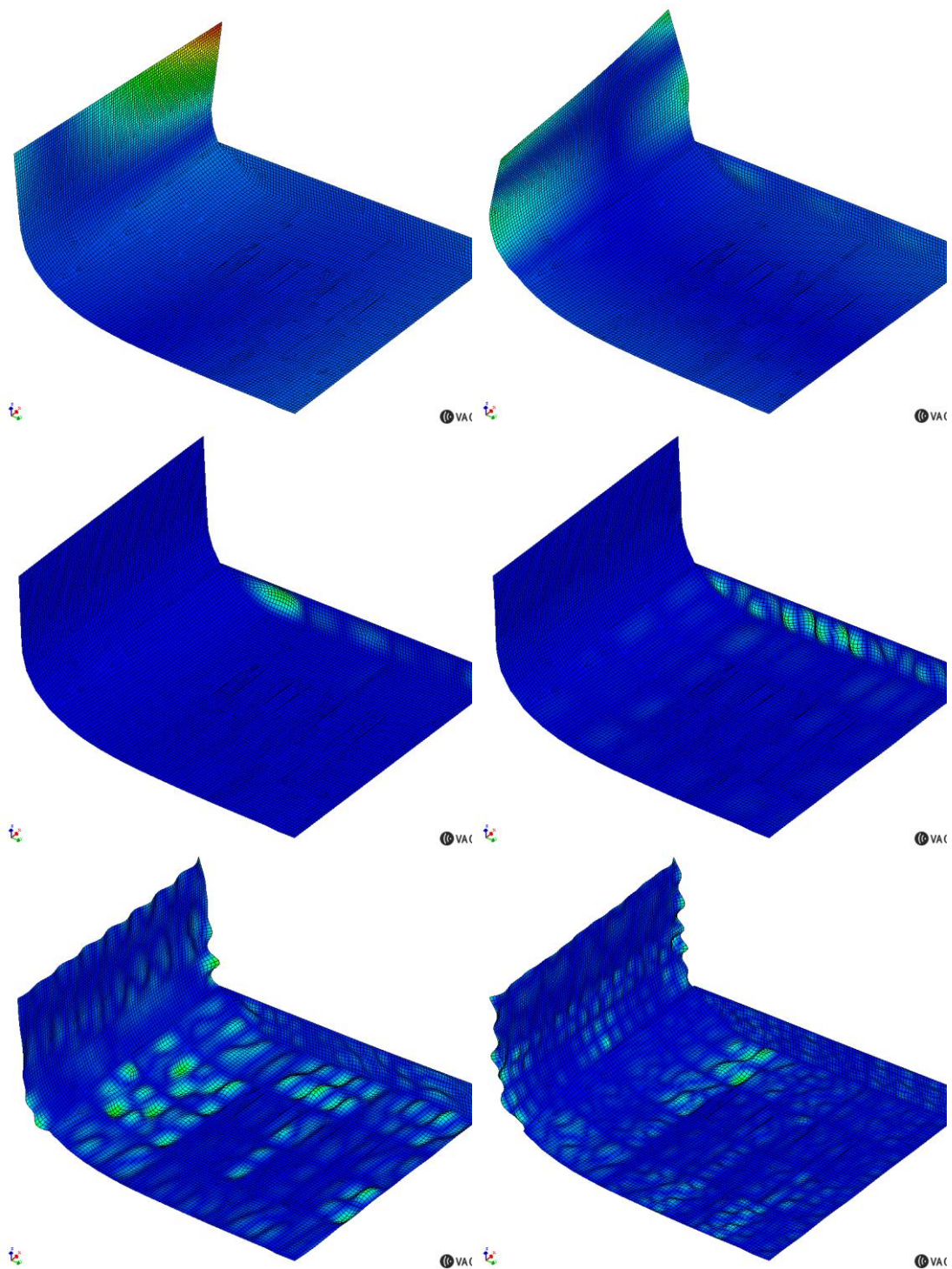
Figure 57. Modes of the candidate 2B seen from below. Top row: modes #7 (0.99 Hz) and #21 (10.4 Hz); second row: modes #46 (20.7 Hz) and #225 (50.2 Hz); bottom row: modes #617 (100.5 Hz) and #1674 (199.3 Hz).
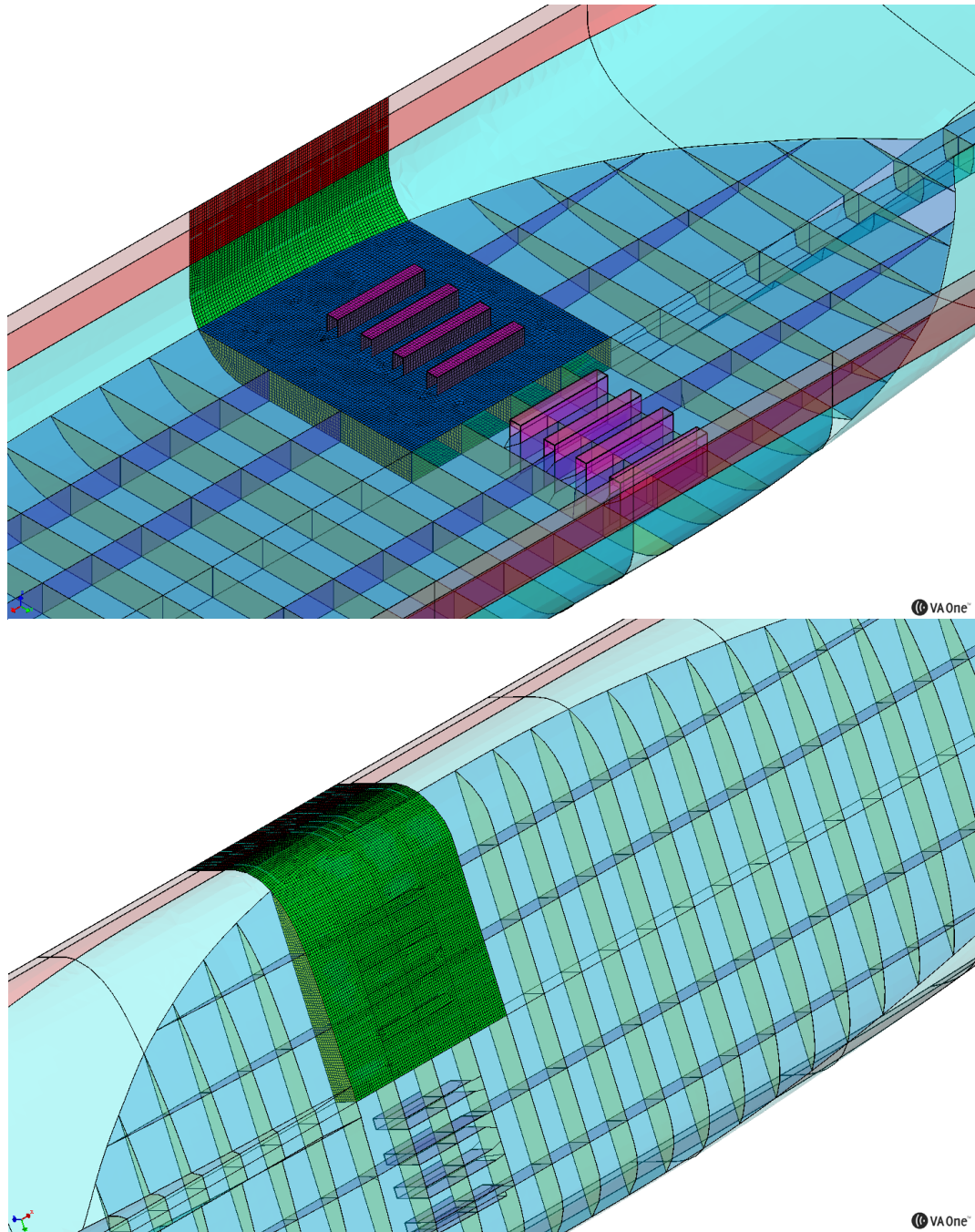
Figure 58. FE-part of FE-SEA model 2 to be assembled into SEA-model.

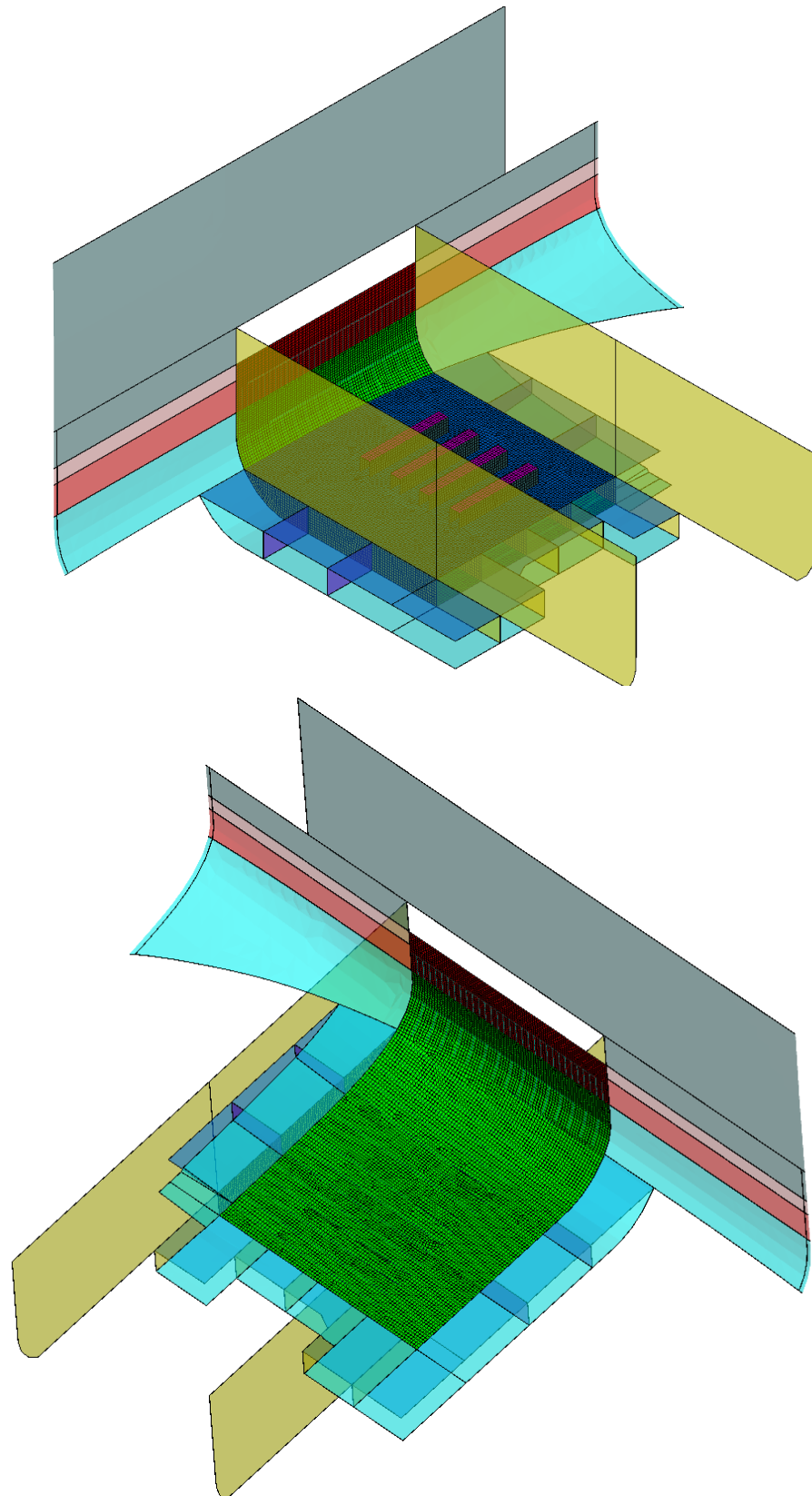*Figure 59. SEA subsystems around the densely meshed FE-part to be re-created for FE-SEA model 2.*
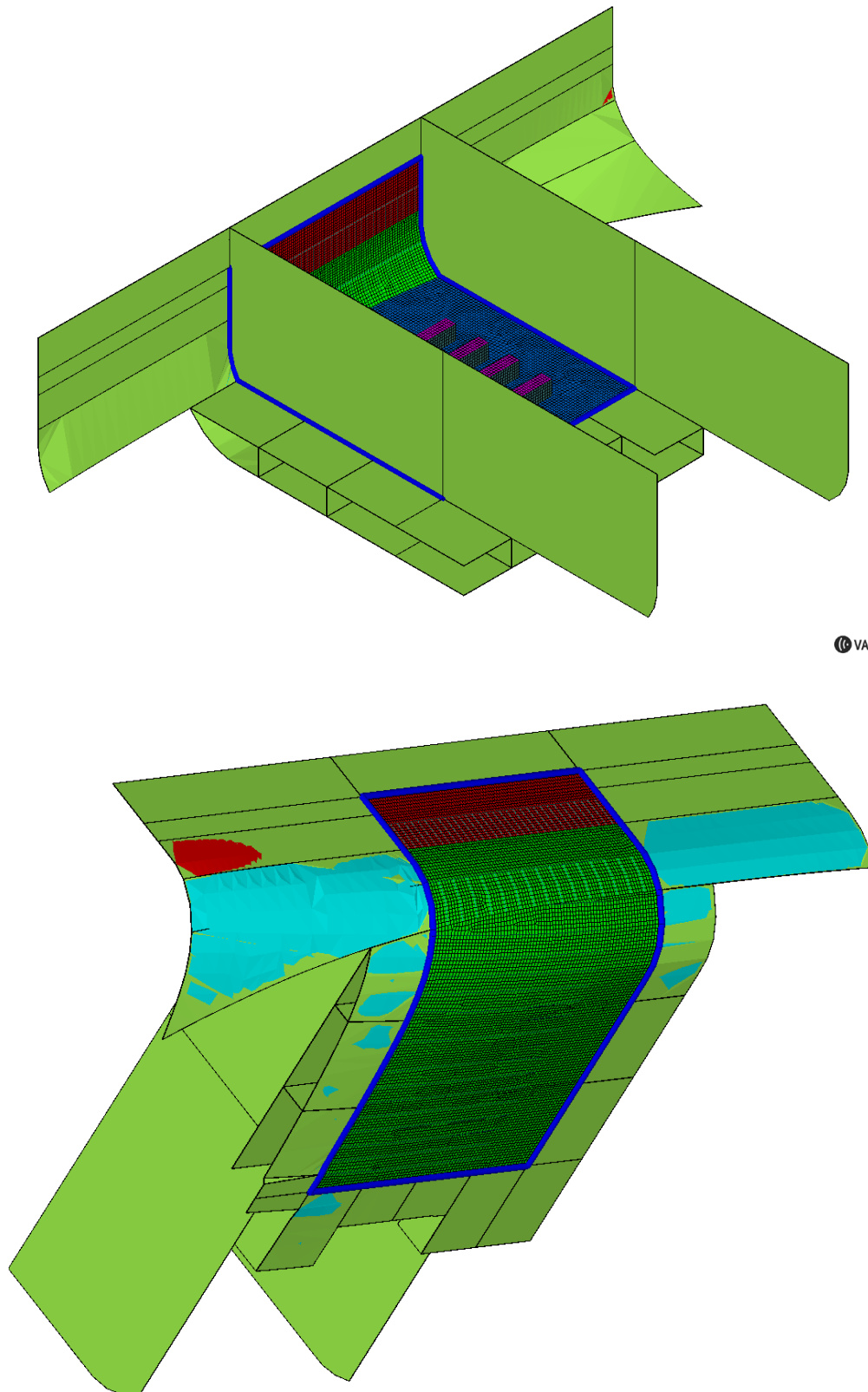
Figure 60. SEA subsystems being re-created for FE-SEA model 2. Some subsystems had to be splitted because high number of nodes in the FE-edge leads to "too distorted" shapes to be modeled as SEA flat plates. Every subsystem sharing nodes with FE was re-created. Temporary SEA-subsystems are green.
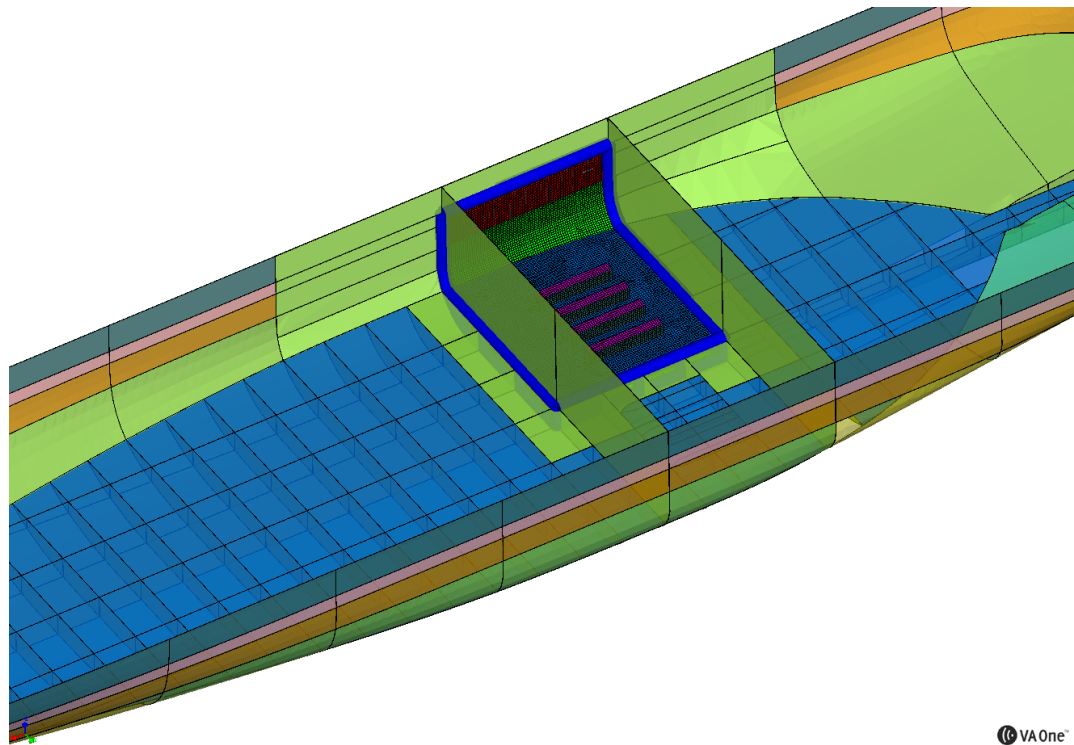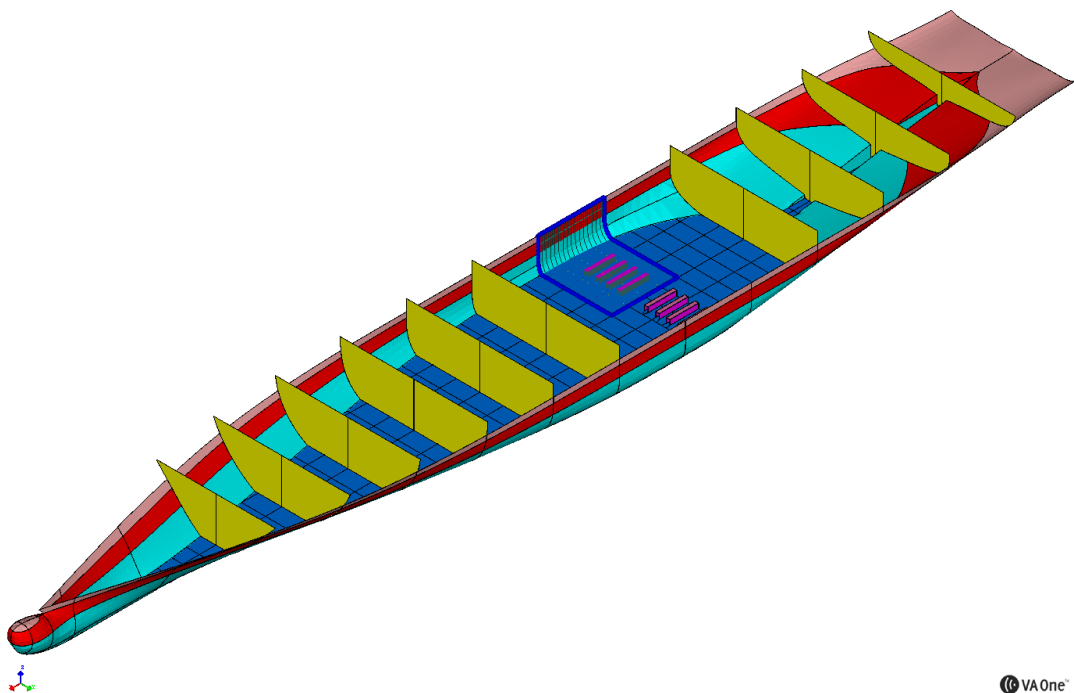
Figure 61. FE-SEA model creation. Lower part of the FE-SEA model 2 ready.

Figure 62. Junction structure of the FE-SEA model 2.Red: SEA junctions, Blue: FE-SEA hybrid junctions. All cavities are modeled using SEA. The wetted FE-part was merged to a single subsystem and a single face was defined to enable the coupling to the water SIF.

6.6 A BEM model

A trial radiation model based on the standard Boundary Element Method (BEM) was created. The model is an extension of the model FE-SEA1 with the same random forces on the engine foundation. The SIF was repla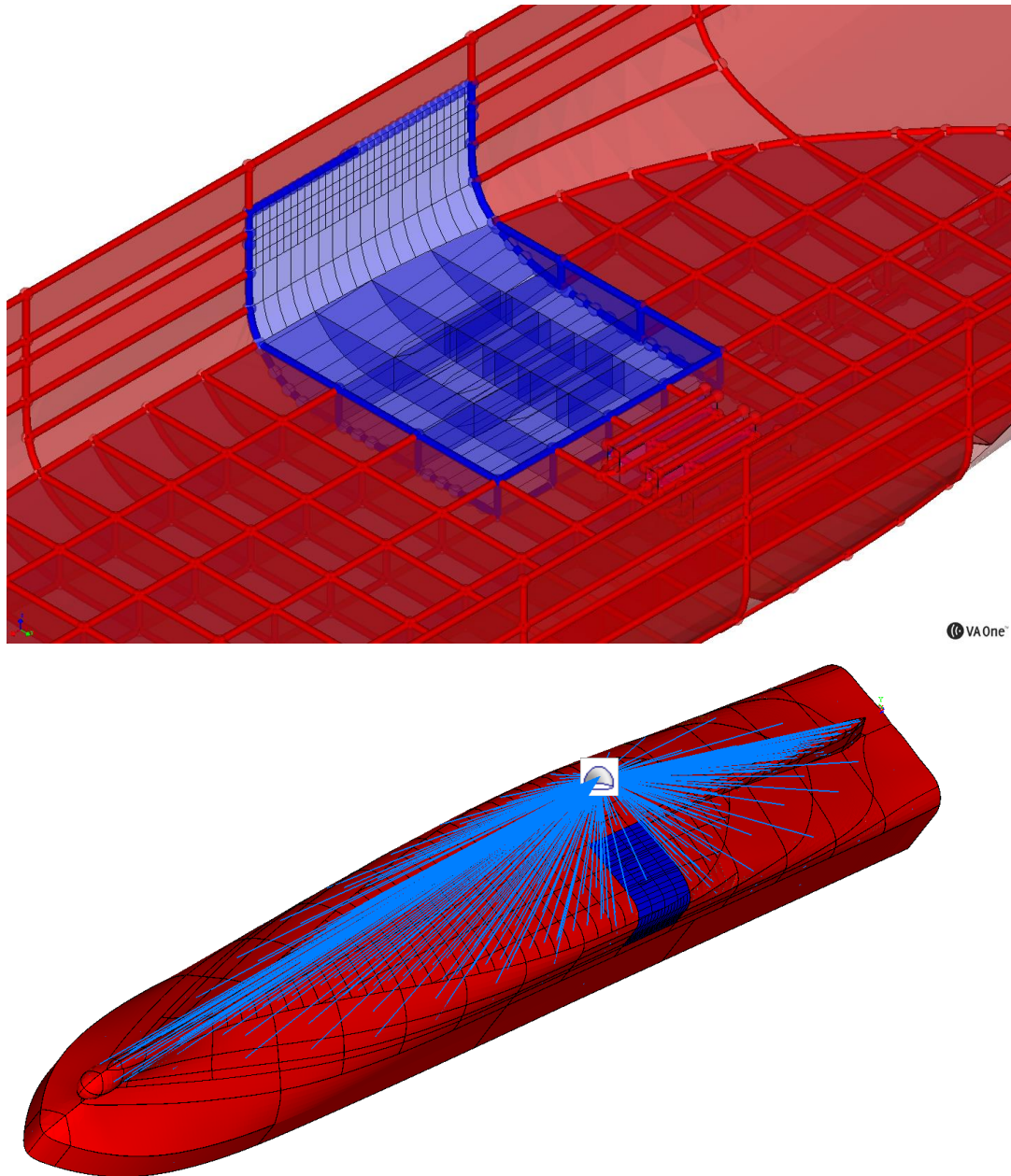ced with a BEM radiation loading connection and an underwater data recovery mesh for visualisation of the underwater sound field.

The use of fast FMM-BEM is not possible is not possible for this kind of random model. The idea of Blanchet [28] is to

i)   run coupled analysis with acoustic loading from SEA SIF, then
ii)   convert the modal structural FE subsystem to forced response subsystem and then run radiation analysis FMM-BEM.

Since complex velocity field is needed for forced response subsystem, the original model cannot be a random model like FE-SEA, but a full deterministic FE model. It is also presently not possible to use FMM-BEM in a coupled analysis, so if SEA subsystems are included, the only possibility is to use standard BEM coupled to FE subsystem of a FE-SEA model.

Modes up to 40 Hz and full solve at 1/3-octave centre frequencies up to 20/25 Hz was used. Figure 63 shows the general arrangement of the model.
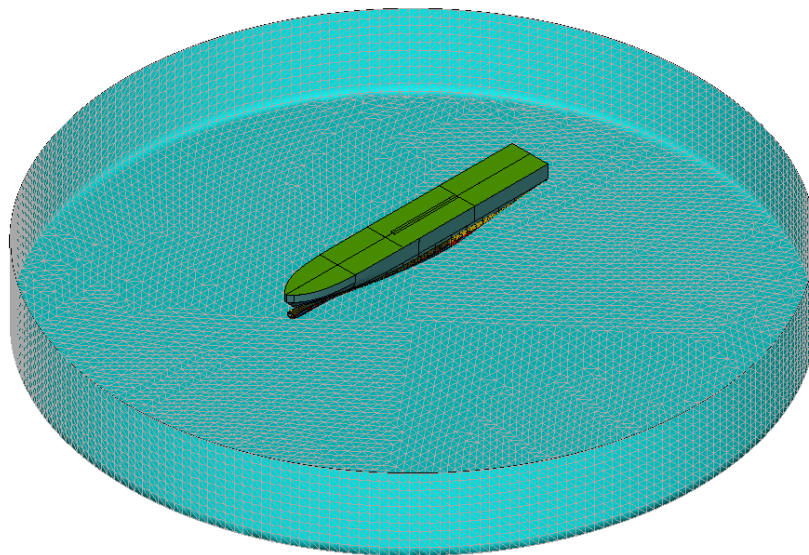

Figure 63. Model BEM1. Data recovery face shown in pale blue. Diameter of the face is 400 meters and depth 50 meters.

6.7 A note on undefined masses (weights)

Summary on weights of VTT ROPAX/RORO is presented in Table 4. The steel in FE- and SEA models correspond quite accurately to the steel-weight of 3400 tons. The steel-weight is roughly 24 % of the total displacement. The weight not explicitly present in the model is 14156.7 - 3400 ≈ 10750 tons, 76 % of the total displacement.

The question is if this nonspecific weight should be added to the model in a way or another. From the "static" point it should; from the "dynamic" point, maybe, at least some of it. When a mass is in a way or another isolated from the steel structure, the structure does not "see" the extra mass as a simple point or area mass, but as coupled dynamic properties of the isolation and the whole mass/structure. For example, a truck is in contact with the ship via tires, which are more or less distributed, flexible components. There are many means of addition exist (like non-structural mass on elements, weakly coupled noise control treatments etc.). But, if the extra weight is not described explicitly, arbitrary addition of it to the model has no added value. No weight additions were done in this report. The subject is worth a study with an aim to develop best practices on that.

Table 4. Weights of the VTT ROPAX/RORO.

Weight group	Tons	
Steelweight +	~3400	
Buildup, machinery	~6300	
= Lightweight		**~9700**
Fresh water +	352.6	
Heavy fuel oil +	1226.2	
Water ballast +	277.9	
Load (40 Trucks)	2600.0	
= Deadweight		**~4460**
Lightweight +	~9700	
Deadweight	4456.7	
= Displacement		**~14160**

6.8 Simulations

Basic and supplementary simulations were done. These are summarized in Table 5 and Table 6 respectively. No cavities were included in any basic simulations. All models containing water wetted SEA panels were run both with and without the Fluid Loading. Two issues were studied in supplementary simulations: 1) refinements of SEA-model at low frequencies by using structural power input from model FE-SEA2 and 2) effect of cavities active in supplementary simulations.

Eight random point forces, each 1N rms at 1/24-octaves, were applied on S-side engine foundation, see Figure 64.

Table 5.Model configurations in basic simulations.

Model	N modes_up to Hz	Freq. range of full solve [Hz] / N of freq. bands	Solve time per freq [min] /	Notes
FE1	2054/18	1.27...11.7 1/24-okt 78	~ 1.5	No cavities
FE-SEA1	1806/40	1.6...20 1/3-okt 12	~ 35	No cavities, no SEA or Hybrid point junctions. Solved both with and without "Fluid Loading"
FE-SEA2	1119/150	5.36...111.36 1/24-okt 105	~ 12	No cavities, no SEA or Hybrid point junctions. Solved both with and without "Fluid Loading"
SEA1	-	1.6...160000 1/3-okt 51	~ 1	No cavities included. Solved both with and without "Fluid Loading"

Table 6.Model configurations in supplementary simulations.

Model	Notes
BEM1	Model FE-SEA1 simulated with fully coupled standard BEM from 1.6 to 25 Hz with 1806 modes up to 40 Hz. Pressure release boundary, no cavities. 18 mins per freq for BEM intermediate results and 13 mins per frequency for full solve. To limit solve time only sound pressure recovered in the data recovery mesh
SEA1_equalized	Simulation at 6.3...100 Hz 1/3 octave bands using structural power input from FE-SEA2. Solved both with and without "Fluid Loading"
SEA1_cavities	Simulation at 1.6...160000 Hz 1/3 octaves with cavities active
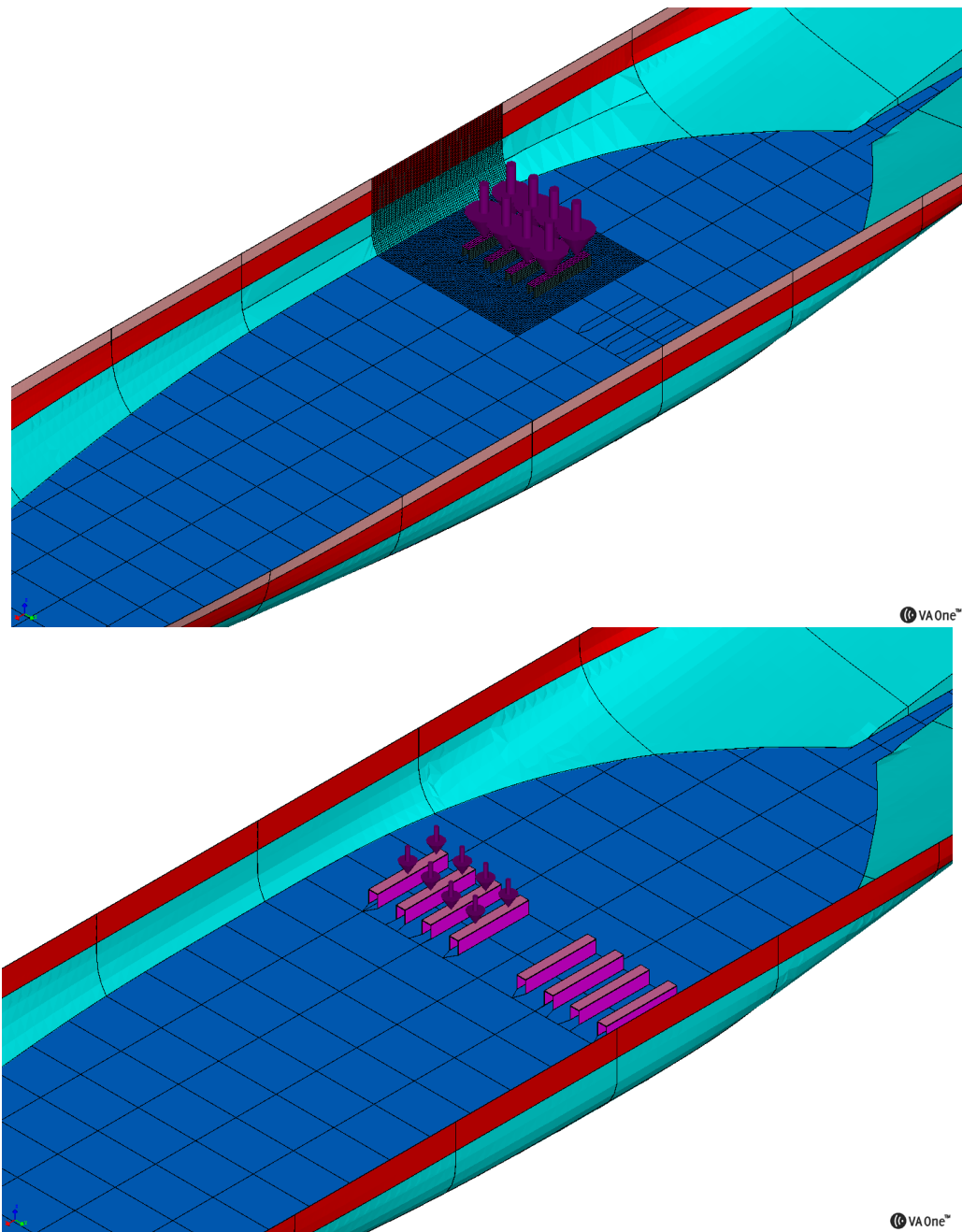
Figure 64. Point forces on S-side foundation. Above: FE-SEA2; below:SEA.

6.9 Results of basic simulations

Main results of simulations are shown in Figure 66 and Figure 67. Sound power levels are registered at the Underwater SIF visible in Figure 49 and Figure 62. Scaling to sound pressure is a matter of converting sound power W to sound pressure p using free-field propagation relation $p^2 = W*\rho c/A$.

Vibration velocities were registered in a certain area in the bottom, see Figure 65.
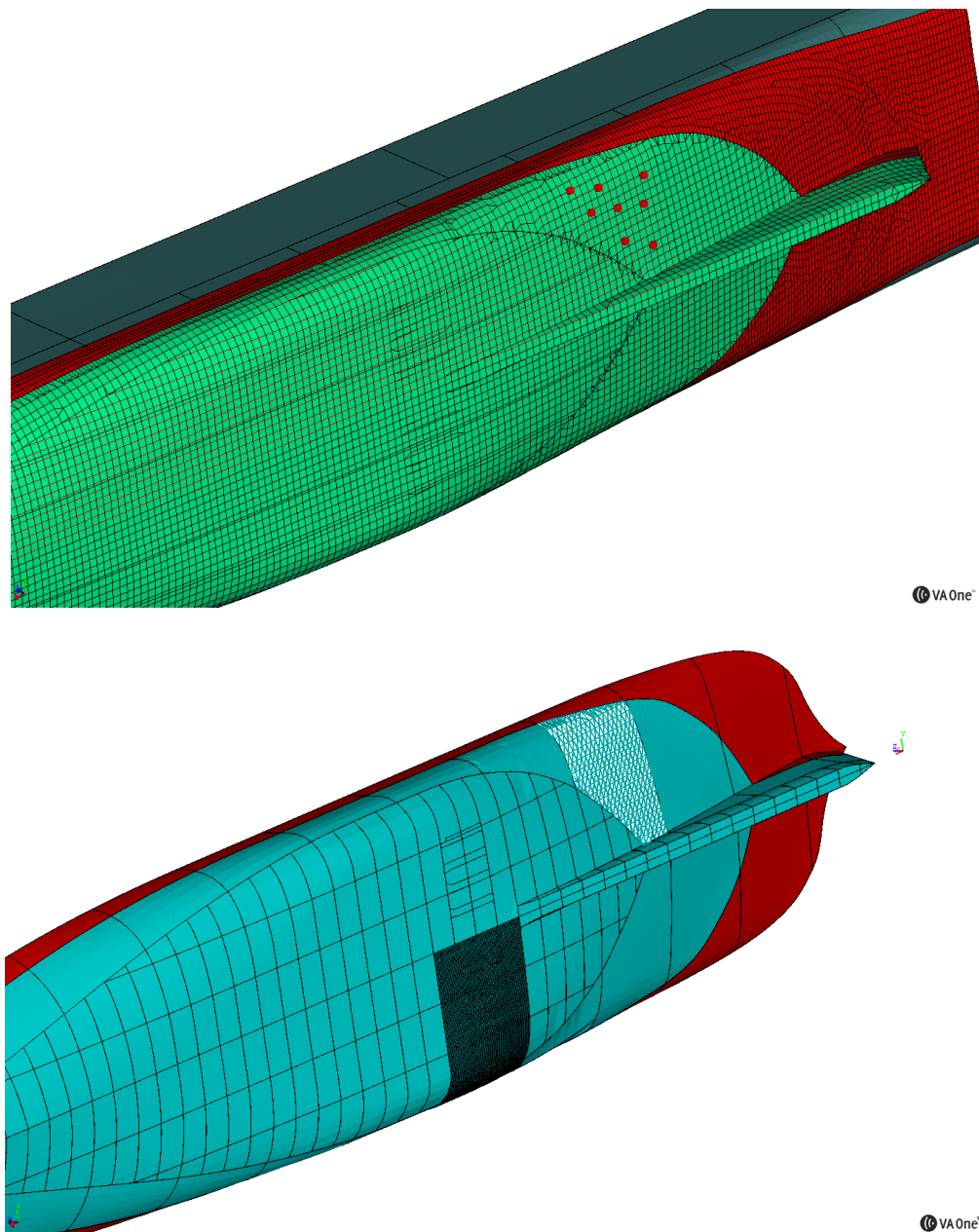
Figure 65. Target bottom structure for vibration velocity comparison. In FE-model and FE-SEA#1 the subsystem partition was different and the average velocity of a SEA plate was approximated using 8 sensors (red dots, top figure). In FE-SEA#2 and SEA –models the subsystem average for flexural wavefield is used.
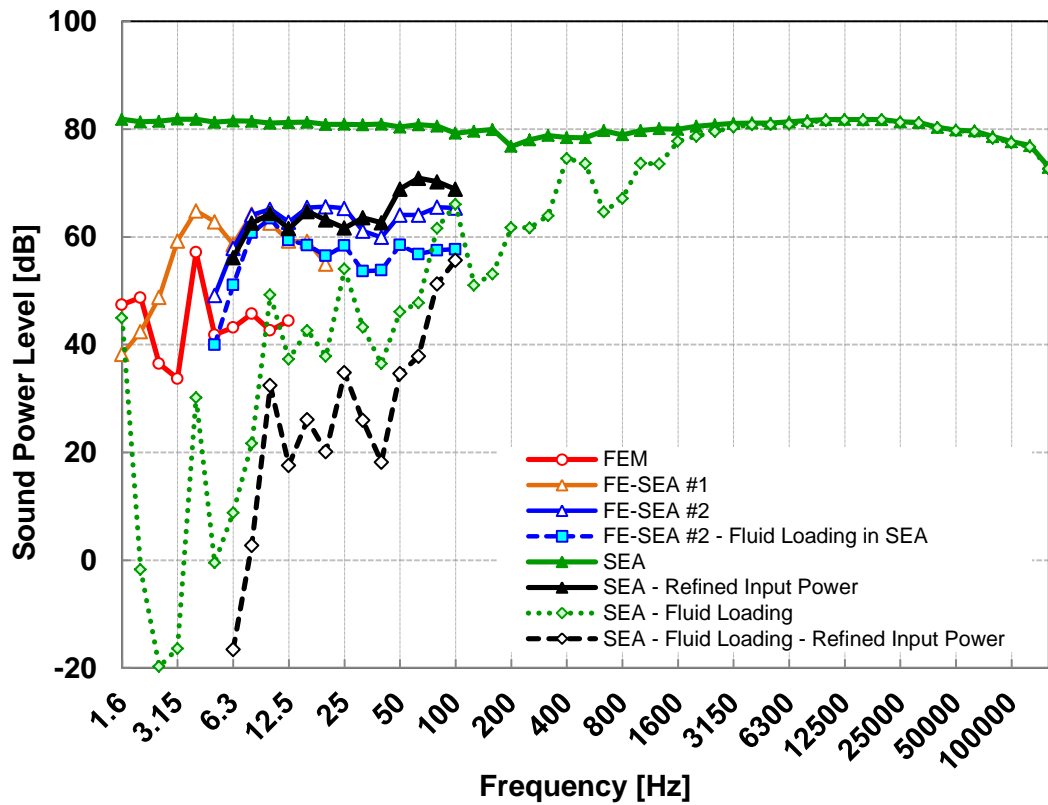
Figure 66. Underwater sound power levels at 1/3 octaves predicted using different methods.
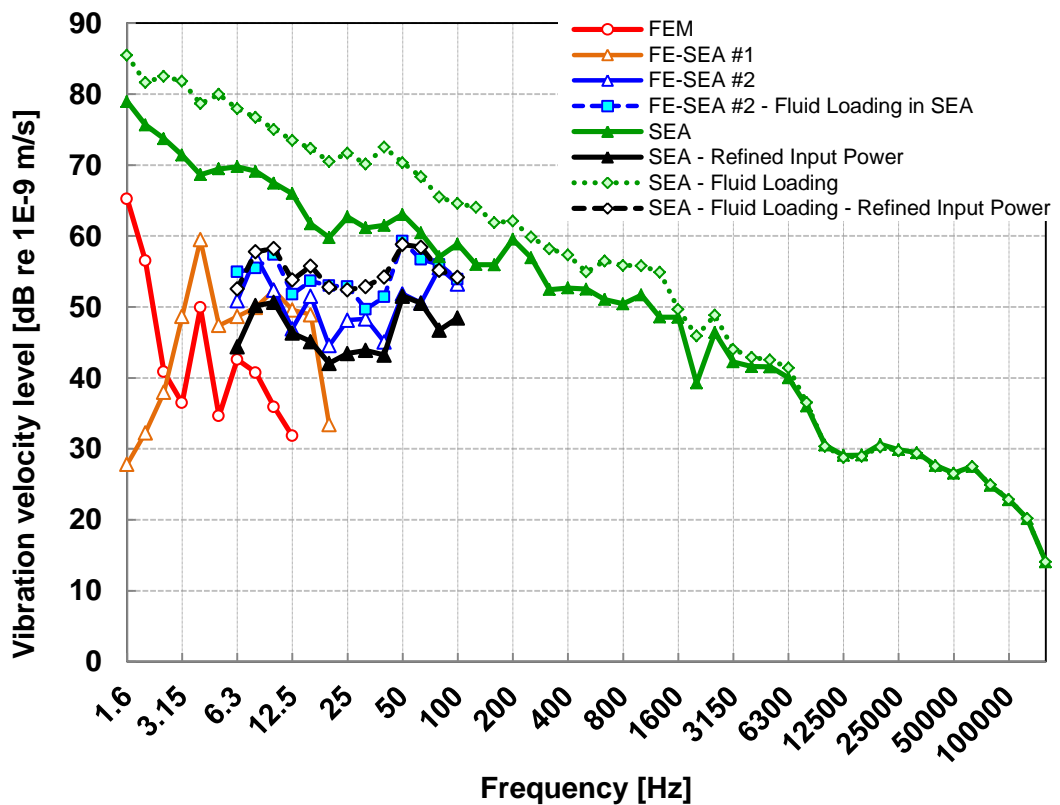
Figure 67. Vibration velocity levels of a bottom plate area at 1/3 octaves predicted using different methods.

6.10   Results of supplementary simulations

Inclusion of cavities in SEA model did not change the results, Figure 68. Instead, almost identical curves were obtained in both with and without Fluid Loading.
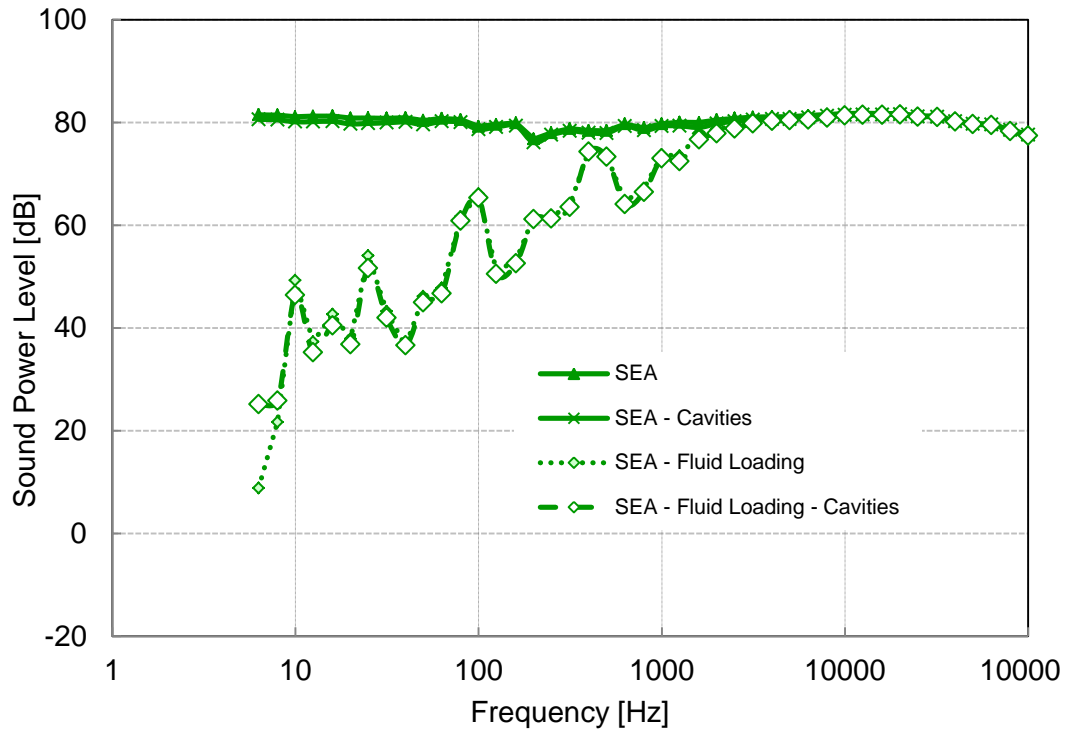
Figure 68. Effect of including acoustic cavities to sound radiation in SEA model.

The Boundary element model described in 6.6 was solved mainly in an exemplary manner. Results of sound pressure field in the data recovery face are shown in Figure 69.
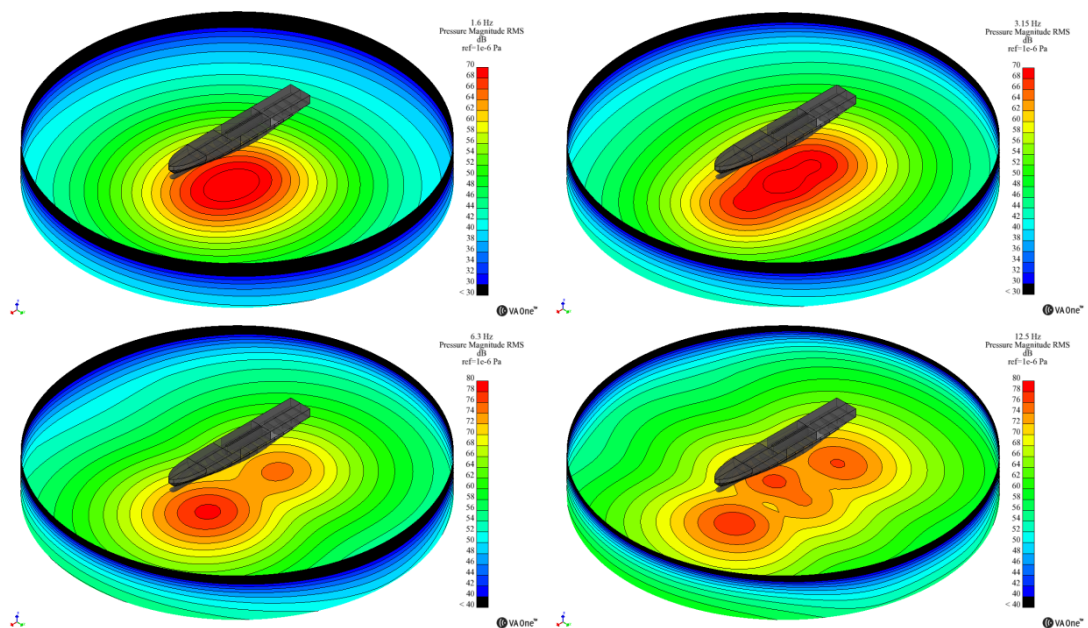
Figure 69. Sound pressure levels re 1 µPa at the data recovery face. Scales are -40 dB from top levels (nearest 5 dB).

Selected low-frequency sound power levels are presented in Figure 70. The BEM-result is approximated from the average pressure on the data recovery face shown in Figure 69 and thus not strictly comparable. On the average, the BEM-curve shows slightly lower levels than FE-SEA1. This should be the case as the surface is included in the BEM model as a pressure release boundary. At 4 Hz the BEM-simulation gave no result. The reason is unknown.
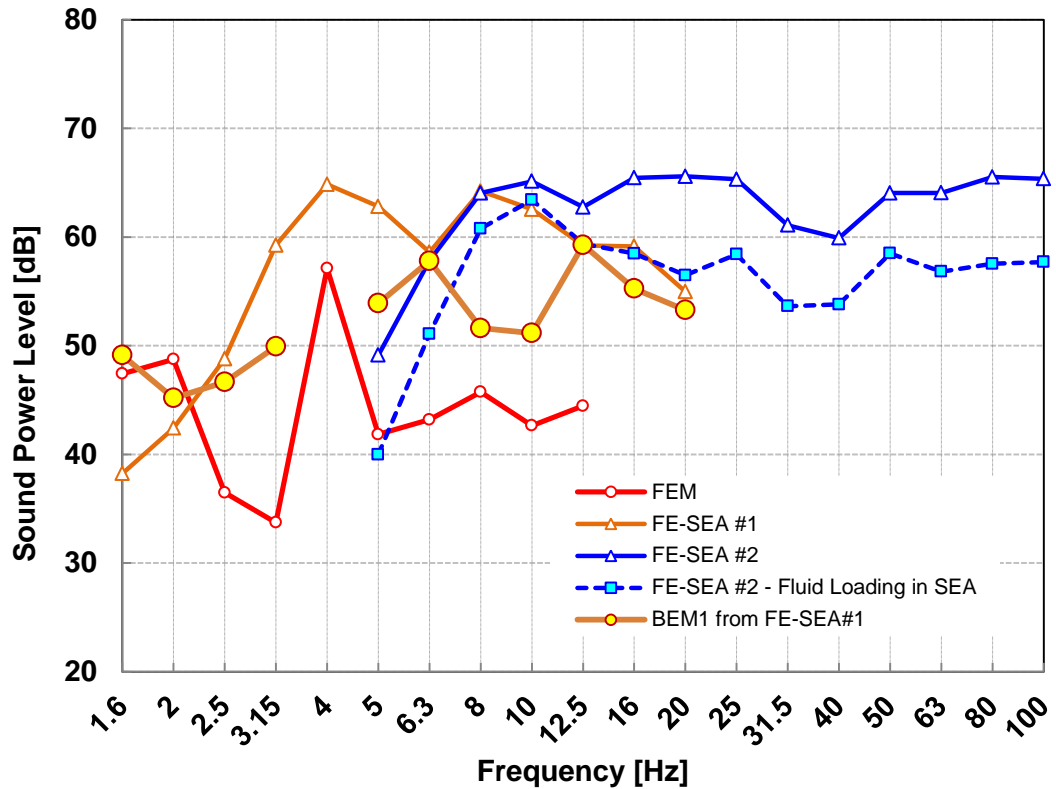
Figure 70. Low-frequency sound power levels at 1/3-octaves.

7 Conclusions

Regulations for underwater noise emission of ships put pressure on accurately predicting the emission. The frequency range defined in those regulations and recommendations is remarkably wide, even from 1 Hz to 100000 kHz. This is much more than the usual range handled in airborne noise emission of machinery and equipment.

Prediction methods of sound radiation from vibrating bodies as well as associated software tools are quite mature today. However, the wide frequency range and the sheer physical size of ships make the task of predicting very demanding.

Usual procedure of dividing the frequency range to low-, mid-, and high frequency ranges is problematic. In case of small (length under 30 m, say) vessels the task may be straightforward. In case of large ships the feasible upper frequency limit of standard low-frequency methods (FEM/BEM) might be 10 Hz or less.

It is technically possible to use Statistical Energy Analysis (SEA) throughout the frequency range. However, a SEA model must be refined at low and mid-frequencies (below 100 Hz, say) with estimations input powers more accurate than those based on infinite subsystem impedances. One possibility is to use FE-SEA model to do that and use a pure SEA-model at high frequencies only. Another possibility is to make a "sidemodel" using FEM for calculation of input powers and feed them to a SEA-model. Anyway, some discontinuity problems with different methods are expected to occur. Another issue in predictions with the particular software (VA One) is the use of "Fluid Loading" on water-wetted panels. This option seems to underestimate the radiated power by setting the radiation efficiency to a very low value.

Anyway, prediction of sound pressure in discrete points or a small area far from a ship is subject to large uncertainty even is totally isotropic unbounded conditions.

The best starting point for a model is a FE-geometry in which the whole structure is divided into manifold parts which can directly serve as a basis for SEA-plate subsystem creation. The number of beams/frames in a large ship is so extensive that modeling of panels as ribbed plates is the recommended option.

The inclusion of unspecified mass (engines, cargo, pipes, furniture, etc.) is a question with no good solution. These artefacts have also stiffness properties and arbitrary addition of non-structural mass does not improve the model. It is always better to make models with as few fictitious details as possible.

8   Summary

To goal was to review and demonstrate methods available for prediction of underwater sound radiation from large ship structures for full frequency (ca. 10...100000 Hz) range.

Background, based on associated recommendations and standards, was reviewed first. The frequency range dealt with is extensive, even from 1 Hz to 100 kHz. Physical background and prediction methods available were reviewed next. Although most prediction methods are quite mature today, the sheer size of ships as well as extended frequency range makes the prediction task very demanding. There is a lack of reliable examples of prediction examples and correlation between experiments. Prediction of sound pressure in discrete points or a small area far from a ship is inherently subject to large uncertainty, even is totally isotropic unbounded conditions.

A small structure was the first example. The (ideal) low-frequency range extends up to ca 250 Hz and high-frequency range upwards from 2500 Hz. Point forces were used as excitation. The methods were used over whole possible frequency range. The most drastic finding is the remarkable effect of "Fluid Loading" option of VA One on sound radiation in SEA-models. It was concluded that SEA without "Fluid Loading" overestimates the radiation and a model with it underestimates. However, it is not wise to draw strict conclusions from a single example. This question that should be studied more.

A part of a 164 m long ship was then modeled. It was noticed that a standard "local" type FE model is not feasible to simulations at frequencies over 10 Hz. By modeling only the lower part of the ship with FE and the rest with SEA the upper frequency range could be raised up to ca. 25-30 Hz. To reach 100 Hz or more with a meaningful sized model, the FE part must be smaller. This was tried. A full SEA model was also created as well as a BEM model. The results again scatter quite much. It was also demonstrated how the SEA-prediction at low frequencies could be refined by using input power calculated using FEM.

An analyst must be aware of differences in methods. A SEA model does not account for global vibration fields, only "local" ones. HAJ formulations used between FE-structure and fluid used assume that the structure is baffled. Better approximation is obtained using BEM. SEA and FE-SEA models assume random excitations, whereas correlation effects can be taken into account in full FE. Radiation analysis using BEM is possible in both random and deterministic excitation cases.

This kind of modeling project is instructive. Much of the learned is in the form of tacit knowledge.

References

1. Arveson, P.T. % Vendittis, D.J. Radiated noise characteristics of a modern cargo ship. J.Acoust.Soc.Am 107(2000)1, p. 118-129.

2. De Robertis, A., Hjellvik, V. Williamson, N. J., and Wilson, C. D. 2008. Silent ships do not always encounter more fish: comparison of acoustic backscatter recorded by a noise-reduced and a conventional research vessel. ICES Journal of Marine Science, 65: 623–635.

3. McKenna, M.F. Underwater radiated noise from modern commercial ships. J.Acoust.Soc.Am 131(2012)1, p. 92-103.

4. Underwater noise of research vessels. Review and Recommendations. International Council for the Exploration of the Sea. ICES Cooperative Research Report no 209. Copenhagen 1995. ed. Mitson, R.B. 61 p.

5. Bahtiarian, M. A standard for the measurement of underwater noise. Presentations from the 2007 NOAA Vessel-Quieting Symposium. http://www.nmfs.noaa.gov/pr/pdfs/acoustics/session1_bahtiarian.pdf. 03.09.2012.

6. Powering the world's navies. Wärtsilä Corporation 2011. 16 p.

7. American National Standard. Quantities and Procedures for Description and Measurements of Underwater Sound from Ships – Part 1: General Requirements. ANSI/ASA S12.64-2009/Part1. 23 p.

8. Rules for Classification of Ships. Part 6 Chapter 24. Silent Class Notation. Det Norske Veritas, January 2010. 18 p.

9. Lankila, A. Full scale underwater noise measurements. Report VTT-R-03893-11. "Unno" project Deliverable D.2.5. 89 p. Espoo 2011.

10. de Jong, C.A.F. Characterization of ships as sources of underwater noise. Proceedings, NAG/DAGA 2009, Rotterdam. p. 271 – 274.

11. Fischer, R. & Collier, R.D. Noise Prediction and Prevention on Ships. In: Handbook of Noise and Vibration Control. Ed. Crocker, M.J. Chapter 101, p. 1216 – 1232. John Wiley, 2007.

12. Ross, D. Mechanics of Underwater Noise. Peninsula Publishing, 1987. 375 s.

13. Feit, D. Sound Radiation from Marine Structures. In: Encyclopedia of Acoustics, ed. Malcolm J. Crocker. Chapter 41, p. 459-468. John Wiley, 2007.

14. Blake, W. Fundamental Underwater Noise Sources. In: Encyclopedia of Acoustics, ed. Malcolm J. Crocker. Chapter 45, p. 501-520. John Wiley, 2007.

15. Collier, R.D. Ship and Platform Noise, Propeller Noise. In: Encyclopedia of Acoustics, ed. Malcolm J. Crocker. Chapter 46, p. 521-537. John Wiley, 2007.

16. Fahy, F.J. Foundations of Engineering Acoustics. Academic Press, 2001. 443 p.

17. Uosukainen, S. D2.2b Report on vibro-acoustic source models of ships. RESEARCH REPORT VTT-R-00434-13. Espoo 22.1.2013. 17 p.

18. Urick, R.J. Principles of Underwater Sound. 3rd edition. Peninsula Publishing, 1983. 423 p.

19. Principles of Underwater Sound. ed. Carl Eckard. Reprinted and distributed by the Research Analysis Group, Committee on Undersea warfare, National Research Council. Originally issued as Division 6, Volume 7, NDRC summary technical reports. books.google.com. Original publishing date unknown. 295 p.

20. Carey, W.M. Lloyd's mirror-image interference effects. Acoustics Today, April 2009. p. 14-20.

21. Fahy, F. Gardonio, P. Sound and structural vibration. Radiation, transmission and response. 2nd edition, Academic Press, 2008. 633 s.

22. Cremer, L., Heckl, M. & Petersson, B.A.T. Structure-Borne sound. Structural vibrations and sound radiation at audio frequencies. 3rd edition, Springer 2005. 607 p.

23. Shorter, P. Modeling noise and vibration transmission in complex systems. In: A.K. Belyaev, R.S. Langley (eds.), IUTAM Symposium on the Vibration Analysis of Structures with Uncertainties, IUTAM Book series 27, Springer 2011. p. 141 – 156.

24. Cotoni, V., Shorter, P., & Langley, R. Numerical and experimental validation of a hybrid finite element-statistical energy analysis method. J. Acoust. Soc. Am. 122(2007), 259-270.

25. Petyt, M. & Jones, C.J.C. Numerical methods in acoustics. In: Advanced applications in acoustics, noise and vibration. Eds. Fahy, F. & Walker, J. Taylor&Francis, 2004. Chapter 2, p 53-99.

26. Gilroy, L. Predicting very low frequency underwater radiated noise from full-scale ships. CFA/DAGA '04. Strasbourg.

27. Blanchet, D. & Caillet, A. Design of Acoustic Insulation in Ships Based on Predictive Vibro-Acoustic Models. Proceedings of DAGA 2011 – Dusseldorf. 2p.

28. Blanchet, D. Use of FE/SEA hybrid methodology for predicting low frequency response in marine structures. VAUC 2013 Conference, Paris France June 5-6, 2013. ESI-Group.

29. Lyon, R.H: & DeJong, R.G. Theory and Application of Statistical Energy Analysis, Second Edition. Butterworth-Heinemann, Boston, 1995. 227 p.

30. Blanchet, D. & Matla, A.S. Building SEA predictive models to support vibro-acoustic ship design. Proceedings of NAG/DAGA 2009 – Rotterdam. 4 p.

31. Boroditsky, L. et al. Shipboard noise prediction for naval architects. Euronoise 2006, 30 May – 1 June 2006, Tampere, Finland. 7 p.

32. Shorter, P.J. & Langley, R.S. Vibro-acoustic analysis of complex system, Journal of Sound and Vibration, Vol. 288(2005), p. 669-699.

33. Shorter, P.J. & Langley, R.S, On the reciprocity relationship between direct field radiation and diffuse reverberant loading, Journal of Sound and Vibration, Vol. 117(2005) no 1, p. 85-95.

34. VA One 2012 EFM & VSEA Modules. User's guide, theory & QA. ESI Group 2012. 46 p.

35. Borello, G. Virtual SEA analysis of a warship classification. 10eme Congres Francais d'Acoustique, Lyon 12-16 April 2010. 6 p.

36. Mace, B. & Shorter, P. Energy flow models from finite element analysis. Journal of Sound and Vibration, 233(2000)3, p. 369-389.

37. Bernhard, R.J. The family of EFA equations and their relationship to SEA. Novem Conference 2000. 12 p.

38. Cabos, C. et al. Application of an Energy Finite Element Method to the Prediction of Structure Borne Sound Propagation in Ships. internoise 2001,The Hague, The Netherlands, 2001 August 27-30. 6 p.

39. Gilroy, L. et al. Energy Finite Element Analysis (EFEA) algorithms & software for ship noise. Technical Memo NCE TM 05-029. Noise Control Engineering, Inc 2005. 59 p

40. Kim, S-H. et al. Exterior noise predictions of commercial ships using energy flow analysis methods. ICSV15 Conference, 6-10 July 2008, Daejeon, Korea. 8 p.

41. Parunov, J. et al. Review of Methods for Structure Born Noise Prediction on Ships. Prodogradnja 63(2012)2, 134-139.

42. Han, J.-B. et al. Radiated noise analysis for naval ship using energy flow analysis with fluid

loading. NOVEM 2012 Conference, Sorrento 1-4 April, 2012. 9p.

43. Nilsson, A.C. Noise Prediction and Prevention in Ships. Ship Vibration Symposium, Arlington, VA, October 16-17, 1978. 18 p.

44. Abrahamsen, K.A. Structure-borne noise transmission in high-speed craft. ICSV10, Stockholm 2003. p. 4877-4884.

45. Actran: http://www.fft.be/index.php?pageID=1. 24.08.2012.

46. lms Virtual Lab / Acoustics: http://www.lmsintl.com/acoustic-simulation. 28.02.2013.

47. VA One: http://www.esi-group.com/products/vibro-acoustics/va-one. 24.08.2012.

48. SEAM: http://www.seam.com/software.htm. 24.08.2012.

49. SEA+: http://www.lmsintl.com/simulation/statistical-energy-analysis. 24.08.2012.

50. Designer-Noise: http://www.noise-control.com/designernoise.php. 24.08.2012.

51. Comet Enflow. http://www.globalcomet.com/home/acoustics/products/enflow. 2012-08-23.

52. Langley, R.S. Numerical evaluation of the acoustic radiation from planar structures with general baffle conditions using wavelets. J. Acoust. Soc. Am. 121(2007)2, p. 766-777.

53. Leppington, F.G. et al., The acoustic radiation efficiency of rectangular panels. Proc.R.Soc.Lond. A382(1982), p. 245-271.

54. Maidanik, G. & Kerwin, E.M. Jr. Influence of Fluid Loading on the Radiation from Infinite Plates below the Critical Frequency. J. Acoust. Soc. Am. 40(1966)5, 1034-1038.

55. Rumerman, M.L. The effect of fluid loading on radiation efficiency. J. Acoust. Soc. Am. 111(2002)1 Pt 1, 75-79.

56. Blakemore, M. & Burton, T. Predicting radiation from underwater bodies using AutoSEA2. Part 1: Strong fluid coupling. Proceedings of the Second International AutoSEA Users Conference. april 17, 2002. Detroit, USA.

57. Leino, O. VTT ROPAX/RORO. Report 74017-001, Elomatic Oy 1.11.2012. 4 p. In Finnish.

58. Wärtsilä 32 product quide. Wärtsilä, Ship Power Technology, Vaasa, April 2012. 182 p.